ABSTRACT

Title of Document:	AN EMPIRICAL RE-EVALUATION OF THE BORON ISOTOPE/PH PROXY IN MARINE CARBONATES
	Kateryna Klochko, Ph.D., 2009
Directed By:	Professor Alan J. Kaufman Department of Geology

The boron isotopic composition measured in marine carbonates is considered to be a tracer of seawater pH. However, an accurate application of this proxy has been hampered by our lack of intimate understanding of chemical kinetics and thermodynamic isotope exchange between the two dominant boron-bearing species in seawater: boric acid $B(OH)_3^o$ and borate ions $B(OH)_4^-$, as well as their subsequent partitioning into a carbonate lattice. In this dissertation I have taken on a task of a systematic empirical re-evaluation of the fundamental parameters and assumptions on which the boron isotope paleo-pH proxy is based. As a result of this research strikingly different values of the boron isotope exchange constant in solution (Klochko et al., 2006) and boron speciation and partitioning in carbonates (Klochko et al., 2009) were determined, suggesting that the most parameters and assumptions that were believed to be previously constrained and have been widely applied to the $\delta^{11}B$-pH reconstructions were incorrect.

Recognizing that both biological and inorganic processes may potentially affect boron speciation and isotopic composition in carbonates, to isolate purely inorganic effects on the boron isotope co-precipitation with carbonates, we have designed a series of pH-controlled $\delta^{11}B$ calibration experiments of inorganic calcite and inorganic aragonite. Results to date reveal that precipitates from our experiments at pH = 8.7 fall exactly along the borate ion $\delta^{11}B$ curve predicted by our empirically determined boron isotope fractionation factor (Byrne et al., 2005; Klochko et al., 2006).

Extending these experiments to wider range of pH conditions will provide the necessary inorganic baseline for paleo-studies of inorganic carbonate and future investigations of the purely biological effects on the boron isotope distributions in carbonates.

AN EMPIRICAL RE-EVALUATION OF THE BORON ISOTOPE/PH PROXY IN
MARINE CARBONATES

By

Kateryna Klochko

Dissertation submitted to the Faculty of the Graduate School of the
University of Maryland, College Park, in partial fulfillment
of the requirements for the degree of
Doctor of Philosophy
2009

Advisory Committee:
Professor Alan J. Kaufman, Chair
Professor John A. Tossell
Professor William F. McDonough
Professor Michael Evans
Dr. Steven Shirey

PREFACE

Much of the work presented in this dissertation was previously published as articles in peer-reviewed journals. I am grateful to the efforts and comments of all my co-authors on those studies. Chapters 1, 3, 5 and 6 represent original contributions; however the experimental part for chapter 5 has been conducted in close collaboration with Dr. Sang-Tae Kim. The references for the remaining chapters 2 and 4 are listed below (although all chapters have been modified from their original published form).

Chapter 2:

Klochko, K., Kaufman, A.J., Yao, Wengsheng, Byrne, R.H. and Tossell, J.A. (2006). Experimental measurment of boron isotope fractionation in seawater. *Earth and Planetary Science Letters* **248**: 276-285.

Chapter 4:

Klochko, K., Cody, G., Tossell, J.A., Dera, P. and Kaufman, A.J. (2009) Re-evaluating boron speciation in biogenic calcite and aragonite using ^{11}B MAS NMR. *Geochimica et Cosmochimica Acta* **73**: 1890-1900.

DEDICATION

I dedicate my dissertation and my work to my mother Valentina Ninova

whose unconditional love and support has kept me strong through the years.

ACKNOWLEDGEMENTS

Lastly, I am thankful to my neighbors Lyuda and Oleg Fedulovi, who has been my family ever since I was little. To my husband Jonathan Policarpio, who always believed in me and supported me through my most difficult days. Thank you.

TABLE OF CONTENTS

LIST OF TABLES

LIST OF FIGURES

CHAPTER 1 - INTRODUCTION AND HISTORICAL BACKGROUND

1.1 Atmospheric CO_2 and climate

Over the past several decades there has been growing concern over the increase of anthropogenic greenhouse gases – like CO_2 – in Earth's atmosphere, and their potential influence on our current and future climate. The yearly increase in atmospheric pCO_2 concentration will inevitably change seawater carbonate chemistry as more and more of this soluble gas is taken up by the surface ocean. If atmospheric pCO_2 continues to rise at the present rate, it is expected that surface ocean CO_2 concentrations will increase 3-fold relative to preindustrial values by the end of this century (IPCC, 2001). Such an increase would cause surface ocean pH to drop by 0.35 units, which would overwhelm the ocean's neutralizing capacity (Feely et al., 2004) and have devastating effects on marine ecosystems, especially coral reefs and other calcifying organisms.

The keys to understanding Earth's current and future climate may be hidden in ancient records of global change. Unfortunately, detailed empirical records of climate and environment have been kept only for the past few decades and then only for certain parts of the globe. Our most convincing record of globally averaged pCO_2 changes in the past comes from ice cores, which only reach back as far as ~420,000 years (Petit et al., 1999) (Fig.1.1). This semi-empirical record shows large cyclic fluctuations in pCO_2 abundances over the Pleistocene glacial cycles. While the driving forces behind these the rapid greenhouse gas variations remain poorly
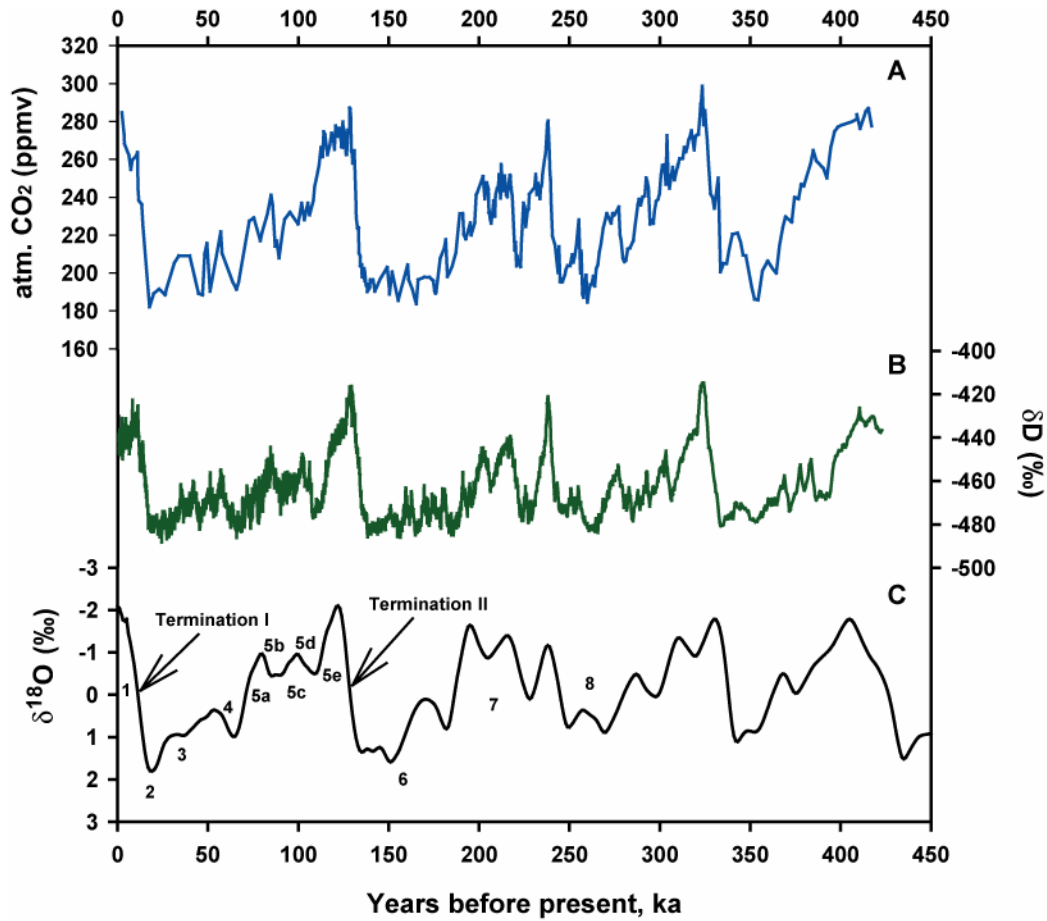
Figure 1.1 – The history of atmospheric pCO_2 over the past 420,000 years as recorded by the gas content in the Vostok ice core from Antarctica (Petit et al., 1999). The ratio of deuterium to hydrogen in ice (expressed as the term δD) provides a record of air temperature over Antarctica, with more negative δD values corresponding to colder conditions. The history of global ice volume based on benthic foraminiferal oxygen isotope data ($\delta^{18}O$) from deep sea sediment cores (Imbrie et al., 1989; McIntyre et al., 1989) is plotted as relative sea level, with more positive values corresponding to sea level minima and peaks in continental ice volume; with a full glacial/interglacial amplitude for sea level change of about 120 m (Fairbanks, 1989).

understood (Broeker and Denton, 1990; Sigman and Boyle, 2000) there is a remarkable agreement between the ice core record and other proxies that record changes in temperature and ice volume (i.e. δD and $\delta^{18}O$) (Fig.1.1), suggesting that CO_2 plays an important role in the Earth's oscillating climate.

For climatically sensitive monitors of even deeper time, paleoceanographers and climatologists are developing additional geochemical proxies, including the analysis of boron isotopes in marine carbonates (McIntyre et al., 1989; Vengosh et al., 1991; Hemming and Hanson, 1992; Imbrie et al., 1993; Petit et al., 1999; Pearson and Palmer, 2000; Quinn and Sampson, 2002). If boron isotope compositions of marine carbonates faithfully record seawater values, these may be used in geochemical models to reconstruct ancient pH and pCO_2 (Vengosh et al., 1991; Spivack et al., 1993; Gillardet and Allègre, 1995; Sanyal et al., 1995; Sanyal et al., 1997; Palmer et al., 1998; Pearson and Palmer, 1999; 2000; Palmer and Pearson, 2003; Hönisch and Hemming, 2005; Pelejero et al., 2005; Foster, 2008; Hönisch et al., 2008) assuming the sediments are well preserved and the proxy is fully calibrated.

1.2   Atmospheric CO_2 and surface ocean pH

To understand the relationship between atmospheric CO_2 abundances and surface ocean pH, it is critical to have a detailed understanding of ocean carbonate chemistry. The reactions which regulate the amount of carbon dioxide in the Earth's atmosphere are complex. One of the fundamental processes that control the relationship is the dissolution of the atmospheric CO_2 in the surface waters (Fig. 1.2).

Carbon dioxide is constantly exchanged between the atmosphere and the ocean via equilibration of CO_2 (g) and CO_2 (aq):

$$CO_2\ (g) \Leftrightarrow CO_2\ (aq) \qquad\qquad K_H = \frac{[CO_2(aq)]}{pCO_2} \qquad\qquad (1.1)$$
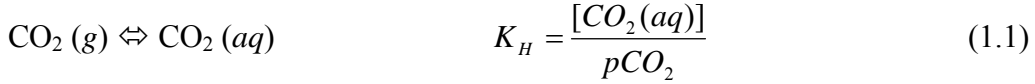
This reaction is characterized by the solubility constant of CO_2 in seawater (K_H), which is controlled by Henry's law (Zeebe and Wolf-Gladrow, 2001).

Further, once dissolved, carbon dioxide in the ocean is speciated into aqueous carbon dioxide: $CO_2(aq)$, carbonic acid: H_2CO_3, bicarbonate: HCO_3^-, and carbonate ion: CO_3^{2-} (Zeebe and Wolf-Gladrow, 2001). The distribution and relative abundances of these species is related to pH of the solution and is controlled by a series of equilibrium reactions with appropriate constants (Fig. 1.2):

$$CO_2(aq) + H_2O \Leftrightarrow H_2CO_3 \qquad\qquad K_0 = \frac{[H_2CO_3]}{[CO_2(aq)][H_2O]} \qquad\qquad (1.2)$$

$$H_2CO_3 \Leftrightarrow HCO_3^- + H^+ \qquad\qquad K_1 = \frac{[HCO_3^-][H^+]}{[H_2CO_3]} \qquad\qquad (1.3)$$

$$HCO_3^- + H^+ \Leftrightarrow CO_3^{2-} + 2H^+ \qquad\qquad K_2 = \frac{[CO_3^{2-}][H^+]}{[HCO_3^-]} \qquad\qquad (1.4)$$
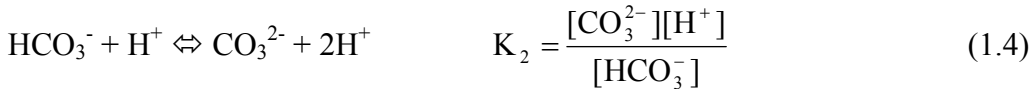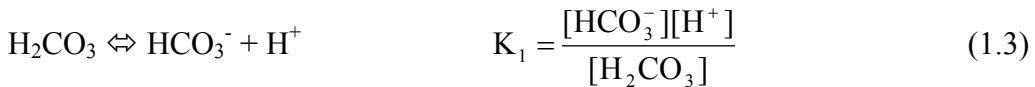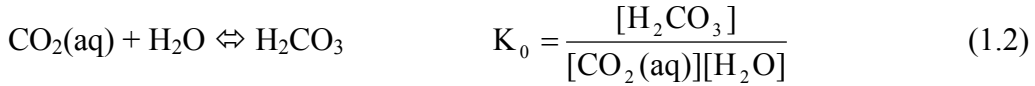
Constants K_H, K_0, K_1 and K_2 are factors of temperature, pressure and salinity of the solution. Stoichiometric equilibrium constants K_1 and K_2 are referred to as first and second carbonic acid dissociation constants. The concentration of the true carbonic acid H_2CO_3 in seawater is negligible compared to $CO_2(aq)$ (< 0.3 %) (Zeebe and Wolf-Gladrow, 2001).
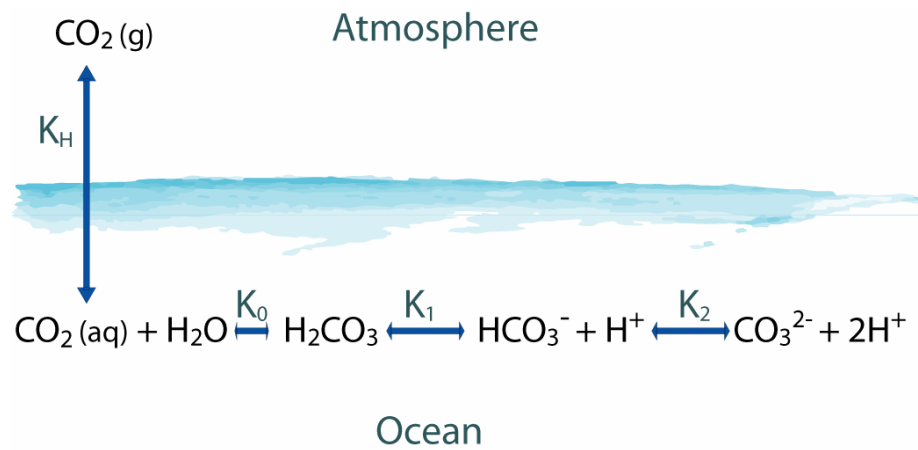
Figure 1.2 - Schematic illustration of the carbonate system equilibria in the ocean.

Therefore, the more commonly used approach (Morse and Mackenzie, 1990) is to combine reactions (1.2) and (1.3) and redefine K_1 (Plummer and Busenberg, 1982):

$$CO_2(aq) + H_2O \Leftrightarrow HCO_3^- + H^+ \qquad K_1 = \frac{[HCO_3^-][H^+]}{[CO_2(aq)][H_2O]} \qquad (1.5)$$
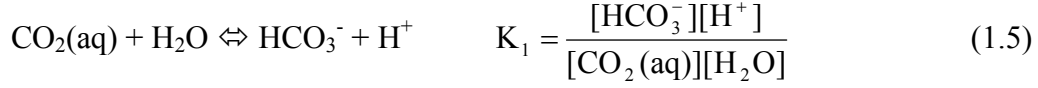
By rearranging equations (1.1), (1.5) and (1.4) for K_H, K_1 and K_2, respectively, it is possible to express surface pCO_2 as a function of pH, which is summarized as:

$$pCO_2 = K_H \left(\frac{K_1}{[H^+]} + \frac{K_1 K_2}{[H^+]^2} \right)^{-1} \sum CO_2 \qquad (1.6)$$

where pCO_2 is partial pressure of CO_2 in the surface waters; pH = - log $[H^+]$; and $\Sigma CO_2 = CO_2(aq) + HCO_3^- + CO_3^{2-}$ is defined as total dissolved inorganic carbon.

Thus, knowledge of the surface paleo-pH allows for a paleo-reconstruction of the surface ocean pCO_2, and subsequently of atmospheric pCO_2, assuming, that surface ocean CO_2 is in equilibrium with atmosphere and ΣCO_2 is constant or known.

1.3   pH and δ^{11}B of marine carbonates

Boron isotope compositions measured in marine carbonates is a potential paleo-pH tool due to pH-sensitive behavior of the boron isotope system in seawater. If reliable, this proxy could provide an invaluable insight into the evolution of ocean pH throughout the Earth's history.

1.3.1   The boron isotope-pH proxy

Boron is a conservative element in seawater, with total concentration of about $4.4 *10^{-4}$ mol/kg H_2O (Byrne and Kester, 1974) and a residence time of ~20 million years. At this concentration, dissolved boron is characterized by two dominant species including trigonally coordinated $B(OH)_3^o$ (boric acid) and tetrahedrally coordinated $B(OH)_4^-$ (borate) (Byrne and Kester, 1974). Distribution of these species in aqueous solution is strongly pH dependent, and described by the following reaction:

$$B(OH)_3^o + H_2O \Leftrightarrow B(OH)_4^- + H^+ \tag{1.7}$$

Although there have been a number of studies attempting to estimate the dissociation constant for reaction (1.7), the most accurate value at 25^oC and salinity of 35 psu is considered to be $pK_B^* = 8.597$ (Dickson, 1990). Thus, at pH > 8.597 borate ions dominate, while at pH < 8.597 boric acid becomes dominant (Fig. 1.3a). In addition, boron has two stable isotopes, ^{11}B and ^{10}B, with average relative abundances of approximately 80% and 20%, respectively. The equilibration of the boron species in solution is accompanied by the isotope exchange reaction:

$$^{10}B(OH)_3^o + {}^{11}B(OH)_4^- \Leftrightarrow {}^{11}B(OH)_3^o + {}^{10}B(OH)_4^- \tag{1.8}$$
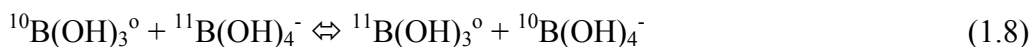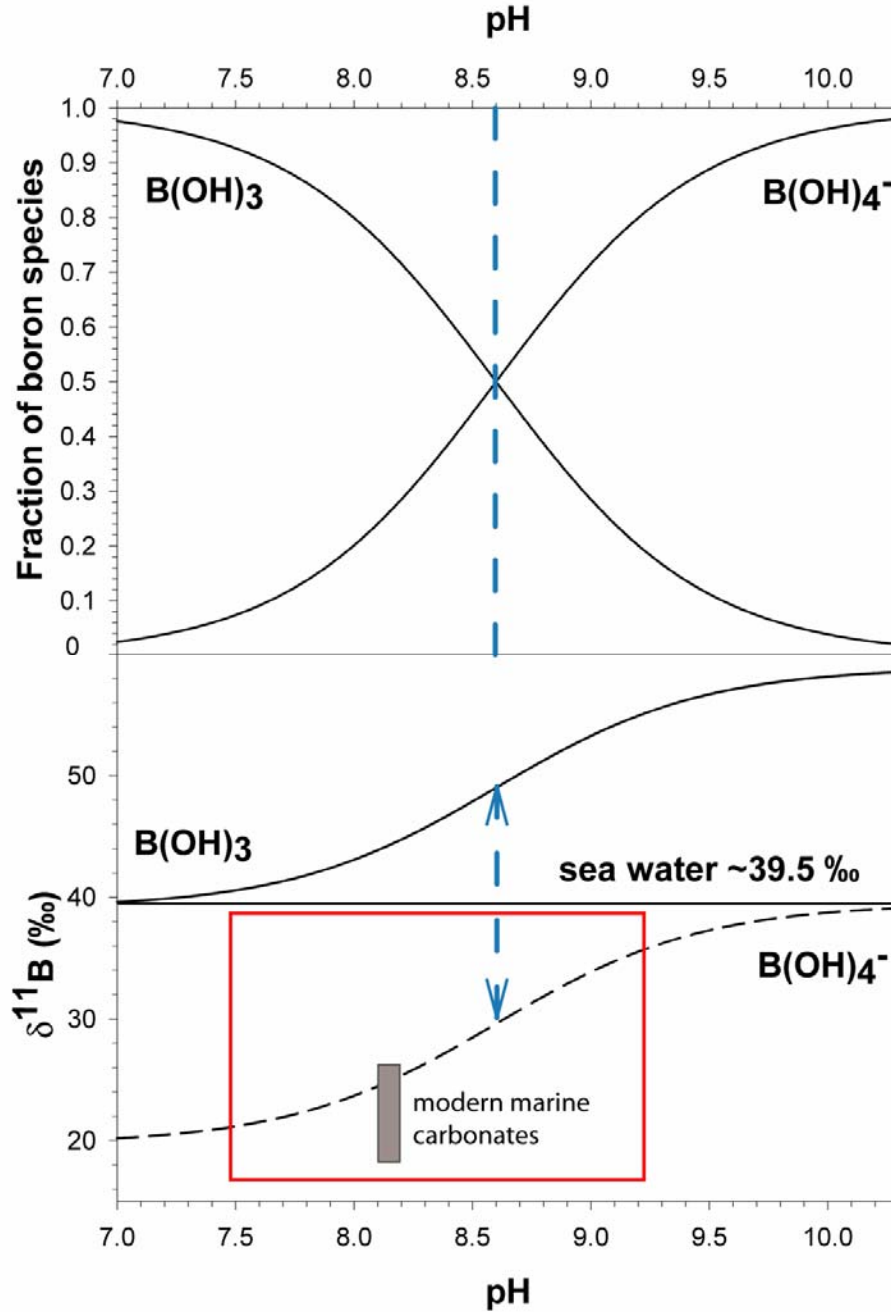
Figure 1.3 - (a) Distribution of two dominant aqueous boron species in seawater vs. pH, calculated using $pK_B^* = 8.597$ (Dickson, 1990); (b) Boron isotopic composition ($\delta^{11}B$) of the aqueous boron species in seawater vs. pH, calculated using $^{11-10}K_B = 1.0194$ (Kakihana et al., 1977). Grey bar represents a range of published boron isotopic composition values measures in various modern marine carbonates. Red square outlines the area of interest depicted in Figs. 4-5.

Boron isotope exchange between boric acid and borate in aqueous solutions results in ^{11}B enrichment in boric acid relative to borate ions (Fig. 1.3b). The magnitude of this enrichment is controlled by the differences in molecular coordination and vibrational frequencies between boron species (Urey, 1947). Until recently, there was no empirical equilibrium constant available for reaction (1.8), and the most commonly used value has been $^{11\text{-}10}K_B = 1.0194$, at 25°C (Kakihana et al., 1977).

The relationship between solution pH and boron isotopic composition of aqueous borate ions can be summarized in the following equation (modified from Gillardet and Allègre, 1995):

$$pH = pK_B^* - \log\left(\frac{\delta^{11}B_{sw} - \delta^{11}B_{borate}}{\delta^{11}B_{sw} - ^{11\text{-}10}K_B \delta^{11}B_{borate} - 1000 \times (^{11\text{-}10}K_B - 1)} \right) \qquad (1.9)$$

where pK_B^* is the boric acid dissociation constant, $^{11\text{-}10}K_B$ is the boron isotope fractionation constant between boric acid and borate, $\delta^{11}B_{borate}$ is the boron isotopic composition of aqueous borate, and the boron isotopic composition of seawater ($\sim$ 39.5‰). Boron isotope ratios are referred to in terms of $\delta^{11}B$ values, where:

$$\delta^{11}B_{sample} = \left\{ \left[\frac{(^{11}B/^{10}B)_{sample}}{(^{11}B/^{10}B)_{standard}} \right] - 1 \right\} \times 1000 \quad ‰ \qquad (1.10)$$

The standard used in most studies is a boric acid (SRM 951) from NIST with $^{11}B/^{10}B$ = 4.04367 (Catanzaro et al., 1970).

Furthermore, it has been assumed that $\delta^{11}B$ of marine carbonates reflects $\delta^{11}B$ of seawater borate (Hemming and Hanson, 1992) ($\delta^{11}B_{borate} = \delta^{11}B_{carb}$). Thus equation (1.9) was applied as:

$$pH = pK_B^* - \log\left(\frac{\delta^{11}B_{sw} - \delta^{11}B_{carb}}{\delta^{11}B_{sw} - {}^{11-10}K_B\delta^{11}B_{carb} - 1000 \times ({}^{11-10}K_B - 1)}\right)$$ (1.11)

where $\delta^{11}B_{carb}$ is the measured boron isotopic composition of a carbonate.

1.3.2 Early applications

Boron isotopes in marine carbonates were first suggested by Vengosh et al. (1991) to be a potential paleo-pH indicator. That study focused on boron sequestration and isotope fractionation in various modern biogenic aragonitic and calcitic skeletons, including corals, foraminifera, ostracodes, pteropodes, gastropods and pelecypodes. The boron isotopic composition of the carbonates analyzed in that study ranged from 14.2 to 32.2‰ (Table 1.1).

These wide variations were initially explained by possible co-precipitation of different proportions of trigonal and tetrahedral species, which are isotopically distinct (i.e. ^{10}B is preferentially partitioned into the tetrahedral borates, Fig. 1.3). Alternatively it was suggested that the range of $\delta^{11}B$ values could also reflect differences in the pH of the microenvironment in which the organisms take up boron into their skeletons.

Later studies, however, reported a narrower range of boron isotope compositions in similar modern biogenic materials (ranging from 19 to 25‰ in (Hemming and Hanson, 1992) and 23.3 to 27.3 in (Gillardet and Allègre, 1995)). Hemming and Hanson (1992) suggested that the narrower range of values was

Table 1.1 - Published data on boron concentration and isotopic composition measured in various modern marine carbonates (adapted from Pagani et al., 2005).

Samples	Carbonate	Boron concentration, ppm	$\delta^{11}B$ range, ‰
Planktonic Foraminifera			
Vengosh et al., 1991	calcite	15 ± 5	14.2-19.8
Sanyal et al., 1995	calcite	-	22.0-23.3
Sanyal et al., 1997	calcite	-	18.4
Benthic Foraminifera			
Vengosh et al., 1991	calcite	-	13.3-32.0
Sanyal et al., 1995	calcite	-	20.5-21.4
Modern Corals			
Vengosh et al., 1991	aragonite	64 ± 11	26.7-31.9
Hemming and Hanson, 1992	aragonite	58 ± 6	23.0-24.7
Gaillardet and Allègre, 1995	aragonite	53 ± 4	23.5-27.0
Hemming et al., 1998	aragonite	51 ± 2	23.9-26.2
Other carbonates			
Hemming and Hanson, 1992	calcite	45 ± 11	20.8-23.2
Hemming and Hanson, 1992	aragonite	31 ± 19	19.1-24.8

consistent with the isotopic composition of the seawater borate (at assumed modern

seawater pH ~ 8.2) as predicted by the isotope fractionation factor of $^{11\text{-}10}K_B = 1.0194$

(Kakihana et al., 1977). Three main conclusions were drawn from this work: 1)

$\delta^{11}B_{carb} = \delta^{11}B_{borate}$, which suggests that tetrahedral borate must be preferentially

incorporated into the carbonate lattice; 2) there must be no vital effect during

incorporation; and 3) boron isotopic composition measured in marine carbonates may

be used as a paleo-pH proxy.

Among the large number of ancient pH and pCO_2 reconstructions that

followed (Sanyal et al., 1995; Sanyal et al., 1997; Palmer et al., 1998; Pearson and

Palmer, 1999; 2000; Palmer and Pearson, 2003; Hönisch and Hemming, 2005;

Pelejero et al., 2005; Foster, 2008; Hönisch et al., 2008) perhaps the most interesting

is the reconstruction of surface ocean pH and surface pCO_2 of the Western Equatorial

Pacific ocean over the last 23,000 years (Palmer and Pearson, 2003) (Fig. 1.4). This

study is notable for two reasons. First, it allowed for a test of pCO_2 during the Last

Glacial Maximum, and second, the earlier part of the record could be directly

compared to the results obtained from the Vostok ice core spanning ~420,000 years

back from the present day.

Figure 1.4 shows $\delta^{11}B$ values measured in planktonic foraminifera

Globigerina sacculifer as well as profiles of surface water pH reconstructed from

$\delta^{11}B$, and of surface pCO_2 reconstructed from surface pH. While the pCO_2 values

reconstructed from pH/$\delta^{11}B$ reflect the overall trend obtained from the Vostok ice

core, there are notable offsets between the two proxy measurements. The most

prominent of these
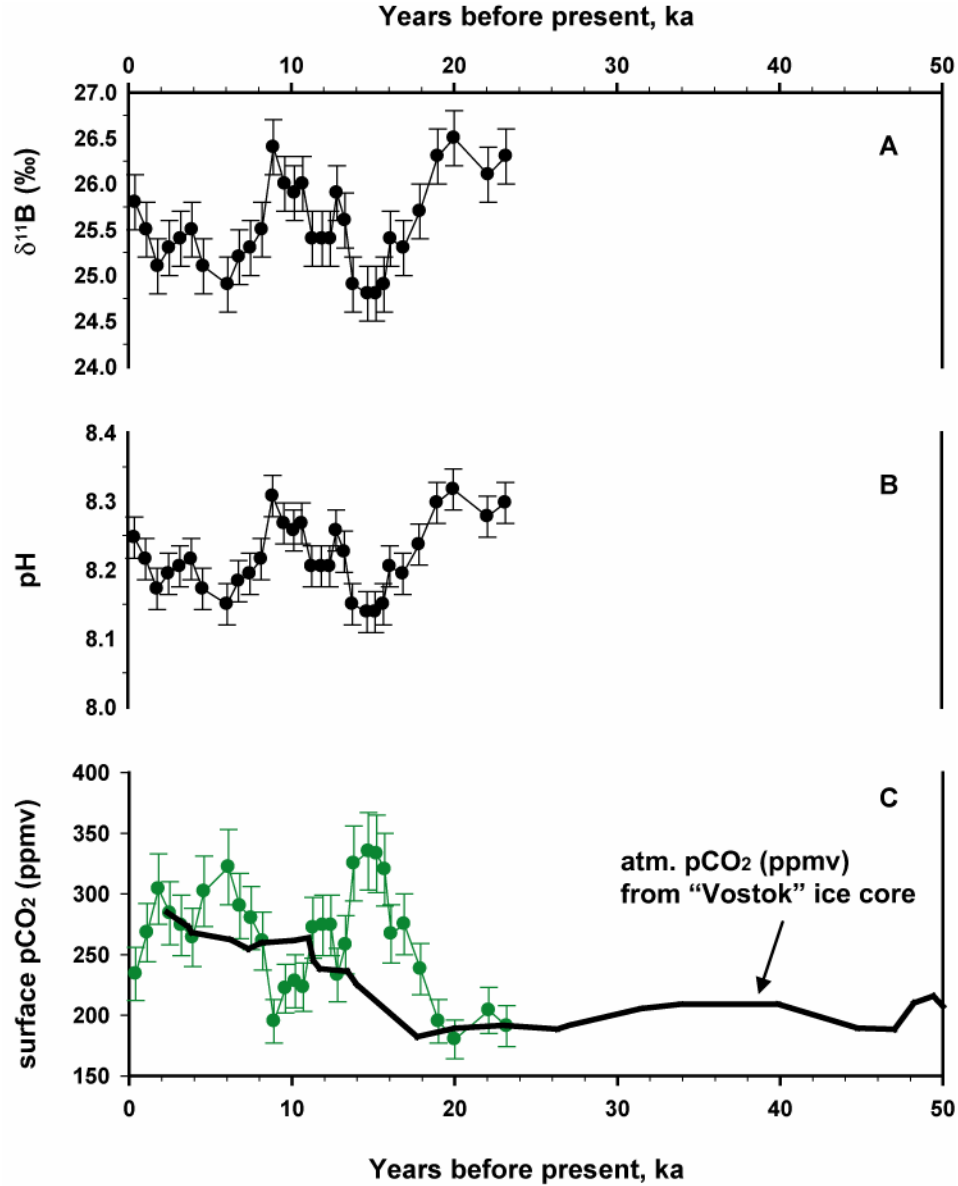
Figure 1.4 – (A) Boron isotope composition ($\delta^{11}B$) measured in planktonic foraminifera *Globigerina succulifer*, collected from the box core ERDC – 92, which was raised from Western equatorial Pacific ($2^o13.5$'S, $156^o59.9$'E; 1598 m). (B) Surface ocean pH in the Western equatorial Pacific reconstructed from $\delta^{11}B$ values. (C)Surface ocean pCO_2 of the Western equatorial Pacific for the last 23,000 years, calculated from the reconstructed surface ocean pH values, and compared with the atmospheric pCO_2, reconstructed from the Vostok core ice records (adopted from Palmer and Pearson, 2003).

occurs between ~13,800 and 15,600 years ago (Fig. 1.4). The authors suggested that this anomaly has resulted from increased La Niña activity in the Western Pacific during this interval. If this view is correct, it would require the wind-driven delivery of high nutrient and high CO_2 waters from the Eastern Pacific to the Western equatorial Pacific Ocean. These surface waters may then have become a powerful source of CO_2 to the atmosphere, which further may have contributed to the termination of the Pleistocene ice age (Palmer and Pearson, 2003).

The work of Palmer and Pearson (2003) is also notably the last pCO_2 reconstruction obtained using the boron isotope pH proxy. This is possibly due to our lack of understanding of variations in carbonate system parameters through time, in particular, ΣCO_2 (total dissolved carbon) and alkalinity. Values used in earlier studies assumed ΣCO_2 to be equivalent to modern seawater (Palmer et al., 1998; Pearson and Palmer, 1999; 2000). This approach has received serious criticism (Caldeira and Berner, 1999; Sundquist, 1999), however, as it is more likely that ΣCO_2 has varied widely in the past. Alternatively, alkalinity could be used instead of ΣCO_2 for pCO_2 estimates. However, there is no clear consensus on the history of alkalinity in the oceans either. To address this issue, Palmer and Pearson (2003) used alkalinity/salinity relationships (Millero et al., 1998) deduced from sea level estimates (Blanchon and Shaw, 1995) to estimate alkalinity values for the past 25,000 years.

1.4 Empirical calibration studies

While armed only with recognition of the aqueous borate species pH-dependant distribution, an untested theoretical isotope exchange constant $^{11-10}K_B$ and an assumption of preferential tetrahedral borate partitioning into the calcium carbonate, the paleo-reconstructions continued. However, the disagreement between $\delta^{11}B$ values provided by the studies of modern biogenic carbonates, which grew in modern seawater of assumed average pH ~ 8.2, remained unresolved. Empirical and more reliable evidence for the pH- $\delta^{11}B_{carb}$ relationship was required. Providing such evidence was an ultimate goal of the several empirical calibration studies carried out over a range of controlled pH conditions.

The five empirical calibration studies included biogenic calcite of two foraminifera species including *G. sacculifer* (Sanyal et al., 2001) and *Orbulina universa* (Sanyal et al., 1996)), biogenic aragonite from two coral species *Acropora nobilis* and *Porites cylindrica* (Hönisch et al., 2004), and inorganic calcite (Sanyal et al., 2000). Results of these studies are presented in Fig. 1.5. These calibration studies reveal that the pH of the solution does have a strong control over the boron isotopic composition of biogenic and inorganic carbonates. All carbonates precipitated at higher pH had higher $\delta^{11}B$ values relative to those that formed at lower pH. Furthermore, boron isotope compositions of these controlled precipitates fell either near or below the expected value for seawater borate (given an assumption from a theoretical – but unmeasured – isotope exchange constant: Kakihana et al., 1977), suggesting little to no incorporation of boric acid into the carbonate lattice.

15
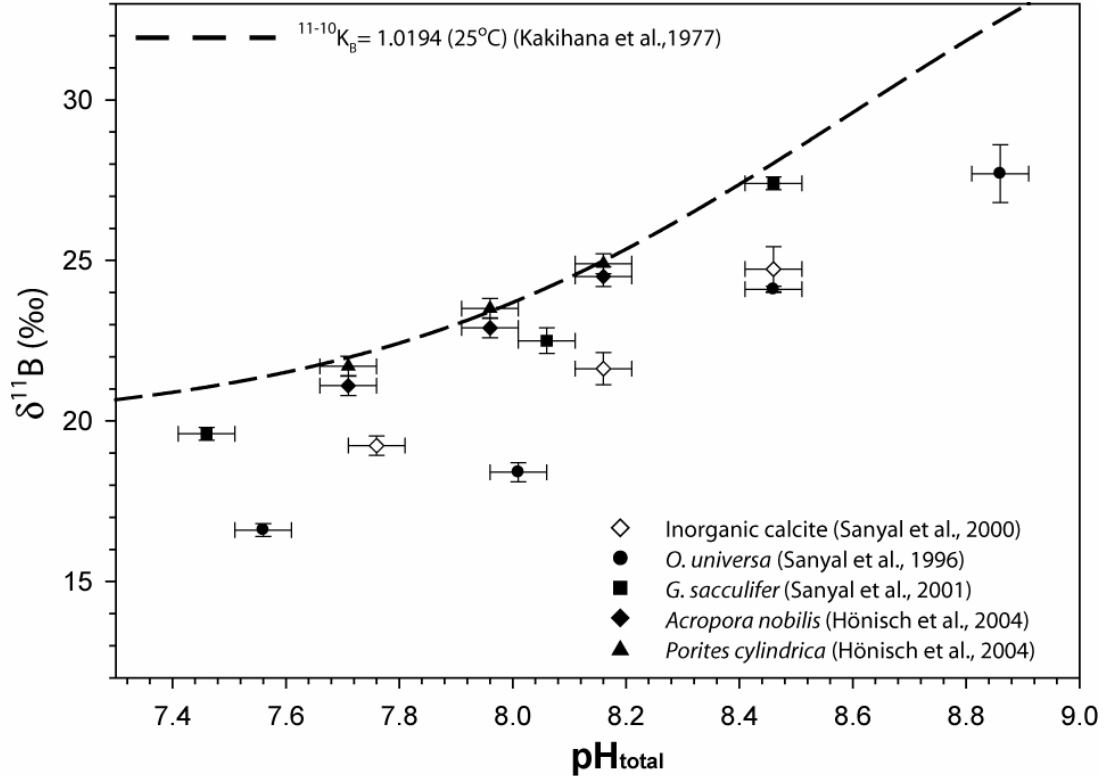
Figure 1.5 – Boron isotopic composition (δ^{11}B) of aqueous borate ion in seawater vs. pH, calculated using $^{11\text{-}10}$K$_B$ = 1.0194 (Kakihana et al., 1977); and the results of the inorganic calcite precipitation experiments (Sanyal et al., 2000), cultured *Orbulina universa* and *Globigerina sacculifer* foraminifera species (Sanyal et al., 1996; Sanyal et al., 2001) and cultured scleractinian corals *Acropora nobilis* and *Porites cylindrica* (Hönisch et al., 2004). The pH$_{NBS}$ values from (Sanyal et al., 1996, 2000, 2001) were recalculated to fit the seawater pH scale (pH$_{total}$= pH$_{NBS}$ - 0.14) (*cf.* Hönisch et al., 2004).

What these researchers found but did not expect, however, were values that fell below isotopic composition of aqueous borate represented by a curve and predicted by a theoretical isotope exchange constant (Kakihana et al., 1977) used in paleo-pH reconstructions. No known processes could explain such downward offset (Zeebe et al., 2003). To satisfy the mass balance of the boron isotope systematics in solution, the isotopic composition of a carbonate precipitated in a given solution should be equal or larger than the isotopic composition of borate ions in that solution. Carbonate $\delta^{11}B$ values lighter than aqueous borate, which is the lowest (hence, the lightest) end member in the boron isotope systematics in solution, are contradictory to the mass balance. Hence, the "borate curve" itself is a source of the discrepancy and the $^{11\text{-}10}K_B$ value is most likely underestimated (Zeebe et al., 2003; Pagani et al., 2005; Zeebe, 2005).

Furthermore, boron isotope differences between the two calcitic foraminifera species *O.universa* and *G.saccilifer* grown under identical ambient pH conditions suggests that metabolic or "species" effects might be present. Similarly, $\delta^{11}B$ differences between aragonite and calcite samples show that the former is systematically enriched in ^{11}B, suggesting the likelihood of a mineralogical effect.

These inconsistencies suggest that the parameters in the pH/pCO$_2$ proxy are poorly constrained. The importance of this proxy to understanding past and future changes in Earth's oceanic environment and climate thus warrants a closer investigation of the fundamental parameters and assumptions of the proxy, which is the over-arching goal of this dissertation.

1.5 Fundamental parameters of the δ^{11}B-pH system

As described above, the δ^{11}B/pH pH proxy depends on an accurate estimate of the pH-dependent distribution of two dominant borate species in aqueous solution (characterized by pK_B^*), the magnitude of isotope exchange between boric acid and borate in a given solution (characterized by $^{11-10}K_B$), and boron species partitioning into biogenic and inorganic carbonate minerals.

1.5.1 Boric acid dissociation constant

The boric acid dissociation constant for the reaction

$$B(OH)_3^o + H_2O \Leftrightarrow B(OH)_4^- + H^+ \tag{1.7}$$

is given by the equation:

$$pK_B^* = -\log \frac{\left[B(OH)_4^-\right]\cdot\left[H^+\right]}{\left[B(OH)_3^0\right]} = pH - \log \frac{\left[B(OH)_4^-\right]}{\left[B(OH)_3^0\right]} \tag{1.12}$$

where pK_B^* is an apparent boric acid dissociation constant, which is a function of ionic strength, temperature and pressure of a solution.

The boric acid dissociation has been studied extensively under a range of temperatures and ionic strength solutions, including freshwater and ion-specific media (Dyrssen and Hansson, 1973; Byrne and Kester, 1974; Hershey et al., 1986), and synthetic seawater (Lyman, 1956; Hansson, 1973; Byrne and Kester, 1974; Dickson, 1990; Roy et al., 1993). Pressure effects on the dissociation constant have been evaluated (Culberson and Pytkowicz, 1968). In general, pK_B^* increases with lower ionic strength of the solution (i.e. "pure" water), and decreases with higher ionic strength of the solution (i.e. seawater). In addition, pK_B^* increases with decreasing temperature and pressure.

The discrepancies between various published values for pK_B^* can be attributed to differences in the applied pH scale. Earlier publications (Lyman, 1956; Byrne and Kester, 1974; Hershey et al., 1986) applied the "NBS" pH scale, which relies on the use of standard buffer solutions with a low ionic strength (~0.1) relative to seawater (~0.65). Such differences in solution compositions make NBS standards and seawater samples incompatible for electrode calibration, as they would affect the electric potential differences between the liquid in the electrode and the sample solution. Moreover, specific properties of a pH electrode utilized in the experiments vary with different electrodes. Such data obtained using the NBS "electrode-specific" scale is almost impossible to compare, unless the data has been obtained using the same electrode and/or "NBS" buffer correction factor is applied.

Boric acid dissociation constant values reported in other publications (Hansson, 1973; Dickson, 1990; Roy et al., 1993) have applied "total hydrogen" pH scale, which relied on the use of the "in-house" standard buffer solutions based on synthetic seawater. If the solution contains fluoride ions, then the "seawater" pH scale is applied. Currently, the commonly accepted pH scales are "total hydrogen" and "seawater" scales (Zeebe and Wolf-Gladrow, 2001). pK_B^* values reported in the three studies using "total hydrogen" scale (Hansson, 1973; Dickson, 1990; Roy et al., 1993) were in very good agreement, and the data set reported by Dickson (1990) is considered the most thorough and accurate.

The differences in pH values reported using "total hydrogen" or "seawater" scales are negligible. However, the differences in pH values reported using the latter two and "NBS" pH scale could be up 0.14 pH units. In addition, ionic media itself as

well as measurement techniques employed might have even larger contribution to the discrepancies between various reported pK_B^* datasets.

Potential effects of pK_B^* on the $\delta^{11}B$-pH relationship are significant (Fig. 1.6). These effects manifest themselves in the shape and the position of the $\delta^{11}B$-pH curve. Therefore, careful consideration of the constant is necessary prior to its application. pK_B^* values applied to the $\delta^{11}B$-pH reconstructions have varied over the history of the proxy. Sanyal et al. (1995) have applied $pK_B^* = 8.77$ at 2^oC and 296 atm obtained by Lyman (1956). Other early $\delta^{11}B$-pH reconstructions (Vengosh et al., 1991; Hemming and Hanson, 1992; Gillardet and Allègre, 1995) have used $pK_B^* = 8.83$ at 25^oC and 1 atm. Later, the most accurate accepted value $pK_B^* = 8.597$ at 25^oC and 1 atm (Dickson, 1990) have been uniformly applied to the $\delta^{11}B$-pH relationship (Palmer and Pearson, 2003; Hönisch and Hemming, 2005; Pelejero et al., 2005; Klochko et al., 2006; Foster, 2008).
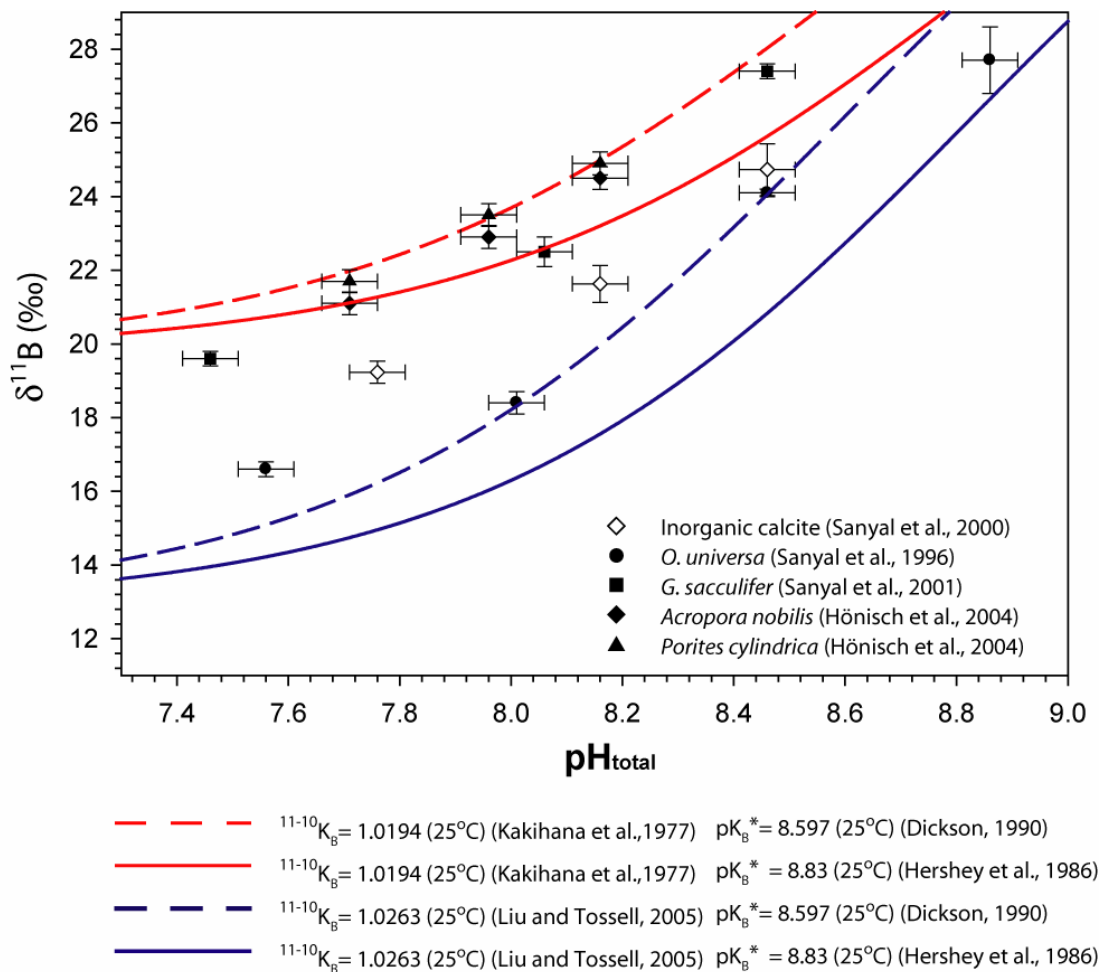
Figure 1.6 – The sensitivity analysis of the potential influence of boric acid dissociation constant (pK_B^*) and boron isotope fractionation constant ($^{11-10}K_B$) on the $\delta^{11}B_{borate}$-pH relationship in solution.

1.5.2 Boron isotope fractionation constant

The boron isotope fractionation constant [11-10]K_B, which characterizes boron

isotope exchange between dominant boron species:

$$^{10}B(OH)_3 + {}^{11}B(OH)_4^- \Leftrightarrow {}^{11}B(OH)_3 + {}^{10}B(OH)_4^- \tag{1.8}$$
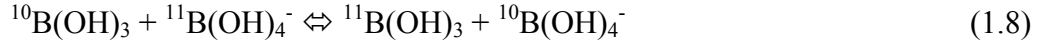
is the second most important parameter of the $\delta^{11}B$-pH relationship in aqueous

solution, and is given by the following equation:

$$^{11-10}K_B = \frac{\left[{}^{11}B(OH)_3^0\right] \cdot \left[{}^{10}B(OH)_4^-\right]}{\left[{}^{10}B(OH)_3^0\right] \cdot \left[{}^{11}B(OH)_4^-\right]} \tag{1.13}$$

or

$$\alpha = \frac{1}{{}^{11-10}K_B}, \tag{1.14}$$

which is another notation for the boron isotope fractionation constant also commonly

used in the literature.

The theoretical result [11-10]$K_B = 1.0194$ at $25^\circ C$ (Kakihana et al., 1977) has

been widely used in the paleo-pH reconstructions (Sanyal et al., 1995; Sanyal et al.,

1997; Palmer et al., 1998; Pearson and Palmer, 1999; 2000; Palmer and Pearson,

2003; Hönisch and Hemming, 2005; Pelejero et al., 2005; Hönisch et al., 2008).

However, the comparison of the carbonate calibration data from the culture

experiments (Sanyal et al., 1996; Sanyal et al., 2000; Sanyal et al., 2001; Hönisch et

al., 2004) and the fractionation curve for aqueous borate characterized by [11-10]K_B =

1.0194 (Kakihana et al., 1977), suggests that the [11-10]K_B has been underestimated.

More recent ab-initio calculations have supported this view and have reported a larger

value for [11-10]K_B in solution ~ 1.0260 (Oi, 2000a; 2000b; Oi and Yanase, 2001) and ~

1.0267 (Liu and Tossell, 2005). Empirically constraining this constant is one of the central goals of this dissertation as reported in detail in Chapters 2 and 3.

1.5.3 *Boron partitioning in carbonates*

The last key parameter of the proxy is an assumption of preferential borate ion incorporation into the calcium carbonate structure. This assumption has been inferred through various approaches. In the early study by Palmer et al. (1987) boron incorporation onto clay surfaces was examined over a range of solution pH. Both the boron concentration and boron isotopic composition of the clays increased with an increase in pH. Furthermore, the isotopic composition of the clays fell close to that predicted by Kakihana et al. (1977) for seawater borate, suggesting that the charged tetrahedral boron species were preferentially attracted to clay surfaces, and by analogy to carbonate surfaces as well.

The only previous investigation of boron coordination in modern marine carbonates was done by NMR spectroscopy (Sen et al., 1994). This study, however, reported conflicting results indicating that boron in aragonite occurs as tetrahedrally-coordinated $B(OH)_4^-$, while in calcite 90% of boron was in trigonal $B(OH)_3^o$ form. The $\delta^{11}B$ measurements of these samples revealed a range of values between +20 and +25‰, which is roughly consistent with the isotopic composition of seawater borate. Thus, it was concluded that the mode of tetrahedral borate ion incorporation into the calcite structure was very different from that of aragonite, which should be accompanied by a subsequent change in coordination to trigonal boric acid.

In Chapter 4, the results of a similar NMR study (Klochko et al., 2009) on boron coordination in biogenic aragonite and calcite, as well as their implications for the δ^{11}B-pH proxy are discussed.

1.6 Proxy material

Marine carbonates, especially scleractinian corals and planktonic foraminifera are very useful environmental archives. For example, marine carbonates have been used as proxy material in paleo-reconstructions of temperature, ice volume, productivity, and respiration (Gallup et al., 1994; Quinn et al., 1996; Quinn et al., 1998; Fallon et al., 1999; Cobb et al., 2001; Gallup et al., 2002; Quinn and Sampson, 2002; Cobb et al., 2003; Kilbourne et al., 2004a; Kilbourne et al., 2004b).

While the modern seawater total boron concentration is around 4.8 ppm, the boron concentrations in marine carbonates analyzed to date are relatively high and range from 40 to 100 ppm, suggesting that marine calcification could be a substantial sink for boron. Relatively high boron abundances in carbonates combined with its long residence time of about 20 million years makes the boron system especially attractive for ocean geochemical studies. However, understanding of boron partitioning from the seawater reservoir into marine carbonates is complicated by metabolic "vital" effects, which remain poorly understood.

1.6.1 *Metabolic considerations*

Modern oceanic surface waters (water depth of a few hundred meters or less) are supersaturated with respect to calcite and aragonite, yet direct precipitation of inorganic calcium carbonate in the modern surface oceans is a rare phenomenon (Morse and Mackenzie, 1990). It has been suggested that various elements or ions, such as: magnesium, phosphates and dissolved organic compounds, make surface waters unfavorable for carbonate precipitation by inhibiting the formation of $CaCO_3$ nuclei (Berner, 1975; 1978; Mucci, 1986; Morse and Mackenzie, 1990).

The bulk of marine calcium carbonate is produced by calcifying organisms, which manage to initiate calcification via the manipulation of seawater chemistry in order to build their skeletons. The strategies employed by these organisms are extremely complex and hence are poorly understood. The simplified chemical reaction of calcification is represented by:

$$Ca^{2+} + CO_2 + H_2O \Leftrightarrow CaCO_3 + 2H^+ \qquad (1.15)$$

To overcome the inhibitions, marine calcifiers have two options: to remove the inhibiting ions and/or increase the $CaCO_3$ saturation state of the fluid. One thing is certain that the first step in both organisms is occurring via this seawater isolation, where corals and foraminifera are able to control chemistry of the calcifying fluid, concentrate necessary ions and actively remove ions that inhibit $CaCO_3$ growth.

Most planktonic foraminifera produce low-Mg calcite. Some models suggest that seawater modification in foraminifera is controlled through initial seawater vacuolization (Erez, 2003). Then, in order to enhance calcification, foraminifera possibly remove Mg^{2+} and H^+ ions from the calcifying fluid. Removal of Mg^{2+}

appears to be very energetically inefficient (Zeebe and Sanyal, 2002). Therefore the question of how foraminifera result in low-Mg calcite remains unanswered. On the other hand, it was shown that H^+ removal could be a very advantageous process in foraminifera (Zeebe and Sanyal, 2002). Photosynthesis of symbiotic algae in foraminifera assists in removing H^+ from the calcifying fluid. Removal of the protons from the solution ultimately increases the pH of the calcifying fluid, thus shifting reaction (1.15) to the right towards increased calcification. Calcification itself works towards reducing pH in isolated solution chambers; therefore the cycle of fluid modification has to be constant to maintain chemistry favorable for $CaCO_3$ formation. The study had shown pH increases of about 1.7 units, which correspond to ~13 fold increase in CO_3^{2-} concentration (Zeebe and Sanyal, 2002).

Jorgensen et al. (1985) succeeded in recording pH changes within the planktonic foraminifera *G. sacculifer* using micro-electrodes, and they discovered that increases in pH of the calcifying fluid of up to 0.6 pH units are possible. However, the pH increase enhanced by photosynthesis in the calcification space would be counteracted by respiration in dark conditions.

Scleractinian corals excrete aragonite. Corals have several chambers for the water to pass through. It is believed that in corals, the enzyme Ca^{2+} - ATPase plays an important role in the calcification mechanism. In corals, this enzyme has a dual function: to transport Ca^{2+} ions to the site of calcification, at the same time removes protons away from it, thus shifting the reaction (1.15) towards calcification.

Evidence of such processes is found in a detailed study of the coral calcification mechanism by Al-Horani and colleagues (Al-Horani et al., 2003). In this

study, diurnal pH variations (light/dark conditions) of the various layers of coral *Galaxea fascicularis*, including calcifying fluid, was monitored with micro-electrodes.

This study proposed that Ca^{2+} - ATPase, present in the calicoblastic layer of a coral, pumps Ca^{2+} against its concentration gradient in exchange for protons, thereby increasing the saturation states of Ca^{2+} and CO_3^{2-}, resulting in $CaCO_3$ precipitation (see Fig. 1.7). Light triggers enzyme function, while ATP need for the reaction is supplied mainly from photosynthetic respiration of zooxathellae. This study found, that the pH of the calcifying fluid was close to 9.3 in light, while in the dark, it fell to 8.13 (Table 1.2). Similarly, the aragonite saturation state (Ω) in calcifying fluid has increased from ca. 3.2 in dark to ca. 25 in light conditions compared to seawater value of ca. 4.

If correct, active modification of the calcifying fluid and substantial diurnal pH fluctuations should have a profound effect on boron isotope distribution within the calcifying space, insofar as it is directly linked to the pH of the solution (see Chapter 4).

Table 1.2 – Summarized table for measured calcium and pH levels in the three compartments of a modern coral Galaxea fascicularis and the calculated aragonite saturation state of the calcifying fluid under calicoblastic layer in light and dark conditions (from Al-Horani et al., 2003).

	pH		Ca^{2+}, mM		saturation state	
	light	dark	light	dark	light	dark
Seawater	8.2		ca. 10.0		ca. 4	
Polyp surface	8.49 ± 0.25	7.60 ± 0.22	9.82 ± 0.06	10.04 ± 0.06		
Coethelon	8.19 ± 0.20	7.61 ± 0.19	9.76 ± 0.05	9.94 ± 0.13		
Calcifying fluid	9.28 ± 0.03	8.13 ± 0.08	10.58 ± 0.29	10.21 ± 0.25	ca. 25	ca. 3.2
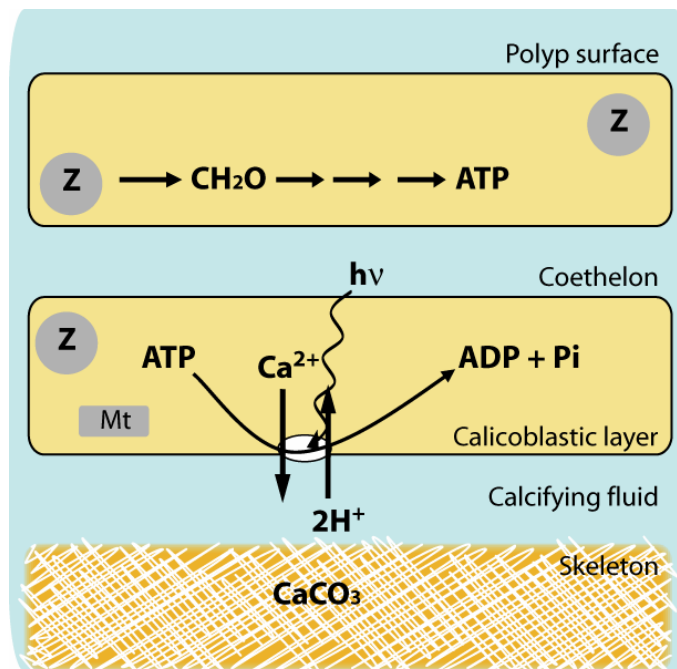
Figure 1.7 – A conceptual model to explain the mechanism of light-enhanced calcification in coral *Galaxea fascicularis* illustrated on a simplified cross-section of a coral (adopted from Al-Horani et al., 2003). ATP - Adenosine Triphosphate; ADP - Adenosine diphosphate; Pi - inorganic Phosphate; Z – zooxathellae; Mt – mitochondria; hυ – photon.

1.7   Conclusions

Boron isotope systematics in solution and marine biogenic carbonates holds a great promise for paleo-pH reconstructions. However, the accurate application of the proxy to the paleo-pH reconstructions depends on our intimate understanding of the chemical kinetics and thermodynamic isotope exchange reactions between the two dominant boron-bearing species in seawater, boron partitioning in carbonate minerals, as well as metabolic effects in biological carbonates used as proxy material.

To summarize, the application of the proxy is possible if:
1) The boric acid dissociation (pK_B^*) is known;
2) The boron isotope fractionation constant ($^{11\text{-}10}K_B$) for isotope exchange between aqueous boron species - borate ion $[B(OH)_4^-]$ and boric acid $[B(OH)_3^o]$ – is known;
3) Boron partitioning and coordination in calcium carbonates is characterized and constrained at any pH;
4) Vital effects on $\delta^{11}B$ of biogenic carbonates are absent or known.

Unfortunately, the proxy has been insufficiently characterized with respect to all the aspects listed above. In this dissertation, I have taken on the task of constraining two of the four main aspects of the pH proxy, namely two fundamental parameters that characterize the $\delta^{11}B$-pH relationship:

1) Empirical determination of the boron isotope fractionation constant ($^{11\text{-}10}K_B$)
   in aqueous solution under a range of temperatures, ionic strengths, media and
   total boron concentrations (Chapters 2 and 3);

2) Re-evaluation of the boron speciation in various modern marine carbonates by
   ^{11}B MAS NMR spectroscopy (Chapter 4).

In collaboration with other colleagues (Sang-Tae Kim, George Cody, Gavin Foster and others), we have initiated a project on synthetic carbonate precipitation in controlled pH conditions to evaluate the effects of pH on boron speciation in carbonates and to re-evaluate the effects of pH on the concentration and boron isotopic composition of carbonates. The preliminary results of this study are presented in Chapter 5.

CHAPTER 2 - EXPERIMENTAL MEASUREMENT OF BORON ISOTOPE FRACTIONATION IN SEAWATER

ABSTRACT: The boron isotopic composition of marine carbonates is considered to be a tracer of seawater pH. Use of this proxy benefits from an intimate understanding of chemical kinetics and thermodynamic isotope exchange reactions between the two dominant boron-bearing species in seawater: boric acid $B(OH)_3$ and borate ion $B(OH)_4^-$. However, because of our inability to quantitatively separate these species in solution, the degree of boron isotope exchange has only been known through theoretical estimates. In this study, we present results of a spectrophotometric procedure wherein the boron isotope equilibrium constant ($^{11-10}K_B$) is determined empirically as the difference in the dissociation constants of $^{11}B(OH)_3$ and $^{10}B(OH)_3$ in pure water, 0.6 mol kg^{-1} H$_2$O KCl and artificial seawater. Within experimental uncertainty, our results show no dependence of $^{11-10}K_B$ on temperature, but $^{11-10}K_B$ at 25°C in the pure water was statistically different than results obtained in solutions at high ionic strength. $^{11-10}K_B$ of the seawater (S = 35, B_T = 0.01 mol kg^{-1} H$_2$O) at 25°C is 1.0272 ± 0.0006. This result is significantly larger than the theoretical value used in numerous previous paleo-pH studies ($^{11-10}K_B$ = 1.0194).

2.1 Introduction

In aqueous solution, the equilibrium distribution of $B(OH)_3$ and $B(OH)_4^-$ is known to be strongly pH dependent, such that at values higher than 8.6 borate ion dominates while at lower pH boric acid is the dominant species (Hershey et al., 1986):

$$B(OH)_3 + H_2O \Leftrightarrow B(OH)_4^- + H^+ \tag{2.1}$$

In modern seawater (pH = 8.2) borate ion comprises ~28.5% of boron species (assuming the dissociation constant of boric acid $pK_B^* = 8.597$ (at 25^oC); (Dickson, 1990)), representing ca. 6% of seawater alkalinity, a measure of the capacity of the ocean to neutralize anthropogenic CO_2 and thus resist changes in pH. Increases in pCO_2 over the next 50 years are predicted to overwhelm the ocean's neutralizing capacity (Feely et al., 2004), resulting in declining pH and potentially devastating effects on marine ecosystems, especially corals and other calcifying organisms in shallow oceanic environments. Boron isotope measurements of coral and foraminiferal carbonate over the past century, and through the recent geological past (Vengosh et al., 1991; Hemming and Hanson, 1992; Spivack et al., 1993; Gillardet and Allègre, 1995; Sanyal et al., 1995; Sanyal et al., 1997; Palmer et al., 1998; Pearson and Palmer, 1999; 2000; Palmer and Pearson, 2003; Hönisch and Hemming, 2005; Pelejero et al., 2005), hold the promise of charting temporal pH changes, but this requires quantitative estimates of isotope exchange reactions between aqueous species, as well as evaluation of possible of microenvironmental effects at the sites of calcification within organisms (Jorgensen et al., 1985; Al-Horani et al., 2003).

Differences in molecular coordination and vibrational frequencies between boron species in solution control the magnitude of isotope fractionation ($\alpha = 1/^{11\text{-}10}K_B$) (Urey, 1947). The isotope exchange of ^{10}B and ^{11}B between the two species is described by the reaction:

$$^{10}B(OH)_3 + {}^{11}B(OH)_4^- \Leftrightarrow {}^{11}B(OH)_3 + {}^{10}B(OH)_4^- \tag{2.2}$$
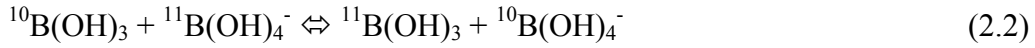
with an isotopic equilibrium constant defined by:

$$^{11\text{-}10}K_B = \frac{\left[^{11}B(OH)_3^0\right] \cdot \left[^{10}B(OH)_4^-\right]}{\left[^{10}B(OH)_3^0\right] \cdot \left[^{11}B(OH)_4^-\right]} \tag{2.3}$$

In 1977, Kakihana et al. (Kakihana and Kotaka, 1977; Kakihana et al., 1977) provided the first theoretical estimate of the magnitude of isotope exchange between borate and boric acid ($^{11\text{-}10}K_B = 1.0194$ at 25^oC), based on reduced partition function ratio calculations from spectroscopic data on molecular vibrations (Table 2.1). In spite of the fact that in a later publication with new collaborators (Oi et al., 1991) it was suggested that the boron isotope equilibrium constant could be much larger than that predicted in 1977, it is the earlier value (Kakihana et al., 1977) that has been consistently used in paleo-pH reconstructions. Supporting the lower value, a recent analysis based on experimental vibrational frequencies from various sources using force field modeling reported $^{11\text{-}10}K_B = 1.0176 \pm 0.0002$ (Sanchez-Valle et al., 2005). In contrast, more rigorous theoretical treatments of the spectroscopic data (Oi, 2000a; Oi and Yanase, 2001; Liu and Tossell, 2005) using *ab initio* molecular orbital theory have indicated significantly higher $^{11\text{-}10}K_B$ values (ranging from 1.0260 to 1.0267 at 25^oC) for these species.

Table 2.1 – Published estimates of $^{11\text{-}10}K_B$ in seawater.

Estimates based on spectroscopic data on molecular vibrations Treatment (T°C)	$^{11\text{-}10}\mathbf{K_B}$
Empirical spectra and Force Field modeling (26.8°C) (Kakihana and Kotaka, 1977; Kakihana et al., 1977)	1.0194
Empirical spectra and Force Field modeling (26.8°C) (Sanchez-Valle et al., 2005)	1.0176(2)
Ab-initio molecular orbital theory (25°C) (Oi, 2000a; Oi and Yanase, 2001)	1.0260
Ab-initio molecular orbital theory (25°C) (Liu and Tossell, 2005)	1.0267
Evaluation of all of the above treatments (Zeebe, 2005)	≥ 1.0300

Estimates from adsorption and precipitation experiments Method (T°C)	$^{11\text{-}10}K_B$
Boron adsorption on marine clay (25°C) (Palmer et al., 1987)	1.0330(20)
Boron mineral precipitation (25°C) (Oi et al., 1991)	1.0395(190)
Best fit value for boron adsorption on resin (10 and 30°C) (Sonoda et al., 2000)	1.0290
Best fit value (Pagani et al., 2005) for inorganic calcite precipitation (Sanyal et al., 2000)	1.0260

An important drawback of both *ab-initio* calculations and calculations that rely on experimental frequencies is that their outcome is extremely sensitive to both the choice of vibrational frequencies and the detailed theoretical methods applied to calculate molecular forces. The most detailed overview and comparison of various quantum methods of computation was presented in (Zeebe, 2005), which demonstrated that $^{11-10}K_B$ could range between ~1.020 and ~1.050 depending on the data used and the theoretical methods applied. The best way to avoid errors is to follow one of the main rules of thumb in computational science, which requires the use of strictly comparable methods for obtaining and treatment of the data (e.g. experimental vibrational frequencies).

Several studies have been conducted to estimate boron isotope fractionation that accompany adsorption of dissolved boron species on various substances such as marine clay (Palmer et al., 1987), N-methyl-D-glucamine resin phase (Sonoda et al., 2000), and boron minerals (Oi et al., 1991) (Table 2.1). Others (Pagani et al., 2005) estimated boron isotope fractionation by fitting through the inorganic calcite precipitation data (Sanyal et al., 2000). However, to the best of our knowledge, although $^{11-10}K_B$ has been determined in 0.6 mol kg^{-1} H$_2$O KCl (Byrne et al., 2006), no direct experimental $^{11-10}K_B$ value for seawater has yet been reported.

The method applied here and in (Byrne et al., 2006) is purely experimental and based upon fundamental observations of chemical equilibrium. Experiments in this study were designed to directly determine the boron isotope equilibrium constant over a range of solution conditions. These were specifically considered in order to evaluate the effect of different temperatures, medium composition and total boron on

the isotopic equilibrium constant. Thousands of at-sea measurements of seawater pH

(Clayton and Byrne, 1993; Clayton et al., 1995; Byrne et al., 1999) demonstrate that

the precision of spectrophotometric pH measurements obtained via absorbance ratios

is on the order of $\pm$ 0.0004 units or better. In this work we have used precise

spectrophotometric pH measurement procedures to accurately determine $^{11\text{-}10}K_B$ from

differences in the dissociation constants of $^{11}B(OH)_3$ and $^{10}B(OH)_3$ (Byrne et al.,

2006).

2.2   Methods

2.2.1   *Theory*

Measurements of $^{11\text{-}10}K_B$ can be obtained through pH observations in

borate/boric acid buffers composed exclusively of ^{11}B on one hand and exclusively

^{10}B on the other. The pH of solutions containing $B(OH)_3^0$ and $B(OH)_4^-$ can be written

as:

$$pH = pK_B^* + \log\left(\frac{[B(OH)_4^-]}{[B(OH)_3^0]}\right) \tag{2.4}$$

where pH = -log [H$^+$], pK$_B^*$ = -log K$_B^*$, K$_B^*$ is an equilibrium constant appropriate to

equation (2.1) and square brackets denote total concentrations of $B(OH)_3^0$ and

$B(OH)_4^-$ in all forms (e.g., free $B(OH)_4^-$ plus ion pairs). The difference between pH

measured in solutions of ^{11}B (^{11}pH) and the pH of solutions containing solely ^{10}B

(^{10}pH) can be written as:

$$^{11}pH - {}^{10}pH = p^{11}K_B^* - p^{10}K_B^* + \log\left(\frac{\left[{}^{11}B(OH)_3^0\right]\cdot\left[{}^{10}B(OH)_4^-\right]}{\left[{}^{10}B(OH)_3^0\right]\cdot\left[{}^{11}B(OH)_4^-\right]}\right) \tag{2.5}$$

where

$$p^{11}K_B^* - p^{10}K_B^* = \log\left(^{11-10}K_B\right) \tag{2.6}$$

In the case that the ^{11}B and ^{10}B buffers are prepared using identical procedures, and buffering by H^+ exchange couples other than $B(OH)_3^0$ and $B(OH)_4^-$ are negligible, the $[^{11}B(OH)_3^0]/[^{11}B(OH)_4^-]$ and $[^{10}B(OH)_3^0]/[^{10}B(OH)_4^-]$ ratios in (Equation 2.5) are identical. In this case, the final term in equation 2.5 is $\log(1) = 0$ and the equation can be written as:

$$\Delta pH = {}^{11}pH - {}^{10}pH = \log\left(^{11-10}K_B\right) \tag{2.7}$$

Equation (2.7) shows that $^{11-10}K_B$ is measured as a small difference in pH between two solutions, one composed using ^{11}B, and the other composed using ^{10}B. As such, highly precise pH measurements are required. Very precise measurements of pH can be obtained via spectrophotometric analysis of indicator absorbance ratios R in the following form (Byrne, 1987; Zhang and Byrne, 1996; Byrne et al., 2006):

$$pH = pK_I + \log\left(\frac{R - e_1}{e_2 - R \cdot e_3}\right) \tag{2.8}$$

where pK_I quantifies the equilibrium characteristics of H^+ exchange between protonated and unprotonated forms of thymol blue, and e_1, e_2 and e_3 are constants that are dependent on the molar absorbance vs. wavelength characteristics of fully protonated (intense yellow color) and fully unprotonated (intense blue color) forms of thymol blue. The physical/chemical characteristics of the various terms in equation (2.8) are presented in (Zhang and Byrne, 1996).

For solutions at constant temperature, ionic strength and composition, pK_I is constant and equations (2.7) and (2.8) can be combined in the following form:

$$\Delta pH = \log\left(^{11-10}K_B\right) = \log\left(\frac{^{11}R - e_1}{e_2 - ^{11}R \cdot e_3}\right) - \log\left(\frac{^{10}R - e_1}{e_2 - ^{10}R \cdot e_3}\right) \qquad (2.9)$$

Equation (2.9) shows that $^{11-10}K_B$ can be measured solely through observations of thymol blue absorbance ratios:

$$R = \frac{_{596}A}{_{435}A} \qquad (2.10)$$

where $_{596}A$ and $_{435}A$ are absorbances at 596 and 435 nanometers measured in buffered solutions that contain the thymol blue indicator.

A rigorous treatment of $^{11-10}K_B$ determinations in solutions buffered not only by $B(OH)_3{}^0/B(OH)_4{}^-$ but also by hydrolysis ($H_2O \leftrightarrow H^+ + OH^-$) and H^+ exchange by the spectrophotometric indicator ($I^{2-} + H^+ \leftrightarrow HI^-$) is given by (Byrne et al., 2006). Including the influence of hydrolysis and several micromolar concentrations of indicator, it can be shown (Byrne et al., 2006) that

$$\log\left(^{11-10}K_B\right) = \log\left(\frac{^{11}R - e_1}{e_2 - ^{11}Re_3}\right) - \log\left(\frac{^{10}R - e_1}{e_2 - ^{10}Re_3}\right) - \log\left(\frac{^{11}x}{^{10}x}\right) \qquad (2.11)$$

where

$$x = \frac{\left[Na^+\right] + \left[H^+\right] - K_w\left[H^+\right]^{-1} - \left[I^{2-}\right] - I_T}{B_T - \left[Na^+\right] - \left[H^+\right] + K_w\left[H^+\right]^{-1} + \left[I^{2-}\right] + I_T} \qquad (2.12)$$

Within equation (2.12), B_T is the total boron concentration; $[Na^+]$ is the solution concentration of Na^+ that is added as both NaOH and the sodium form of thymol blue; I_T is a total indicator concentration, and the concentration of unprotonated indicator ($[I^{2-}]$) is calculated using the thymol blue equilibrium characteristics determined by (Zhang and Byrne, 1996).

The final term in equation (2.11) is insignificant if $[Na^+] >> ([H^+] - K_w[H^+]^{-1} -$

$[I^{2-}] - I_T)$ and $(B_T-[Na^+]) >> (-[H^+] + K_w[H^+]^{-1} + [I^{2-}] + I_T)$. Under our experimental

conditions, wherein $[Na^+]$ ranges between 0.004 and 0.02 mol kg^{-1} H$_2$O, and $(B_T -$

$[Na^+])$ ranges between 0.006 and 0.03 mol kg^{-1} H$_2$O, pH $\approx$ 8.6, $I_T \approx$ 3 x 10^{-6} mol kg^{-1}

H$_2$O and ΔpH $\leq$ 0.03, the term log (^{11}x/^{10}x) is smaller than 0.0001 and can be

neglected in calculations of $^{11-10}$K$_B$.

2.2.2   Sample preparation and materials

2.2.2.1   Sample solutions

Boron is one of the major constituents of natural seawater and has a

concentration of 4.4 * 10^{-4} mol kg^{-1} H$_2$O at a ~34.8 salinity (Byrne and Kester, 1974).

The spectrophotometric measurements in (Byrne et al., 2006) were obtained at a total

boron concentration of 0.05 mol kg^{-1} H$_2$O, which is significantly higher than the

concentration of boron in natural seawater. To investigate the potential significance of

polyborate formation on the $^{11-10}$K$_B$ determinations, experiments were conducted at a

range of total boron concentrations, including: 0.01, 0.025 and 0.05 mol kg^{-1} H$_2$O.

Insofar as the activity quotient for the reaction (2) is very close to unity, the

value for the isotope exchange in this reaction ($^{11-10}$K$_B$) should be applicable over a

wide range of solution compositions and ionic strengths (Byrne et al., 2006). To

evaluate this contention, experiments were conducted in three different synthetic

solutions: "pure water", 0.6 mol kg^{-1} H$_2$O KCl and synthetic seawater. To assess the

effects of temperature on $^{11-10}K_B$, experiments in "pure water", 0.6 mol kg^{-1} H$_2$O KCl and seawater were performed at 25 and 40°C.

Equimolal ^{10}B(OH)$_3$ and ^{11}B(OH)$_3$ in "pure water" were prepared by weight in 15 MΩ Milli-Q water. Approximately 25 grams (± 0.0005 1 s.d.) of each solution were then weighed into 10 cm spectrophotometric cells. Equal amounts of 1.0 M NaOH approximately 0.5 gram (± 0.0001 1 s.d.), were then added (by weight) to each cell. These procedures resulted in two solutions that were equimolal in Na$^+$, and whose concentrations of ^{10}B and ^{11}B were identical. For all "pure water" solutions, $B_T \approx 0.05$ mol kg^{-1} H$_2$O, [Na$^+$] ≈ 0.02 mol kg^{-1} H$_2$O, and pH ≈ 8.6. In each experiment usually four to six sample cells (n = 4-6) were prepared for both isotopically labeled solutions. Upon preparation each sample cell was promptly transferred from the scale into a custom designed thermostated cell holder, where the cells were left to thermally equilibrate for at least 45 minutes.

A second set of solutions was prepared in 0.6 mol kg^{-1} H$_2$O KCl medium, resulting in an ionic strength close of that of natural seawater. A single batch of 0.6 mol kg^{-1} H$_2$O KCl was prepared by weight in 15 MΩ Milli-Q water. Similar to the procedure using "pure water", equimolal ^{10}B(OH)$_3$ and ^{11}B(OH)$_3$ solutions were prepared by gravimetric addition of boric acid and 1.0 M NaOH to the 0.6 mol kg^{-1} H$_2$O KCl solution. For the 0.6 mol kg^{-1} H$_2$O KCl solutions, $B_T \approx 0.01, 0.025$ and 0.05 mol kg^{-1} H$_2$O.

Synthetic seawater was prepared using a standard recipe (Dickson and Goyet, 1994) and had an ionic strength of 0.70 mol kg^{-1} H$_2$O and salinity of ~35. The only boron in this solution, as well as the solutions prepared using "pure water" and 0.6

mol kg^{-1} H$_2$O KCl, came from the isotopically labeled boric acid. A single batch of synthetic seawater was prepared by adding seawater constituent salts (NaCl, KCl, Na$_2$SO$_4$, CaCl$_2$, MgCl$_2$) by weight to 15 MΩ Milli-Q water. The preparation of equimolal ^{10}B(OH)$_3$ and ^{11}B(OH)$_3$ solutions in seawater was identical to the procedures used for "pure water" and 0.6 mol kg^{-1} H$_2$O KCl. For the synthetic seawater, B$_T$ ≈ 0.01 and 0.05 mol kg^{-1} H$_2$O.

2.2.2.2   *Materials*

Experimental reagents including boric acid as ^{10}B(OH)$_3$ and ^{11}B(OH)$_3$ (99+ atom % pure ^{10}B and ^{11}B respectively, 99.95% by weight boric acid), 1.0 M NaOH, and the pH indicator thymol blue, were obtained from Sigma-Aldrich. The boric acid and KCl were stored in a desiccator containing P$_2$O$_5$ for three days prior to use. Salts used in this work (NaCl, KCl, Na$_2$SO$_4$, CaCl$_2$, MgCl$_2$) were analytical grade reagents also obtained from Sigma-Aldrich. We calculate that a 1% isotopic impurity of the ^{10}B and ^{11}B labeled boric acids would result in a pH uncertainty of around 0.0001 units. Given 0.05% neutral impurity of the labeled boric acids we calculate an additional uncertainty of 0.00036 pH units. Either of these uncertainties are less than our analytical precision.

2.2.3   *Instrumental procedures*

Absorbance measurements for determination of pH in ^{10}B(OH)$_3$^{0}/^{10}B(OH)$_4$$^-$ and ^{11}B(OH)$_3$^{0}/^{11}B(OH)$_4$$^-$ buffers prepared as described above were obtained using an HP 8453 and CARY 400 Bio UV-Vis spectrophotometers. Both instruments are

41

equipped with water-jacketed sample cell holders, which were thermostated at 25 or 40°C within ± 0.1°C and maintained with a Neslab refrigerating circulator. First, the sample was transferred to the instrument cell holder for a blank absorbance measurement. Then, indicator was added to the sample for simultaneous measurements of absorbances ($_\lambda A$) at wavelength λ = 730, 596 and 435 nm. When calculating the absorbance ratio R (Eq. 2.10) the absorbance measurement at 730 nm ($_{730}A$) was subtracted from $_{596}A$ and $_{435}A$ as means of compensating for possible baseline shifts:

$$R = \frac{_{596}A - _{730}A}{_{435}A - _{730}A}$$
(2.13)

2.2.4 Data analysis

For each of the experimental conditions described above (various B_T, temperature and medium composition) four to six samples were prepared for each isotope. For example, in seawater experiments (B_T = 0.01 mol kg^{-1} H$_2$O, at 25°C), each sample was analyzed at least five times, producing a maximal instrumental error of ± 0.0004 (1 s.d.). For n = 5 (number of samples of each isotope) there were five values of ΔpH calculated using Eq.(2.9) by pairing the mixtures. The grand mean ΔpH of these five values was 0.0117 ± 0.0003 (1 s.d.). Instrumental contributions to uncertainties were only ± 0.0001 (1 s.d.). Therefore, the larger uncertainty associated with the grand mean ΔpH was chosen as an upper bound uncertainty estimate. The standard error of the mean with 95% confidence interval ($2\sigma_m$) was determined as:

$$2\sigma_m = \frac{2 \cdot 1 \text{s.d.}}{\sqrt{n}} \qquad (2.14)$$

where n = number of samples for each isotope or number of pairs.

$^{11\text{-}10}K_B$ was calculated using Eq.(2.9) and the uncertainty ($2\sigma_m$) associated with the grand mean ΔpH was propagated as:

$$2\sigma_m{}' = 2.302 \cdot \left(^{11\text{-}10}K_B\right) \cdot 2\sigma_m \qquad (2.15)$$

The results from multiple experiments conducted under identical experimental conditions were combined in a weighted mean with the individual uncertainties incorporated into a weighted error as (Bevington and Robinson, 2003):

$$\text{weighted mean} = \Sigma \frac{\overline{x}}{\left(2\sigma_m{}'\right)^2} \Bigg/ \Sigma \frac{1}{\left(2\sigma_m{}'\right)^2} \qquad (2.16)$$

$$\text{variation on mean} = \sqrt{\frac{1}{\Sigma \dfrac{1}{\left(2\sigma_m{}'\right)^2}}} \qquad (2.17)$$

where $\overline{x}$ are $^{11\text{-}10}K_B$ values obtained in each of the multiple experiments under identical experimental conditions and $2\sigma_m{}'$ - are uncertainties associated with each $^{11\text{-}10}K_B$.

Table 2.2 – $^{11\text{-}10}K_B$ determined for three different media at 25 and 40°C.

Media	T°C	[H₃BO₃], (mol kg⁻¹ H₂O)	Ionic strength (mol kg⁻¹ H₂O)	Instrument	ΔpH = ^{11}pH − ^{10}pH	2σ$_m$	$^{11\text{-}10}K_B$	2σ$_m$´	n	Weighted mean of N experiments	2σ$_m$ of weighted mean	N
Pure water	25	0.05	~0.02	HP 8453	0.0132	0.0010	1.0308	0.0023	6			
	40	0.05	~0.02	HP 8453	0.0124	0.0020	1.0289	0.0048	6			
KCl (0.6 mol kg⁻¹ H₂O)	25	0.01	~0.60	CARY 400*	0.0109	0.0006	1.0254	0.0014	4			
	25	0.025	~0.61	CARY 400*	0.0107	0.0003	1.0249	0.0008	5	1.0251	0.0007	2
	25	0.025	~0.61	CARY 400*	0.0109	0.0005	1.0253	0.0011	5			
	25	0.05	~0.62	CARY 400*	0.0104	0.0004	1.0242	0.0009	5	1.0250	0.0005	4
	25	0.05	~0.62	CARY 400*	0.0104	0.0003	1.0241	0.0008	4			
	25	0.05	~0.62	CARY 400*	0.0115	0.0004	1.0268	0.0011	5			
	25	0.05	~0.62	HP 8453	0.0116	0.0007	1.0271	0.0017	6			
	40	0.05	~0.62	HP 8453	0.0112	0.0015	1.0262	0.0035	6			
Seawater	25	0.01	~0.72	CARY 400*	0.0117	0.0002	1.0272	0.0006	5			
	25	0.05	~0.74	CARY 400*	0.0110	0.0005	1.0257	0.0012	4	1.0272	0.0003	3
	25	0.05	~0.74	CARY 400*	0.0117	0.0001	1.0273	0.0003	4			
	25	0.05	~0.74	HP 8453	0.0116	0.0008	1.0270	0.0019	6			
	40	0.05	~0.74	HP 8453	0.0115	0.0011	1.0269	0.0027	6			

*CARY 400 Bio UV-Vis double-beam spectrophotometer

2.3   Results

$^{11\text{-}10}K_B$ results obtained over a wide range of medium composition, total boron

concentrations (B_T = 0.01, 0.025, 0.05 mol kg^{-1} H$_2$O) and 25-40°C temperature range

were quite coherent (Table 2.2 and Figure2.1). Spectroscopic measurements in "pure

water" media (B_T = 0.05 mol kg^{-1} H$_2$O) yielded $^{11\text{-}10}K_B$ values of 1.0308 ± 0.0023 and

1.0289 ± 0.0048 at 25 and 40°C, respectively. $^{11\text{-}10}K_B$ values in 0.6 mol kg^{-1} H$_2$O KCl

with identical B_T at these two temperatures were 1.0250 ± 0.0005 and 1.0262 ±

0.0035. Finally, $^{11\text{-}10}K_B$ values in synthetic seawater (B_T = 0.05 mol kg^{-1} H$_2$O) were

1.0272 ± 0.0003 and 1.0269 ± 0.0027 at 25 and 40°C, respectively. Higher errors

were observed for measurements at 40°C than for the measurements at 25°C,

especially for the "pure" water solutions. Within the experimental uncertainties, our

$^{11\text{-}10}K_B$ results show no temperature dependence within the range 25-40°C. However,

considering only the 25°C analyses, there is a statistical difference between $^{11\text{-}10}K_B$

values obtained in "pure water" solution and at higher ionic strength. It should also

be noted that the measurement uncertainties obtained using CARY 400 double-beam

instrument were much smaller than those obtained using HP 8453.

$^{11\text{-}10}K_B$ results obtained in 0.6 mol kg^{-1} H$_2$O KCl and artificial seawater are

very similar (Table 2.2 and Figure 2.1). Since approximately 44% of the total borate

in seawater is ion paired with Na$^+$, Ca^{2+} and Mg^{2+} (Byrne and Kester, 1974), it can be

concluded that the relatively weak ion paring of borate with major seawater cations

has a negligible influence on $^{11\text{-}10}K_B$. Furthermore, the excellent agreement in $^{11\text{-}10}K_B$

results obtained using total boron concentration between 0.01 and 0.05 mol kg^{-1} H$_2$O
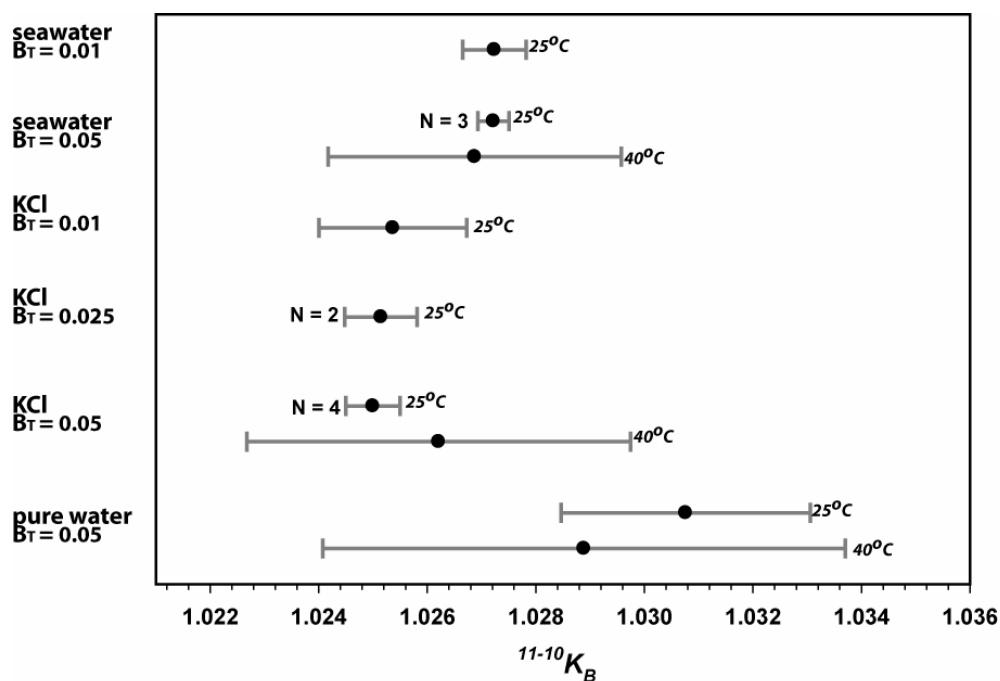
Figure 2.1 – Boron isotope equilibrium constant ($^{11\text{-}10}K_B$) determined in "pure water", 0.6 mol kg^{-1} H$_2$O KCl and seawater (S = 35) over a range of total boron concentrations (B$_T$ ≈ 0.01, 0.025 and 0.05 mol kg^{-1} H$_2$O) and two temperatures (25, and 40°C). The error bars represent 95% confidence interval ($\pm\ 2\sigma_m'$ – standard error of a mean) of the analyses within each experiment. The results of multiple experiments (N > 1) conducted under the same experimental conditions are presented as weighted mean of these results with the associated weighted uncertainty of the mean ($\pm\ 2\sigma_m$).

indicates that polyborate formation has a negligible influence on the equilibrium results obtained in this work. In a recent publication (Byrne et al., 2006) it was pointed out that experiments conducted over a range of boron concentrations would allow extrapolation of $^{11-10}K_B$ results to values appropriate at the natural boron levels of seawater (416 micromoles/kg seawater). This appears to be unnecessary because there is no statistically discernable trend in $^{11-10}K_B$ results over a substantial range of boron concentrations. The likely mechanism behind this constancy in $^{11-10}K_B$ is seen in the observation (Oi, 2000b) that boron fractionations into the four coordinate sites of $B(OH)_4^-$ and $B_3O_3(OH)_4^-$ are very similar (Byrne et al., 2006).

2.4   Discussion

Of greatest interest to oceanic pH reconstructions, the $^{11-10}K_B$ result for artificial seawater [$^{11-10}K_B = 1.0272 \pm 0.0006 \ (2\sigma_m')$ at 25°C ($B_T = 0.01$ mol kg^{-1} H_2O)] is significantly larger than the 1977 estimate of 1.0194 (Kakihana and Kotaka, 1977; Kakihana et al., 1977) and the spectral and the force field modeling estimate of 1.0176 (Sanchez-Valle et al., 2005). On the other hand, our empirical result is in agreement with the recent *ab initio* calculations (Oi, 2000a; Oi and Yanase, 2001; Liu and Tossell, 2005), which indicate $^{11-10}K_B$ values between 1.0260 to 1.0267.

The relationship between pH and boron isotopic composition of borate in seawater ($\delta^{11}B_{borate}$), given $pK_B = 8.597$ at 25°C (Dickson, 1990), $^{11-10}K_B$ as either 1.0272 ± 0.0006 (this study) or 1.0194 (Kakihana and Kotaka, 1977; Kakihana et al., 1977) and boron isotopic composition of seawater ($\delta^{11}B_{sw} = 39.5$‰) can be summarized as:

$$pH = pK_B - \log\left(\frac{\delta^{11}B_{sw} - \delta^{11}B_{borate}}{\delta^{11}B_{sw} - {}^{11-10}K_B \delta^{11}B_{borate} - 1000 \times ({}^{11-10}K_B - 1)}\right) \qquad (2.18)$$

The experimental ${}^{11\text{-}10}K_B$ value obtained in this work results in a calculated relationship between $\delta^{11}B_{borate}$ and pH, that lies below than the curve based on the previous theoretical estimate (Figure 2.2). It is important to recognize that both curves intend to display the boron isotopic composition of borate species ($B(OH)_4^-$) in seawater, not the carbonate minerals that serve as a proxy for seawater isotopic compositions.

Calibrations of the $\delta^{11}B$ of carbonate materials vs. pH have been conducted using controlled experiments with inorganic calcite precipitates and both coral and foraminifera species grown under constant pH conditions in modified seawater solutions (Sanyal et al., 1996; Sanyal et al., 2000; Sanyal et al., 2001; Hönisch et al., 2004). While the coral analyses appear to conform to the Kakihana et al. reference curve – calculated using the most widely accepted pK_B value of 8.597 (Dickson, 1990) – it is noteworthy that both foraminiferal and inorganic carbonates had $\delta^{11}B$ values that fell significantly below the theoretical constraint for $B(OH)_4^-$. It has been argued (Hönisch and Hemming, 2004) that because these calibration measurements broadly mirror the "shape" of the Kakihana et al. curve, a constant offset at different pH may be used to correct for each of the studied species. In contrast, the borate-pH curve produced from ${}^{11\text{-}10}K_B$ obtained in this study (1.0272 ± 0.0006) fits best with the data from the controlled *O.universa* measurements (Sanyal et al., 1996), but the slope of this curve is steeper over the studied pH range, and hence does not as
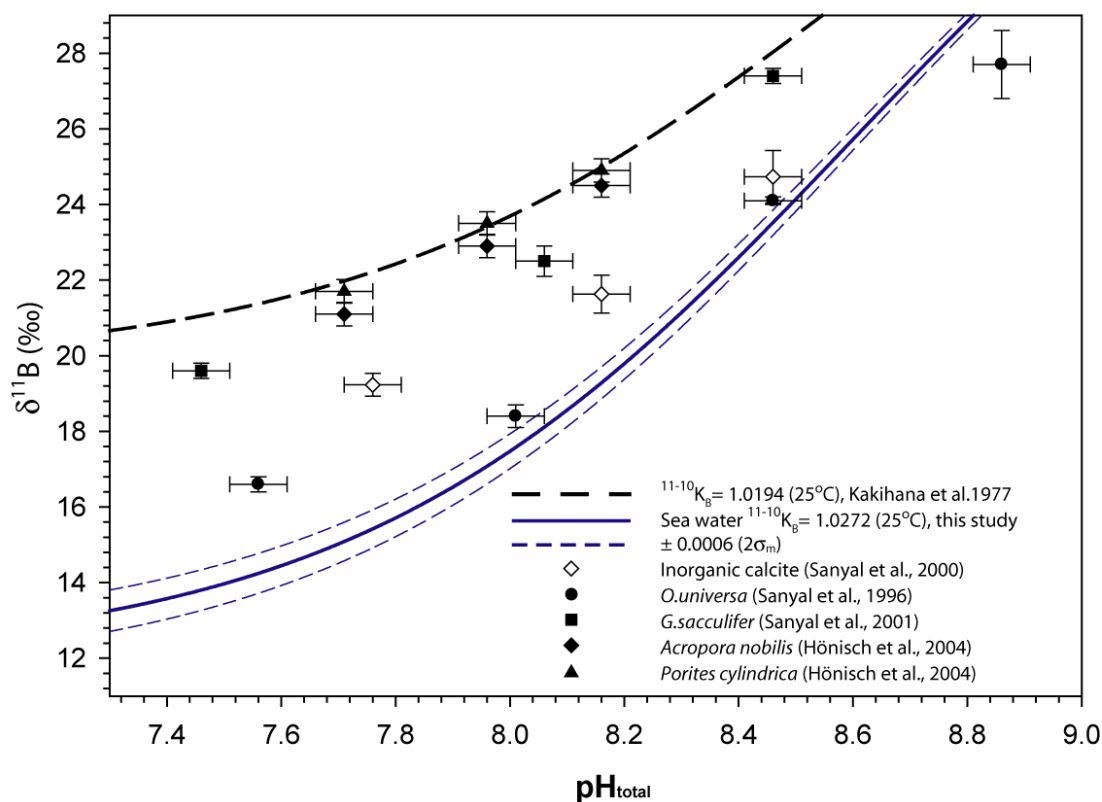
Figure 2.2 – $\delta^{11}B$ of $B(OH)_4^-$ in seawater based on theoretical $^{11-10}K_B = 1.0194$ (Kakihana and Kotaka, 1977; Kakihana et al., 1977) and empirical $^{11-10}K_B = 1.0272 \pm 0.0006$ ($2\sigma_m'$, n=5) obtained in this study at 25°C ($B_T \approx 0.01$ mol kg^{-1} H$_2$O); and the results of the inorganic calcite precipitation experiments (Sanyal et al., 2000), cultured *O.universa* and *G.sacculifer* foraminifera species (Sanyal et al., 1996; Sanyal et al., 2001) and cultured scleractinian corals *Acropora nobilis* and *Porites cylindrica* (Hönisch et al., 2004). The pH$_{NBS}$ values from (Sanyal et al., 1996; Sanyal et al., 2000; Sanyal et al., 2001) were recalculated to fit the seawater pH scale (pH$_{SWS}$= pH$_{NBS}$ − 0.14).

faithfully mirror the control data. Slight differences in pK_B values are shown to have a profound effect on the slope of these curves (Liu and Tossell, 2005) with higher values reversing the orientation of the two calculated slopes, such that our empirical $^{11-10}K_B$ constraint would better mirror the control data. It is evident that the controls on the boron isotopic composition of marine carbonates are more complex than suggested by simple isotope exchange equilibrium reactions. In this regard both vital effects and the chemistry of seawater at the site of carbonate formation warrant further investigation.

Boron isotope redistribution during biosynthesis of carbonate is possible given the requirement that marine calcifiers modify seawater in order to concentrate carbonate ion and maintain saturation at the site of calcification (Erez, 2003; Weiner and Dove, 2003). Saturation is achieved by seawater vacuolization and modification within the cytoplasm, which elevates both pH and alkalinity. In foraminifera photosynthesis plays a critical role in elevating the pH through the uptake of vacuole CO_2 (Erez, 2003), while in corals endergonic enzymatic reactions that exchange protons for Ca^{2+} result in higher pH at the site of calcification (Allemand et al., 1998; Cohen and McConnaughey, 2003). Micro-sensor studies indicate that the pH of the calcifying fluid in the foraminifera *G.sacculifer* rises to as high as 8.6 in daylight (Jorgensen et al., 1985) relative to ambient seawater (pH = 8.2). Similarly, pH in the symbiotic coral *Galaxea* rises from 8.2 to 8.5 at the polyp surface and further to 9.3 in the calcifying fluid (Al-Horani et al., 2003). It is not known whether boron is delivered to the calcifying site in the form of neutral $B(OH)_3^0$ or charged $B(OH)_4^-$. If the neutral species are more likely to pass through to the calcifying site, then ^{11}B

enriched borate would form from the heavier boric acid via re-equilibration due to higher pH of the site. Thus, elevated pH in these biogenically modified solutions would drive both chemical and isotopic equilibrium resulting in ^{11}B enrichment of borate ion by as much as 4-5‰.

Mineralogic differences between marine calcifiers may also play an important role in boron isotope distributions. While it has been concluded that the main boron-bearing species incorporated into the carbonate lattice of aragonite is the borate ion, with no observed fractionation (Sen et al., 1994; Hemming et al., 1995), in calcite up to 90% of the incorporated species may be boric acid (Sen et al., 1994), which could result in heavier boron isotopic composition of calcite relative to aragonite provided no other processes are involved (e.g. biological).

Both biological and mineralogical effects would appear to result in enrichments of the heavy isotope in carbonates, which is consistent with the larger value of the boron isotope equilibrium constant empirically determined in this study (Figure 2.2). Thus we presently find no logical basis for offset corrections to lower measured δ^{11}B values in marine carbonates, based on the use of the 1977 equilibrium constant.

For the time being, while relative time series changes in pH are valid (Hönisch and Hemming, 2005; Pelejero et al., 2005), obtaining absolute values for paleo-pH using the carbonate proxy remains a challenge. Existing calibrations (Sanyal et al., 1996; Sanyal et al., 2000; Sanyal et al., 2001; Hönisch et al., 2004) are useful but limited to only two species of foraminifera (*G.sacculifer* and *O.universa*) and two species of relatively fast-growing branching corals (*Acropora nobilis* and *Porites*

cylindrica). Notably, massive corals (e.g. *Porites lutea*) with much slower growth rate are more widely used in paleo-reconstructions and should be the focus of new culture experiments. In our view, progress towards the use of carbonates as absolute pH proxies will require additional controlled culture and micro-sensor studies of pertinent species and better understanding of boron speciation at the site of calcification with respect to boron transport and incorporation into the crystal lattice. Empirical and culture experiments are the key to a better understanding of past changes in oceanic pH, but they will also be critical in charting the course of anthropogenic effects on oceanic pH and marine ecosystems through the next century.

CHAPTER 3 - THE EFFECTS OF BORATE POLYMERIZATION, TEMPERATURE AND ION PAIRING ON BORON ISOTOPE FRACTIONATION IN SOLUTION

3.1   Introduction

The boron isotope compositions of various biogenic and inorganic oceanic carbonates have been used to decipher paleo-pH in a variety of environmental settings including: abyssal oceans using benthic foraminifera (Hönisch et al., 2008), surface oceans during Pleistocene glacial/interglacial cycles using planktonic foraminifera (Palmer and Pearson, 2003), and shallow marine carbonate platforms in the aftermath of Neoproterozoic glaciation using inorganic carbonate precipitates (Kasemann et al., 2005). The accurate application of the boron isotope system for paleo-pH reconstructions, however, requires an understanding of the range of environmental conditions represented by each sedimentary deposit, as the boron isotope equilibrium ($^{11\text{-}10}K_B$) and boric acid dissociation (pK_B^*) constants largely depend on the temperature, total boron concentration, salinity and even the specific ocean chemistry of differing environments.

An evaluation of the temperature effect on $^{11\text{-}10}K_B$ is important, as fluctuations in surface temperature across Earth history have been significant. For example, during the Last Glacial Maximum in the Pleistocene (ca. 18,000 years ago) surface ocean temperatures are believed to have been $\sim 5^oC$ lower than today; in contrast, during glacial minimum temperatures may have been $\sim 3^oC$ higher than today (Sigman and Boyle, 2000). While significant, Pleistocene temperature fluctuations

fade in comparison with those of the Neoproterozoic, when temperatures fluctuations of 50°C or more may have been recorded between icehouse (i.e. Snowball Earth) and hothouse periods (Hoffman et al., 1998). Finally, in the deep sea, where benthic foraminifera used for paleo-pH reconstructions dwell and calcify, average temperatures could dip to 1°C (Hönisch et al., 2008).

Ion pairing of borate ion with major ions in seawater, including Mg^{2+}, Ca^{2+} and Na^{+} may also affect boron isotope distributions in marine carbonates. The major ion composition of the oceans is noted to have varied over the geologic past (Sandberg, 1983; Hardie, 1996; Stanley and Hardie, 1998; Berner, 2004). In particular, the ratio of Mg/Ca is thought to have varied from ~ 1 to ~5 over the past 560 million years based on the dominant mineralogy of the shallow marine carbonates (Wilkinson and Algeo, 1989). Throughout the Phanerozoic, it appears that the oceans have recorded secular oscillations in carbonate mineralogy marked by shifts in Mg/Ca ratios. High Mg/Ca ~ 5 is associated with "aragonitic" seas (from ~340 to ~170 Ma and in the Modern); and low Mg/Ca ~ 1 is associated with "calcitic" seas (~550-340 Ma and ~170-40 Ma) (Stanley and Hardie, 1998). These shifts are believed to be controlled by the changes in spreading rates along mid-ocean ridges (Stanley and Hardie, 1998).

Changes in Mg^{2+} content of seawater may also be controlled by the extent of marine dolomitization (formation of $Ca,Mg(CO_3)_2$ from a $CaCO_3$ precursor by replacing Ca^{2+} with Mg^{2+}) (Wilkinson and Algeo, 1989). Insofar as dolomitization is believed to require significant environmental modifications of seawater (including high Mg/Ca > 8, high temperature, low salinity (i.e. dielectric constant), and the

absence of sulfate (Prothero and Schwab, 2003), boron isotope studies may provide clues to the origin and distribution of this mineral trough time. To this end, it will be important to investigate how changes in Mg^{2+} concentrations, temperature and salinity in modified seawater may affect $^{11-10}K_B$ and subsequently the boron isotope distributions in solution.

Similarly, temporal variations in total boron concentration (B_T) in the oceans may have had an effect on boron isotope fractionation through polymerization of borate into dimer, trimer and tetramer forms. In the present-day ocean B_T is estimated to be 0.4 mmol/kg H_2O (Byrne and Kester, 1974), and this did not likely change much during maximum Pleistocene glaciation. Even at the extreme during Neoproterozoic "Snowball Earth" events when sea level may have dropped by 1 km or more (Hoffman et al., 1998), B_T is estimated to have reached ~0.56 mmol/kg H_2O, assuming present-day boron sources and sinks in the ocean. Unless boron fluxes into past oceans were vastly different from today, it is unlikely that natural variations in total boron concentration have been significant. Nevertheless, an investigation of the potential effects of the boron concentrations on $^{11-10}K_B$ is necessary with regards to various boron isotope laboratory studies conducted in experimental solutions with boron concentrations significantly exceeding natural concentrations (Sanyal et al., 1996; Sanyal et al., 2000; Sanyal et al., 2001; Hönisch et al., 2004; Byrne et al., 2006; Klochko et al., 2006).

In the current study, we systematically evaluate the effects of various degrees of borate polymerization, temperature and ion pairing on the boron isotope

fractionation constant ($^{11-10}K_B$) between boric acid [B(OH)$_3^o$] and borate ions

[B(OH)$_4^-$] in aqueous solution, which is expressed by the reaction:

$$^{10}B(OH)_3^o + {}^{11}B(OH)_4^- \Leftrightarrow {}^{11}B(OH)_3^o + {}^{10}B(OH)_4^- \qquad (3.1)$$
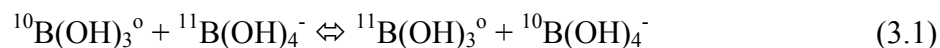
These experimental constraints should provide insight into the boron isotopic

compositions of ancient biogenic and inorganic carbonates that may have

accumulated under radically different environmental conditions than those in the

modern oceans.

3.1.1 Total boron concentration

In our previous experiments $^{11-10}K_B$ determinations were carried out in

solutions with total boron concentrations (B$_T$ = 0.01, 0.025 and 0.05 mol/kg H$_2$O),

which significantly exceeded those of natural seawater (B$_T$ = 4.4 x 10^{-4} mol/kg H$_2$O).

In dilute solutions like modern seawater and our experimental solution with B$_T$ = 0.01

mol/kg H$_2$O, dissolved boron is represented by only mononuclear species including:

boric acid [B(OH)$_3^o$] and borate ions [B(OH)$_4^-$] (Fig. 3.1a). However, boron

polynuclear complexes begin to form at concentrations B$_T$ > 0.025 mol/kg H$_2$O

(Ingri, 1963; Cotton and Wilkinson, 1972). Since the degree of boron polymerization

may potentially affect the $^{11-10}K_B$ in our most concentrated experiments, we

concluded that it is important to investigate this issue further. According to Baes and

Mesmer (1976), at high concentrations > 0.025 mol/kg H$_2$O the boron in solution is

represented by the mononuclear species B(OH)$_3^o$ and B(OH)$_4^-$, as well as

polynuclear species B$_2$O(OH)$_5^-$, B$_3$O$_3$(OH)$_4^-$ and B$_4$O$_5$(OH)$_4^{2-}$.
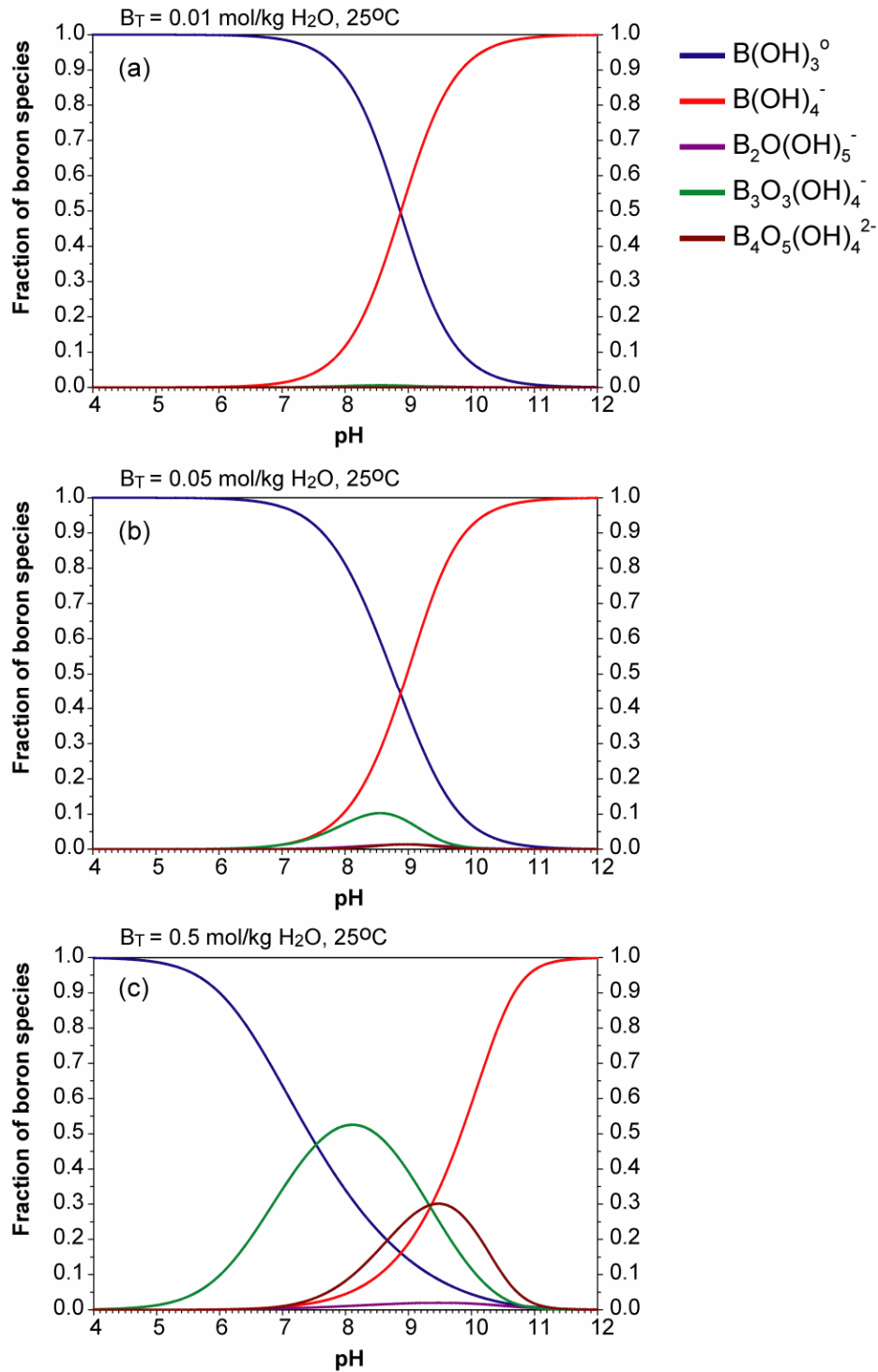
Figure 3.1 – Distribution of boron species in 1 mol/kg H_2O KCl medium at 25^oC and total boron concentrations (B_T): (a) B_T = 0.01 mol/kg H_2O; (b) B_T = 0.05 mol/kg H_2O; and (c) B_T = 0.5 mol/kg H_2O. Graphs are reconstructed using equilibrium quotients and constants determined for the "NBS" acidity scale and reported in Baes and Mesmer (1976).

The relative abundances of these species depend on total boron concentration, temperature and pH of a given solution (Ingri, 1963). Most studies (Ingri, 1963; Baes and Mesmer, 1976; Hirao et al., 1979) agree that the trimer $[B_3O_3(OH)_4^-]$ is the most dominant of the polynuclear complexes across the pH range between ~4 and 9.5. For example, the polyborate equilibrium data determined from a 1 mol/kg H_2O KCl solution at 25^oC (Baes and Mesmer, 1976) suggests that polyborates account for ~12% of total borate at $B_T = 0.05$ mol/kg H_2O, which is the highest concentration in our experiments (Chapter 2; Klochko et al., 2006). The approximate concentrations of each boron species is calculated as a function of pH by using the equilibrium quotients and constants reported in Baes and Mesmer (1976). At pH ~ 8.6, the trimer $[B_3O_3(OH)_4^-]$, dimer $[B_2O(OH)_5^-]$ and tetramer $[B_4O_5(OH)_4^{2-}]$ represent approximately 10%, 1% and 1% of total boron, respectively (Fig. 3.1b). Since all experimental solutions in our studies had pH ~ 8.3-8.6, it is the trimer that might have the greatest potential effect on the final $^{11-10}K_B$ determined in our experiments. The relevant reaction involving boron isotope exchange between boric acid $[B(OH)_3^o]$ and a polyborate trimer $[B_3O_3(OH)_4^-]$ is:

$$^{10}B(OH)_3^o + {}^{11,11,11}B_3O_3(OH)_4^- \Leftrightarrow {}^{11}B(OH)_3^o + {}^{11,11,10}B_3O_3(OH)_4^- \qquad (3.2)$$

Oi (2000b) have applied *ab-initio* molecular orbital calculations to determine $^{11-10}K_B$ values for the isotope exchange between boric acid and various polyborate species. That study concluded that $^{11-10}K_B = 1.030$ for the reaction (3.2), and $^{11-10}K_B = 1.026$ for reaction (3.1), which indicates that the magnitude of isotope exchange between boric acid and mononuclear borate; as well as that between boric acid and

polyborate trimer are similar, with the small increase in $^{11\text{-}10}K_B$ associated with trimerization.

In Klochko et al. (2006) we demonstrated that the $^{11\text{-}10}K_B$ value remained unchanged over a range of experimental solutions (Fig. 2.1 in Chapter 2) with total boron concentrations from 0.01 mol/kg H_2O (where the presence of the polyborates is negligible) to 0.05 mol/kg H_2O (where the presence of the trimer becomes potentially significant for the isotope exchange). These results suggest that either the formation of the trimer in solution has negligible effect on the resulting $^{11\text{-}10}K_B$ or the concentration of the trimer is too low to have any effect on $^{11\text{-}10}K_B$. Increasing the total boron concentration (e.g. by a factor of 10) in experimental solutions could provide an empirical estimate of the boron isotope exchange constant for the reaction (3.2) and its potential effects on the $^{11\text{-}10}K_B$. At $B_T = 0.5$ mol/kg H_2O, the trimer represents $\sim 50\%$ of the total boron, essentially replacing $B(OH)_4^-$ at pH ~ 8.3 (Fig. 3.1c). Therefore, this concentration should be ideal for our investigation of the potential polyborate effects on $^{11\text{-}10}K_B$.

3.1.2 Temperature effects

The $^{11\text{-}10}K_B$ as a function of temperature has been estimated using *ab-initio* molecular orbital theory calculations (Liu and Tossell, 2005; Tossell, unpublished). The results of these studies vary significantly with various methods of quantum mechanical calculations applied to different models of dissolved boron in solution (Table 3.1).

Table 3.1 – $^{11\text{-}10}K_B$ in seawater as a function of temperature, calculated using various models for the solute and quantum mechanical methods of calculation.

T^{o}C	$^{11\text{-}10}K_B$		
	Hartree-Fock, free monomers[1]	Density function, free monomers[2]	Density function, 22 H$_2$O clusters[3]
0	1.029	1.043	1.026
10	-	1.042	1.017
20	-	1.041	1.025
25	1.027	-	-
30	-	1.040	1.025
40	1.026	1.038	1.023
50	-	1.037	1.023
60	1.024	-	-

[1] data from Liu and Tossell (2005)
[2,3] unpublished data from Tossell

Liu and Tossell (2005) applied the "Hartree-Fock" method of calculation to a boron model represented by only free boron monomers. Their data shows a small linear decrease in $^{11-10}K_B$ values (from 1.029 to 1.024) with increasing temperatures over a wide range of temperature conditions spanning from 0 to 60°C (Table 3.1). Application of a "density function" method of calculations to such "free-boron-monomers" model yields unreasonably high $^{11-10}K_B$ values (1.037-1.043), however, the results reveal a similar temperature dependent trend (Tossell, unpublished). It should be noted that free monomer models only take into account bond energies within the monomer clusters; they ignore the bonds between the monomer cluster and the surrounding H_2O molecules. Including H_2O molecules in the cluster would result in more realistic model of dissolved boron speciation. Tossell (unpublished) used a model of boron monomers surrounded by 22 H_2O molecules for the calculations and obtained reasonable $^{11-10}K_B$ values, although the temperature-dependent trend observed in the previous two datasets is lost (Table 3.1).

The purpose of the current study is to empirically constrain temperature effects on $^{11-10}K_B$ values and to determine whether there are systematic trends in the data that could be extrapolated to higher or lower temperatures. To this end, we have investigated $^{11-10}K_B$ behavior at 40, 25, 15 and 9°C. Lower temperature experiments are not yet possible with the current experimental design.

3.1.3 Ion pairing effects

Borate ion [B(OH)$_4$$^-$], being one of the two species of total boron in seawater, has been known to form complexes with a variety of common ions in seawater (Byrne

and Kester, 1974). The cations most likely to show significant ion-pairing with borate in seawater are Na^+, Mg^{2+} and Ca^{2+}, which are the major constituents in seawater. It is estimated that 44% of the borate ions in seawater are represented by $NaB(OH)_4^o$, $MgB(OH)_4^+$ and $CaB(OH)_4^+$ complexes (Byrne and Kester, 1974). Table 3.2 demonstrates the breakdown of the boron species in seawater at 25^oC, salinity of 35 and pH = 8.2. According to this study, free borate $B(OH)_4^-$ represents only 13.3 % of the total boron in modern seawater. Importantly, the magnesium-bearing complex $MgB(OH)_4^+$ appears to be the next important borate compound, representing 5.1 % of total boron.

As it as been discussed above, Mg^{2+} is one of the main inhibitors of the $CaCO_3$ precipitation. Thus, in order to initiate precipitation of the synthetic $CaCO_3$, a number of previous boron isotope/pH calibration studies (Sanyal et al., 1996; Sanyal et al., 2000; Sanyal et al., 2001) have excluded Mg^{2+} cations from their experimental synthetic seawater solutions. In the absence of Mg^{2+}, borate ion will most likely pair with the other two cations Na^+ and Ca^{2+}, which may affect the magnitude of the boron isotope exchange between $B(OH)_3^o$ and $B(OH)_4^-$ - paired ions in solution.

Due to our present lack of understanding of the effects of ion pairing on boron isotope distribution, it is difficult to predict the potential effects of Mg^{2+} exclusion on the results from the calibration studies. Thus this study is designed to quantify these effects using various media including solutions free of Mg and those prepared with $MgCl_2$, NaCl and KCl.

Table 3.2 – Inorganic boron speciation in seawater at $25^{o}C$, salinity of 35 and pH = 8.2. The speciation is inferred from the association constants for $NaB(OH)_4^{o}$, $MgB(OH)_4^{+}$ and $CaB(OH)_4^{+}$ complexes, determined using the "NBS" pH scale (Byrne and Kester, 1974).

Boron species	Percentage of the total boron
$B(OH)_3^{o}$	76.4 ± 1.0 %
$B(OH)_4^{-}$	13.3 ± 0.6 %
$MgB(OH)_4^{+}$	5.1 ± 0.4 %
$NaB(OH)_4^{o}$	3.6 ± 0.4 %
$CaB(OH)_4^{+}$	1.6 ± 0.2 %

3.2   Methods

Solution preparations, instrumental procedures and data analysis for the spectrophotometric experiments conducted in this study are identical to those outlined in Chapter 2 and in (Byrne et al., 2006; Klochko et al., 2006).

Experimental solutions for the polyborate effects study were prepared in synthetic seawater media with total boron concentrations $B_T = 0.01$ and 0.5 mol/kg H_2O. These solutions were analyzed at 25^oC. It should be noted that all solutions for the experiments with $B_T = 0.01$-0.05 mol/kg H_2O were brought up to a pH ~ 8.6 (close to the boric acid dissociation constant in natural seawater solutions $pK_B^* =$ 8.597) by using 1 M NaOH addition (Chapter 2; Klochko et al., 2006). However, in the case of solutions with $B_T = 0.5$ mol/kg H_2O required addition of a more concentrated 10 M NaOH, which triggered the undesired instant precipitation of $Mg(OH)_2$ and $Ca(OH)_2$ complexes:

$$Mg^{2+} +2OH^- \rightarrow Mg(OH)_2\downarrow \qquad\qquad (3.3)$$

$$Ca^{2+} +2OH^- \rightarrow Ca(OH)_2\downarrow \qquad\qquad (3.4)$$

Reducing the volume of 10 M NaOH addition, and hence, lowering the pH to ~ 8.3, eliminated the unwanted $Mg(OH)_2$ and $Ca(OH)_2$ precipitates.

Experimental solutions for the temperature effect study were prepared in synthetic seawater media with total boron concentrations $B_T = 0.01$ mol/kg H_2O. These solutions were analyzed at three different temperature conditions: 9, 15 and 25^oC.

Finally, experimental solutions for the ion pairing effects study were prepared in four different media: synthetic seawater, Mg-free seawater, 0.7 mol/kg H_2O NaCl

and 0.23 mol/kg H_2O $MgCl_2$ with total boron concentration $B_T = 0.01$ mol/kg H_2O.

These solutions were analyzed at 25^oC.

3.3 Results and Discussion

The results of all three spectrophotometric studies: polyborate, temperature

and ion pairing effects on $^{11\text{-}10}K_B$, are summarized in Table 3.3 and shown graphically

in Figs. 3.2-3.4.

3.3.1 Polyborate effects on $^{11\text{-}10}K_B$

$^{11\text{-}10}K_B$ results obtained in the synthetic seawater solutions at 25^oC with total

boron concentrations $B_T = 0.01$ mol/kg H_2O (the lowest concentration) and $B_T = 0.5$

mol/kg H_2O (the highest concentration) are shown in Fig. 3.2. For comparative

purposes, the $^{11\text{-}10}K_B$ data obtained in the earlier study (Klochko et al., 2006) (i.e. 0.6

mol/kg H_2O KCl solutions with $B_T = 0.01$, 0.025 and 0.05 mol/kg H_2O; and synthetic

seawater with $B_T = 0.05$ mol/kg H_2O) are also included.

As previously discussed, the $^{11\text{-}10}K_B$ value remains statistically the same in

both 0.6 mol/kg H_2O KCl and synthetic seawater media over a range of total boron

concentrations (0.01-0.05 mol/kg H_2O), regardless of the fact that 10% of the total

boron in experimental solutions with $B_T = 0.05$ mol/kg H_2O is represented by the

polyborate trimer $B_3O_3(OH)_4^-$. A 10 fold increase in total boron ($B_T = 0.5$ mol/kg

H_2O) in experimental solutions, however, does appear to have resulted in a statistical

Table 3.3 – $^{11\text{-}10}K_B$ determined for various total boron concentrations, media and temperatures conditions.

Media	T°C	[H₃BO₃] (mol kg⁻¹ H₂O)	ΔpH = ^{11}pH – ^{10}pH	2σ_m	$^{11\text{-}10}K_B$	2σ_m′	n	Weighted mean of N experiments	2σ_m of weighted mean	N
Seawater	25	0.5	0.0123	0.0008	1.0286	0.0019	3			
	25	0.5	0.0133	0.0013	1.0310	0.0030	2	1.0298	0.0011	3
	25	0.5	0.0129	0.0007	1.0302	0.0016	2			
	25	0.01	0.0117	0.0002	1.0272*	0.0006	5			
	25	0.01	0.0114	0.0006	1.0266	0.0014	6	1.0270	0.0005	3
	25	0.01	0.0113	0.0005	1.0263	0.0011	3			
	15	0.01	0.0130	0.0015	1.0304	0.0036	6	1.0306	0.0007	3
	15	0.01	0.0131	0.0003	1.0307	0.0007	3			
	9	0.01	0.0121	0.0008	1.0283	0.0018	2	1.0288	0.0015	3
	9	0.01	0.0128	0.0012	1.0299	0.0028	2			
Mg-free seawater	25	0.01	0.0094	0.0003	1.0218	0.0007	3			
	25	0.01	0.0114	0.0008	1.0265	0.0018	3			
	25	0.01	0.0142	0.0004	1.0332	0.0009	3			
	25	0.01	0.0111	0.0001	1.0260	0.0002	3	1.0261	0.0002	7
	25	0.01	0.0126	0.0005	1.0294	0.0012	3			
	25	0.01	0.0094	0.0004	1.0218	0.0010	3			
	25	0.01	0.0113	0.0001	1.0263	0.0003	3			
NaCl (0.7 mol/kg H₂O)	25	0.01	0.0126	0.0003	1.0295	0.0007	3			
	25	0.01	0.0132	0.0004	1.0308	0.0008	3			
	25	0.01	0.0107	0.0007	1.0249	0.0016	3	1.0296	0.0004	5
	25	0.01	0.0122	0.0005	1.0286	0.0012	3			
	25	0.01	0.0133	0.0005	1.0312	0.0011	3			
MgCl₂ (0.23 mol/kg H₂O)	25	0.01	0.0104	0.0002	1.0242	0.0005	3			
	25	0.01	0.0114	0.0003	1.0265	0.0007	3	1.0270	0.0003	4
	25	0.01	0.0128	0.0006	1.0299	0.0014	3			
	25	0.01	0.0127	0.0002	1.0297	0.0005	3			

*data from Klochko et al. (2006)

increase of the $^{11\text{-}10}K_B$ to a value of 1.0298 ± 0.0011 ($2\sigma_m$), relative to the experimental solutions with lowest total boron ($B_T = 0.01$ mol/kg H_2O): $^{11\text{-}10}K_B =$ 1.0270 ± 0.0005 ($2\sigma_m$) (Fig. 3.2).

This increase could be attributed to a formation of a trimer, which would represent $\sim 50\%$ of the total boron in solution at pH ~ 8.3. Such an effect was expected since the boron isotope fractionation associated with isotope exchange between boric acid and the trimer in solution was estimated by *ab-initio* calculations to be larger (1.030) than that of the isotope exchange between boric acid and the borate ion monomer (1.026) (Oi, 2000b). It is also possible that the greater $^{11\text{-}10}K_B$ values in the high B_T experimental solutions may also be attributed to the formation of a tetramer $B_4O_5(OH)_4^{2-}$, which would represent $\sim 15\%$ of the total boron in these solutions at pH ~ 8.3 (Fig. 3.1c). Unfortunately, it is not currently possible to estimate relative contributions of the trimer and tetramer to the resulting $^{11\text{-}10}K_B$ values determined in these solutions, since the boron isotope fractionation associated with isotope exchange between boric acid and the tetramer in solution has never been estimated.

Figure 3.2 – Boron isotope equilibrium constant ($^{11\text{-}10}K_B$) determined at 25°C in 0.6 mol/kg H_2O $KCl^{(*)}$ and synthetic seawater over a range of total boron concentrations $B_T = 0.01^{(*)}$, $0.025^{(*)}$ and $0.05^{(*)}$ mol/kg H_2O and $B_T = 0.01$, $0.05^{(*)}$ and 0.5 mol/kg H_2O, respectively. $^{(*)}$ denotes experimental data obtained in an earlier study (Klochko et al., 2006).

3.3.2 Temperature effects on $^{11\text{-}10}K_B$

$^{11\text{-}10}K_B$ values determined in "pure" water and 0.6 mol/kg H_2O KCl media at 25 and 40°C; and in synthetic seawater at 9, 15, 25 and 40°C are graphically illustrated in Fig. 3.3. Data obtained in all three types of media at 25 and 40°C did not demonstrate a statistical temperature effect on the boron isotope fractionation at this temperature range, partially due to a large error associated with the experiments conducted at 40°C. It may be possible to reduce the error by improving temperature control of the instrumental cell.

Experiments conducted in synthetic seawater at temperatures $\leq$ 25°C are of great importance for the paleo-pH reconstructions using boron isotope pH proxy, especially for those studies that use benthic foraminifera, dwelling in the deep ocean and calcifying at temperatures as low as ~ 1°C, as a proxy material (Hönisch et al., 2008). $^{11\text{-}10}K_B$ values in synthetic seawater: $^{11\text{-}10}K_B$ = 1.0288±0.0015(2σ_m), 1.0306±0.0005(2σ_m) and 1.0270±0.0005(2σ_m) were determined at three temperature settings of 9, 15 and 25°C, respectively.

Two observations can be made from this dataset: 1) there are small differences between $^{11\text{-}10}K_B$ across this temperature range; and, 2) there is no overall discernable trend in temperature effects on the $^{11\text{-}10}K_B$ at this temperature range. These observations generally agree with the magnitude of the temperature effects on the $^{11\text{-}10}K_B$ and same lack of a trend in the data set calculated by Tossell (unpublished), using *ab-initio* density functions method and a 22 H_2O molecule cluster model (Table 3.1).

Figure 3.3 – Boron isotope equilibrium constant ($^{11\text{-}10}K_B$) determined in "pure" water[*] and 0.6 mol/kg H_2O KCl[*] at 25 and 40°C; and synthetic seawater over a range of temperatures: 9, 15, 25 and 40[*]°C. [*] denotes experimental data obtained in an earlier study (Klochko et al., 2006). B_T = 0.01 mol/kg H_2O.

This suggests that this particular *ab-initio* method/model of calculations is perhaps more applicable for quantum mechanical estimates of the equilibrium fractionation constants associated with boron isotope exchange in solutions.

3.3.3 Ion pairing effects on $^{11\text{-}10}K_B$

Results obtained in various media: seawater, Mg-free seawater, 0.7 mol/kg H_2O NaCl, 0.23 mol/kg H_2O $MgCl_2$ and 0.6 mol/kg H_2O KCl, with total boron concentration $B_T = 0.01$ mol/kg H_2O at 25^oC are illustrated in Fig. 3.4.

The results obtained in Mg-free seawater are of special importance, as this media is widely used for calcite precipitation in various studies, including some significant boron isotope/pH calibration studies (Sanyal et al., 1996; Sanyal et al., 2000; Sanyal et al., 2001). To estimate effects of the ion pairing between borate ion and Mg^{2+} it is best to compare the $^{11\text{-}10}K_B$ values obtained in $MgCl_2$ media, Mg-free seawater and synthetic seawater, which are: $1.0270\pm0.0003(2\sigma_m)$; $1.0261\pm0.0002(2\sigma_m)$ and $1.0270\pm0.0005(2\sigma_m)$, respectively. There is no statistical difference in $^{11\text{-}10}K_B$ between $MgCl_2$ media and synthetic seawater; however there is a small difference between synthetic seawater and Mg-free seawater ($\Delta^{11\text{-}10}K_B = 0.0009$), which translates to 0.9‰ difference in boron isotope fractionation between boric acid and borate ions in aqueous solution.

There is also a notable offset ($\Delta^{11\text{-}10}K_B = 0.0026$ or 2.6‰) between $^{11\text{-}10}K_B$ values obtained in NaCl media and synthetic seawater: $1.0296\pm0.0004(2\sigma_m)$ and $1.0270\pm0.0005(2\sigma_m)$, respectively.

Figure 3.4 – Boron isotope equilibrium constant ($^{11\text{-}10}K_B$) determined at 25°C in different media: synthetic seawater, Mg-free seawater, 0.6 mol/kg H_2O KCl[(*)], 0.7 mol/kg H_2O NaCl and 0.23 mol/kg H_2O MgCl$_2$. [(*)] denotes experimental data obtained in an earlier study (Klochko et al., 2006).

This would suggest that the boron isotope fractionation associated with the isotope exchange between boric acid and NaCl-borate ion pairs is larger than that between boric acid and all borate ion pairs combined in seawater.

It is difficult to predict whether these effects would be propagated to the isotopic composition of a carbonate precipitated in Mg-free seawater or NaCl media, however these observations may help in data interpretation obtained in future calibration studies. Nevertheless, to avoid potential effects resulting from absence/presence of certain borate ion pairs in experimental calibration solutions, it is more advisable to use synthetic seawater media, which would closely mimic natural seawater conditions.

3.4   Conclusions

This study has demonstrated no significant effects of the polyborates on the boron isotope fractionation ($^{11\text{-}10}K_B$) between boric acid and borate ion in aqueous solutions at total boron concentrations ranging from 0.01 to 0.05 mol/kg H_2O, which makes these concentrations safe to use in boron isotope calibration studies. However, polyborate effects may manifest themselves at higher concentrations (0.5 mol/kg H_2O), at which point the effects could be contributed to the formation of the polyborate trimer and tetramer.

Although, the $^{11\text{-}10}K_B$ values obtained in synthetic seawater at temperatures 9, 15, 25 and 40°C are valuable for paleo-pH reconstructions using the boron isotope/pH proxy, lack of a trend in the data obtained below 25°C makes its interpolation to the intermediate temperatures difficult.

Analysis of the data obtained in various solution media suggests that there are potentially important effects on $^{11-10}K_B$ associated with the borate ion pairing with various seawater constituents: in particular with Mg^{2+} and Na^+. One should be particularly careful in a choice of a media for the boron isotope calibration studies, as the effects of ion pairing may become significant enough to compromise the accuracy of the calibration.

Within the range of possible environmental variations recorded in the current study, boron isotope distributions are not expected to change much in the ancient record even under extreme conditions. This is problematic; however, as very different boron isotopic compositions have been found in some ancient deposits, in particular the Neoproterozoic cap carbonates, which have strongly negative $\delta^{11}B$ values (Spivack and You, 1997; Kasemann et al., 2005; Kasemann et al., 2009). Given the lack of environmental effects in our controlled experiments, these unusual values might instead reflect wholesale diagenetic resetting of the signal or that our understanding of the boron isotopic composition of the ancient oceans is poor (Lemarchand et al., 2002; Pagani et al., 2005). Thus until we have a better handle on long-term temporal variations in the $\delta^{11}B$ of ocean proxies we may only be able to interpret stratigraphic patterns in sedimentary successions in terms of relative (but uncalibrated) changes in pH.

CHAPTER 4 - RE-EVALUATING BORON SPECIATION IN BIOGENIC CALCITE AND ARAGONITE USING ^{11}B MAS NMR

ABSTRACT: Understanding the partitioning of aqueous boron species into marine carbonates is critical for constraining the boron isotope system for use as a marine pH proxy. Previous studies have assumed that boron was incorporated into carbonate through the preferential uptake of tetrahedral borate $B(OH)_4^-$. In this study we revisit this assumption through a detailed solid state ^{11}B magic angle spinning (MAS) nuclear magnetic resonance (NMR) spectroscopic study of boron speciation in biogenic and hydrothermal carbonates. Our new results contrast with those of the only previous NMR study of carbonates insofar as we observe both trigonal and tetrahedral coordinated boron in almost equal abundances in our biogenic calcite and aragonite samples. In addition, we observe no strict dependency of boron coordination on carbonate crystal structure. These NMR observations coupled with our earlier re-evaluation of the magnitude of boron isotope fractionation between aqueous species suggest that controls on boron isotope composition in marine carbonates, and hence the pH proxy, are more complex that previously suggested.

4.1   Introduction

Insofar as aqueous boron species are isotopically distinct, their incorporation into marine carbonates is important to our understanding of the boron isotope system as a proxy for ancient ocean pH. Boron speciation in aqueous solution is well established (Dickson, 1990) with the equilibrium distribution of boric acid $[B(OH)_3]$ and borate ion $[B(OH)_4^-]$ being strongly pH dependent:

$$B(OH)_3 + H_2O \Leftrightarrow B(OH)_4^- + H^+ \tag{4.1}$$

The stoichiometric equilibrium constant for reaction (4.1) is a function of salinity, temperature and pressure. At a salinity 35, 25^oC and 1 atm total pressure, $pK^*_B =$ 8.597 on the total proton concentration scale (Dickson, 1990).

The isotopic equilibrium between these two species in aqueous solution is characterized by the exchange reaction:

$$^{10}B(OH)_3 + {}^{11}B(OH)_4^- \Leftrightarrow {}^{11}B(OH)_3 + {}^{10}B(OH)_4^- \tag{4.2}$$
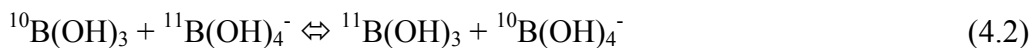
Paleo-pH studies of marine carbonates (Vengosh et al., 1991; Hemming and Hanson, 1992; Spivack et al., 1993; Gillardet and Allègre, 1995; Sanyal et al., 1995; Sanyal et al., 1997; Palmer et al., 1998; Pearson and Palmer, 1999; 2000; Lemarchand et al., 2002; Palmer and Pearson, 2003; Hönisch and Hemming, 2005; Pelejero et al., 2005, etc.) have most commonly used an isotope equilibrium constant ($^{11-10}K_B =$ 1.0194 at 25^oC) for reaction (4.2) that was estimated, over 30 years ago, using reduced partition function calculations from spectroscopic data on molecular vibrations (Kakihana et al., 1977). This constant has been the subject of recent debate, largely based on contrasting interpretations of results from pH-controlled calibration studies of cultured coral, foraminifera and inorganic calcite (Sanyal et al., 1996;

76

Sanyal et al., 2000; Sanyal et al., 2001; Hönisch et al., 2004). Whereas control studies demonstrated a distinct relationship between the $\delta^{11}B$ of precipitated carbonates and the pH of aqueous solutions, carbonate values were systematically <u>depleted</u> in ^{11}B relative to the expected value for aqueous $B(OH)_4^-$, believed to be primarily boron species incorporated into the mineral lattice (Fig. 4.1). It has been argued (Hönisch and Hemming, 2004; Hönisch et al., 2008) that because these calibration measurements broadly mirror the "shape" of the Kakihana's curve, a constant offset at different pH may be used to empirically correct $\delta^{11}B$ values for each of the studied species. While this may be a possible solution, it does not address the underlying mechanism(s) responsible for the ^{11}B depletion. Since all imaginable processes (e.g., boric acid incorporation, metabolic seawater modification at the site of calcification, etc.) would result in ^{11}B enrichment in carbonate relative to aqueous borate, the only logical explanation is that the magnitude of $^{11\text{-}10}K_B$ was underestimated (Zeebe et al., 2003).

Subsequent studies, including new *ab-initio* calculations and semi-empirical modeling, as well as precipitation and adsorption experiments have focused on re-evaluating the magnitude of the boron isotope equilibrium constant (Palmer et al., 1987; Oi et al., 1991; Sanyal et al., 2000; Sonoda et al., 2000; Oi, 2000a; 2000b; Oi and Yanase, 2001; Liu and Tossell, 2005; Pagani et al., 2005; Sanchez-Valle et al., 2005; Zeebe, 2005). However, until recently there have been no experimental measurements of $^{11\text{-}10}K_B$ in aqueous solutions. In our earlier publications (Byrne et al., 2006; Klochko et al., 2006), we used a spectrophotometric technique on
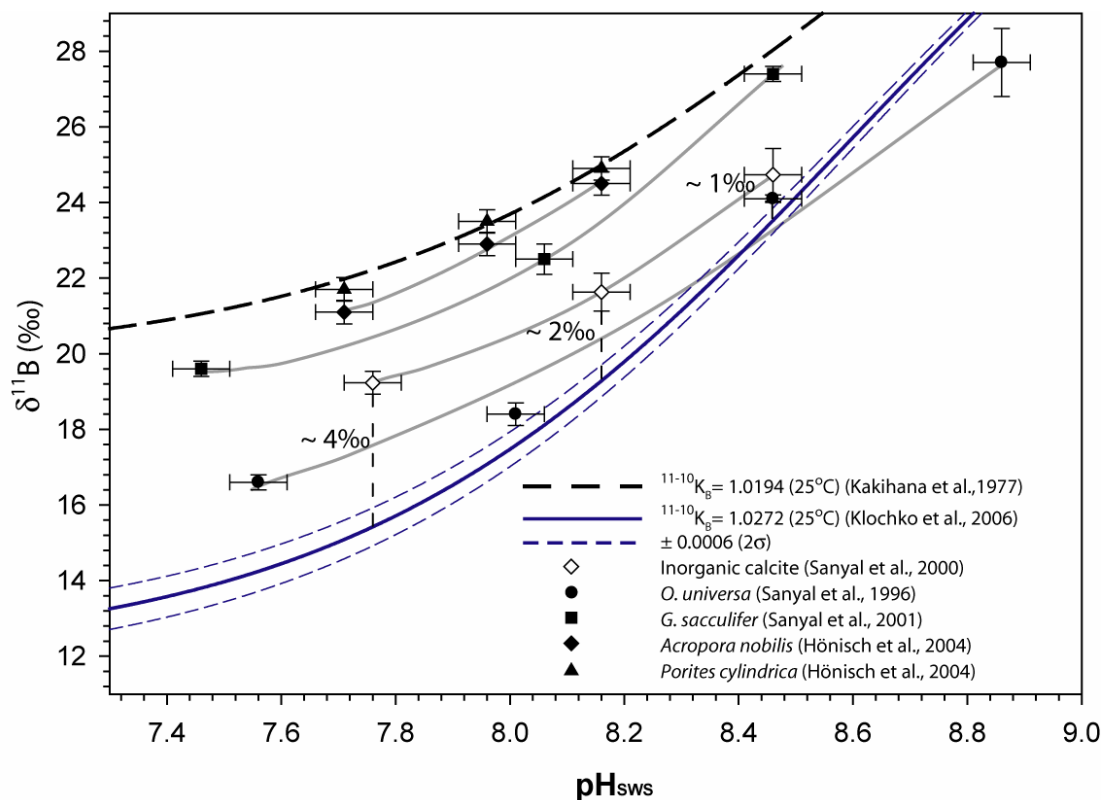
Figure 4.1 – $\delta^{11}B$ of $B(OH)_4^-$ in seawater based on theoretical $^{11-10}K_B$ = 1.0194 (Kakihana et al., 1977) and empirical $^{11-10}K_B$ = 1.0272 ± 0.0006 (2 σ) (Klochko et al., 2006); and the results of the inorganic calcite precipitation experiments (Sanyal et al., 2000), cultured *Orbulina universa* and *Globigerina sacculifer* foraminifera species (Sanyal et al., 1996; Sanyal et al., 2001) and cultured scleractinian corals *Acropora nobilis* and *Porites cylindrica* (Hönisch et al., 2004). The pH_{NBS} values from (Sanyal et al., 1996, 2000, 2001) were recalculated to fit the seawater pH scale (pH_{SWS}= pH_{NBS} - 0.14) (*cf.*, Hönisch et al., 2004). The gray lines represent the polynomial best fits through the $\delta^{11}B$ data-points from precipitation experiments.

isotopically labeled boric acid solutions to determine the magnitude of $^{11\text{-}10}K_B$, which was shown to be ca. 1.0272 ($\pm$ 0.0006, 2σ) regardless of ionic strength or boron concentration. Using the new empirical constant, the boron isotope composition of cultured carbonates in the pH controlled experiments was shown to be <u>enriched</u> in ^{11}B relative to the expected δ^{11}B composition of borate (see Fig. 4.1).

To explain the observed ^{11}B enrichments, we suggested two potential mechanisms (Klochko et al., 2006). First, δ^{11}B of biological carbonates could be affected indirectly via pH adjustment at the site of calcification. Second, boron partitioning in carbonates during mineralization might result in the non-equilibrium enrichment of ^{11}B in the experimental carbonates. Here we suggest that ^{11}B enriched boric acid may be incorporated into the carbonate lattice along with borate; hence the overall boron isotopic composition of the carbonate would be higher than expected from exclusive borate incorporation (see Discussion).

Earlier publications, however, suggested that the charged tetrahedral borate B(OH)$_4^-$ species would be preferentially attracted to mineral surfaces, substituting for the charged carbonate ion (Palmer et al., 1987; Spivack and Edmond, 1987; Hemming and Hanson, 1992). To evaluate this hypothesis, Sen et al. (1994) employed nuclear magnetic resonance (NMR) spectroscopy to quantitatively measure the relative abundance of boron species in synthetic carbonates precipitated from similar starting solutions, as well as some biogenic carbonates. These authors concluded from their NMR data that aragonite contained only tetrahedral-coordinated borate ion, whereas in calcite, whether natural, synthetic, or the product of a high temperature ($\sim$400°C) phase transformation, over 90% of boron was in trigonal

coordination. The inferred species dependence of boron uptake into the crystal structure of carbonates is remarkable insofar as the larger tetrahedral anion appeared to substitute into the smaller lattice sites in aragonite, whereas the smaller trigonal ion substituted into larger lattice sites in calcite. Even more interesting was the observation that the $\delta^{11}B$ of these minerals were similar (Hemming and Hanson, 1992).

To explain this phenomenon it was later suggested that there may be a structural barrier in calcite that causes a quantitative change from tetrahedral to trigonal coordination during incorporation without significant isotopic fractionation (Hemming et al., 1995; Hemming et al., 1998). If correct, this supports the view that only borate ion, $B(OH)_4^-$, is taken up by carbonate minerals from aqueous solutions. However, the variability of $\delta^{11}B$ in calcite samples from later experiments (Sanyal et al., 1996; Sanyal et al., 2000; Sanyal et al., 2001; Hönisch et al., 2004) and the observation that aragonite is consistently enriched in ^{11}B relative to calcite over a range of pH are difficult to reconcile with the NMR results (Sen et al., 1994).

In this study we re-investigate borate speciation in biogenic and hydrothermal carbonates using solid state ^{11}B magic angle spinning (MAS) NMR spectroscopy. Our new results contrast strongly with those of Sen et al. (1994) as we observe both trigonal and tetrahedral coordinated boron in almost equal abundances in the biogenic calcite and aragonite samples. Moreover, we observe no strict dependency of boron coordination on the carbonate crystal structure.

4.2 Methods

4.2.1 Samples

Two scleractinian coral samples, *Diploria strigosa* and *Porites sp.*, originally collected for a detailed study of carbon and nitrogen isotopes (Jabo, 2001), were obtained for the NMR experiments. The *Diploria strigosa* sample was collected from Three Hills Shoal (depth of 3-4.5 m) in Bermuda, and the *Porites sp.* sample was collected from Pickles Reef (depth 4.5-6 m) in Florida. Organic components (i.e. coral animal, algal symbionts, and endolithic algae) within these corals were removed by physical separation with a Waterpik® followed by an overnight treatment with 1M NaOH. Samples were then ultra-sonicated in Milli-Q water (Jabo, 2001). Between 100-200 mg of each prepared coral was isolated with a drill and fragments crushed to a fine powder in an agate mortar with pestle for our ^{11}B NMR analysis. X-ray diffraction (XRD) analyses indicated that aragonite was the only mineral present in both samples.

A foraminifera sample of *Assilina ammonoides* was obtained from the Reef Indicators Lab at the College of Marine Sciences, University of South Florida, St. Petersburg. This sample was collected from Tutum Bay off the coast of Papua New Guinea. The sample was stored and shipped in ethanol, which was removed by repeated sonication with Milli-Q water. After drying, the sample was crushed to a fine powder in an agate mortar with pestle for ^{11}B NMR analysis. XRD analysis identified only calcite in this sample.

For comparative purposes, we analyzed a well characterized carbonate sample (#3651-0908) (Ludwig et al., 2006) from the Lost City Hydrothermal Field carbonate

81

chimneys (Kelley et al., 2001; Kelley et al., 2005). The Lost City carbonate chimneys are remarkable structures that form rapidly during mixing of Ca^{2+} bearing alkaline fluids with ocean water. Based on the chemistry of fluids emitted from active structures in the vicinity, the source water for the sample #3651-0908 had pH > 10 at temperatures near 60^oC (Ludwig et al., 2006). The sample was collected at a depth of 844 m and currently contains a mixture of calcite and high magnesium calcite, but no aragonite.

4.2.2 X-ray diffraction

X-ray diffraction analyses of the samples were performed with a Rigaku RAXIS/RAPID diffractometer with an Ultrax-18, 18kW rotating anode X-ray generator and a hemi-cylindrical image-plate detector at the Carnegie Institution for Science. Twenty minute exposures were taken using monochromatic, Mo Kα radiation. Samples were oscillated over a 40° range to average grain orientations. Crystal structure of the biogenic samples was established via their characteristic diffraction patterns. In either case, the calcite and aragonite samples are determined to be 99% mineralogically pure.

4.2.3 ^{11}B MAS NMR spectroscopy

^{11}B MAS NMR analyses were performed at the W. M. Keck solid-state NMR facility at the Geophysical Laboratory, Carnegie Institution for Science. The instrument used in this study is a three channel Varian-Chemagnetics Infinity solid-

state NMR spectrometer. The static field strength of the magnet is ~ 7.05 T, a lower field than the system used by Sen et al. (9.4 T). As discussed below, peak positions, width and shape depend on the field dependence of the quadrupolar interaction. The Larmor frequency of ^{11}B in this static magnetic field is 96.27 MHz. For the current experiments, 100-200 mg of powdered samples were placed in 5mm diameter zirconia rotar cells. The sample was spun at a magic angle of 54.7^o at a frequency ($\omega_r/2\pi$) of 12 kHz. All experiments employed an excitation RF pulse that corresponds to a 10° tip angle with RF power ($\omega_1/2\pi$) of 56 kHz; high power RF decoupling ($\omega_1/2\pi$ =65 kHz) was applied during signal acquisition to mitigate the effects of ^{1}H-^{11}B dipolar coupling. The recycle delay between acquisitions was 0.5 seconds and a total of 300,000 acquisitions were sufficient to resolve the characteristic borate spectral features. All spectra are referenced to the resonant frequency of boron trifluoride diethyl etherate defined as equal to 0 ppm.

4.3   Results

Solid-state ^{11}B NMR spectroscopy is particularly well suited to provide fundamental information about the speciation of boron in carbonates. Acknowledging that the primary audience for this study are paleo-oceanographers, a brief discussion about ^{11}B NMR is warranted. The ^{11}B nucleus is a spin 3/2 particle that has both a magnetic dipole and electric quadrupole moment. The presence of an electric quadrupole moment means that the nucleus will interact strongly with the local electric field surrounding the nucleus. This interaction has a significant effect on the observed spectrum. The strength of local electric field gradient (EFG) is described by

a second rank tensor with principal axis elements V_{ii} (i = x, y, and z) (Cohen and Reif, 1957). The symmetry of the EFG manifests predictable and large effects in the spectral line shape of ^{11}B species in the solid state and is quantified by the asymmetry parameter, η [$\eta = (V_{xx} - V_{yy})/V_{zz}$)]. In the case of perfect radial symmetry of the EFG around the quadrupolar nucleus ($V_{xx} = V_{yy}$) $\eta = 0$, and in the case maximum deviation away from cylindrical symmetry, $\eta = 1$. In the case where the EFG is perfectly spherically symmetric around the nucleus, Vxx=Vyy=Vzz=0 and the quadrupolar interaction is nonexistent (i.e., the spins respond to radiofrequency pulses through their magnetic dipole interaction only). Static NMR experiments show that the shape of the resultant powder patterns is strongly affected by the value of η. In the case of borate salts and boric acid, the BO_3 species have a nearly perfect trigonal planar distribution of oxygen atoms surrounding the ^{11}B nucleus, consequently η is observed to be nearly equal to zero (note that if BO_3 groups are covalently bonded to other cations through bridging oxygens, then a significant distortion of the EFG away from trigonal symmetry will occur). The BO_4 species have a tetrahedral oxygen arrangement that approaches nearly perfect cubic symmetry; thus, a minimal quadrupolar interaction for these borate species is expected and observed.

In the present experiments, powder samples were spun rapidly at the magic angle, 54.7°, during signal acquisition. Magic angle sample spinning (MAS) is performed in order to average out chemical shielding anisotropy, some of the quadrupolar broadening, as well as to reduce broadening associated with proton dipolar coupling (thus enhancing the effectiveness of RF decoupling). In the case of

Table 4.1 – ^{11}B MAS NMR parameters, where δ_{iso} – isotropic chemical shift, expressed in parts per million; Cq – nuclear quadrupolar coupling constant, expressed in MHz; LB – line broadening, expressed in Hz; η – EFG asymmetry parameter.

Sample	Mineralogy	BO$_3$				BO$_4$			
		δ_{iso}	Cq	LB	η	δ_{iso}	Cq	LB	η
Coral *Diploria strigosa*	100% aragonite	16.8	2.5	469.9	0	2.54	0	-	-
Coral *Porites sp.*	100% aragonite	18.3	2.5	361.5	0	2.0	0	-	-
Foram *Assilina ammonoides*	100% calcite	19.3	2.6	455.9	0	1.67	0	-	-
Lost City carbonate #3651-0908	calcite/ Mg-calcite	-	-	-	-	2.85	0	-	-
Boric acid standard	--	19.5	2.5	114.7	0	-	-	-	-

the quadrupolar interaction, rapid MAS at 54.7°C cannot completely average out the fourth rank tensorial terms of the quadrupolar Hamiltonian (Ganapathy et al., 1982), although it does afford significant line narrowing compared to static NMR improving the signal to noise. This means that even with fast MAS one can readily distinguish between boron sites with dramatically different EFG symmetries (e.g., BO_3 and BO_4).

In Figure 4.2, the ^{11}B MAS NMR spectrum (with ^1H decoupling) is presented for a pure $B(OH)_3$ standard, revealing the characteristic two-peak MAS quadrupolar powder pattern for a single boron site with a radially symmetric EFG. This single site is adequately fit with η set equal to 0, a quadrupolar coupling parameter, Cq, set to 2.5 MHz, an isotropic shift, δ_{iso} set to 19 ppm, and a modest amount of line broadening, 140 Hz (Massiot et al., 2002). In Figures 4.3 (a-c), ^{11}B MAS NMR spectra are presented for three natural biological specimens of carbonate, including calcite (foraminifera *Assilina ammonoides*, Fig. 4.3a) and aragonite (corals *Diploria strigosa*, Fig. 4.3b, and *Porites sp.*, Fig. 4.3c). In each case, satisfactory fits of the spectra are achieved with two boron species, BO_3 fit with η fixed at 0 and adjustment of the line broadening and a BO_4 species fit with a single Lorentzian line, assuming that $Cq = 0$. Slightly better fits (i.e. achieving lower residuals) are achievable if a mixed Lorentzian/Gaussian broadening function is used. For the current purposes, however, the original fits are sufficient to show that each of these biological carbonates contain mixed borate species with a slight predominance of BO_4 over BO_3. The various NMR parameters as well as species abundances are presented in Table 4.1.
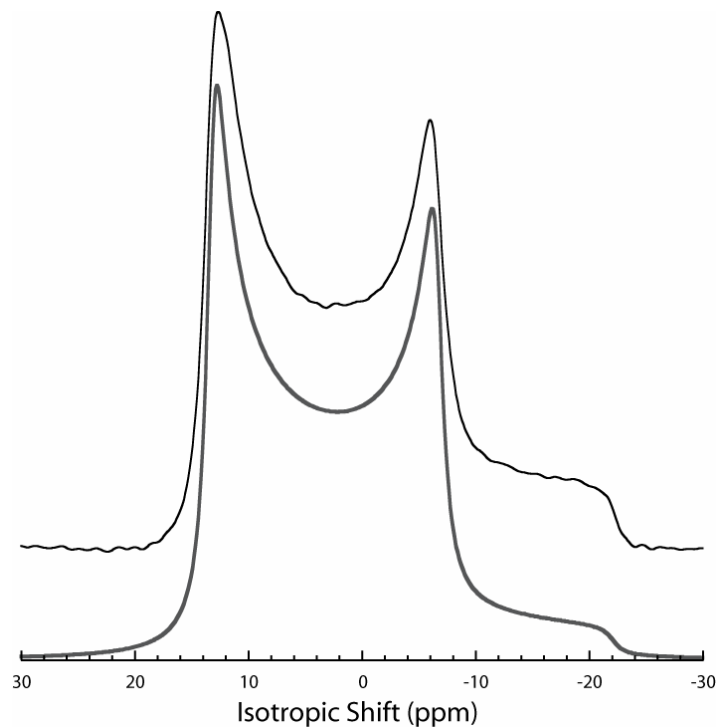
Figure 4.2 – ^{11}B MAS NMR spectrum of boric acid standard, B(OH)$_3$. A single boron site is observed that exhibits a classic MAS quadrupolar power pattern resulting from the inability of spinning at 54.7° to average out fourth rank tensorial terms of the quadrupolar Hamiltonian. A simulation (fit) of this spectrum is presented by the bold line spectrum where the following parameters were used, η = 0.0, C_Q = 2.470 Mhz, and δ_{iso} = 19 ppm. These parameters are consistent with a highly symmetrical trigonal BO$_3$ site. Boric acid B(OH)$_3$ (ACS reagent, $\geq$ 99.5% pure) obtained from Sigma-Aldrich was used as a standard in this study.

(a)

(b)

(c)

Isotropic Shift (ppm)
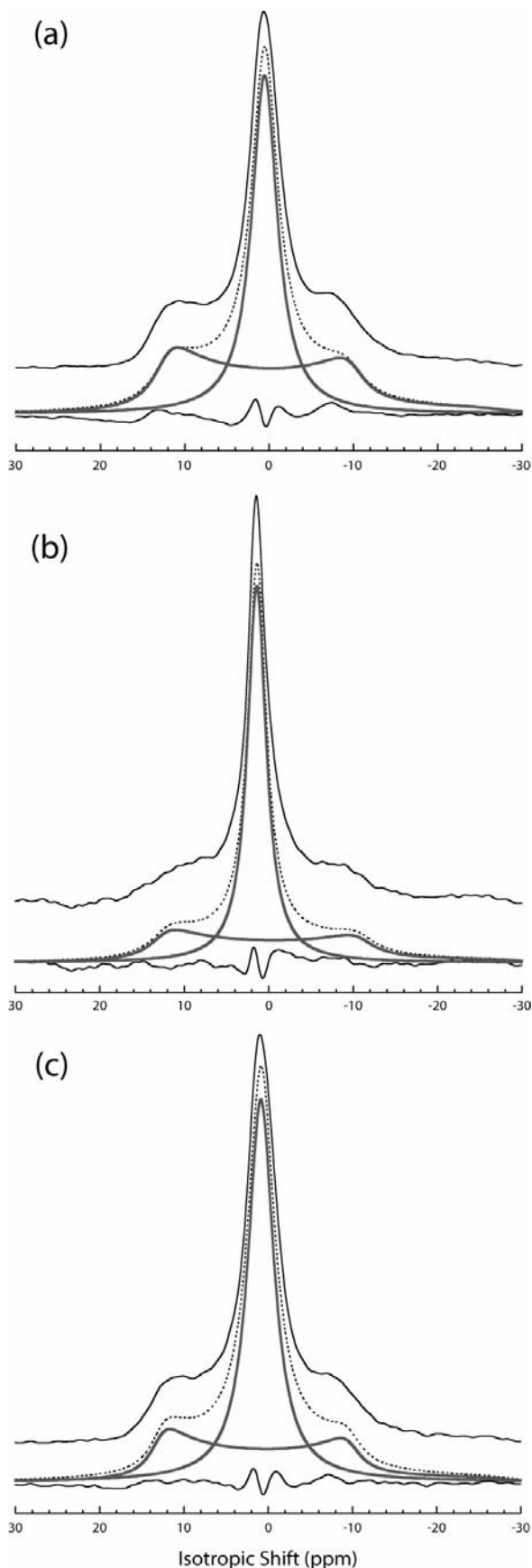
Figure 4.3 - ^{11}B MAS NMR of three biogenic carbonates revealing that borate is present in both trigonal and tetrahedral coordination: (a) calcite from the foraminifera (*Assilina ammonoides*) with BO3 (~46%) and BO4 (~54%); (b) aragonite from the coral (*Diploria strigosa*) with BO3 (~36%) and BO4 (~64%); and (c) aragonite from the coral (*Porites sp.*) with BO3 (~36%) and BO4 (~64%). The total fit is shown as a dotted line; the individual sites are shown in bold black. The difference between the spectrum and the fit is in black. The acquired spectrum is in black and offset vertically from the total fit.

88

To test whether the solution pH has any effect on the borate speciation in the carbonate structure, we analyzed the Lost City carbonate sample which precipitated from solutions of pH > 10 (Ludwig et al., 2006). The ^{11}B MAS NMR spectrum for this sample is presented in Figure 4.4 where only BO_4 was detected. For the present discussion, the presence of essentially pure BO_4 in this hydrothermal calcite is important insofar as it suggests that there exists no structural barrier to the incorporation of the larger tetrahedral borate species in calcite, as was previously suggested (Sen et al., 1994; Hemming et al., 1995; Hemming et al., 1998). We acknowledge that a rapid precipitation rate, as expected for this hydrothermal chimney sample, may favor the incorporation of the dominant species in solution, even if it is less stable in the crystalline structure.

In the present experiments, high power RF ^{1}H decoupling was applied during the signal acquisition phase based on the assumption that boron is incorporated into a growing carbonate as $B(OH)_3$ or $B(OH)_4^-$ (i.e., analogous to recent observations that HCO_3^- groups can be incorporated into growing carbonate as detected in a recent solid state NMR study) (Feng et al., 2006). In the case of spin 1/2 nuclei, ^{1}H decoupling provides greater spectral resolution by reducing the magnitude of this homogeneous source of line broadening. In the case of proton coupling to quadrupolar nuclei (e.g., [11]B), however, there is an additional issue; in addition to broadening there is also distortion of the rotational powder pattern due an orientational dependence on [1]H-[11]B coupling interaction that is moderated by the fast MAS. This combination of line broadening and spectral distortion is clearly
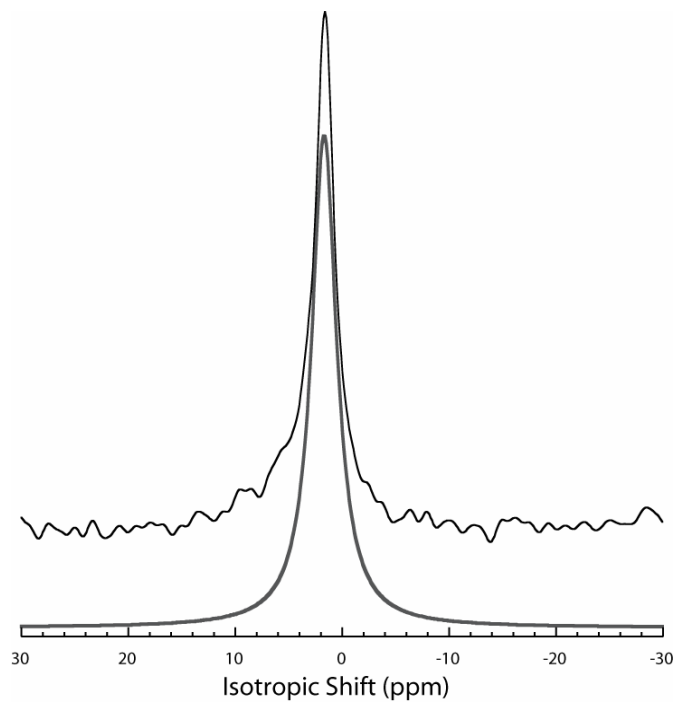
Figure 4.4 – ^{11}B MAS NMR of a deep sea serpentinite carbonate from the Lost City hydrothermal complex and precipitated at high pH. The entire spectrum is adequately fit with single Lorentzian line with similar isotropic shift to that of other BO4 groups in calcite and aragonite.

manifested in Figure 4.5 where B(OH)$_3$ MAS NMR without ^{1}H decoupling is compared with the same experiment with ^{1}H decoupling.

Similarly, the same orientational distortion of the "BO$_3$" MAS powder pattern is clearly observed when comparing the borate spectra of the carbonates (e.g., *Porites sp.*) with and without ^{1}H decoupling, revealing the presence of neighboring H$^+$ atoms (Fig. 4.6). There is, however, a spectral distortion of a different sort that provides additional information. Without decoupling, the "BO$_3$" intensity appears enhanced relative to the "BO$_4$" intensity when normalized to the spectrum obtained with decoupling. The most likely explanation for this distortion is that the "BO$_4$" groups are associated with more hydrogen atoms than the BO$_3$ groups, and hence experience a more intense dipolar perturbation leading to greater line broadening. These results suggest that additional experiments might be performed to gain better insights on the true stoichiometry of the protonated borate structures in these carbonates. It should also be noted that even with ^{1}H RF decoupling, the BO$_3$ resonance features in the biogenic carbonates are broader than that of the B(OH)$_3$ standard (Table 4.1). This residual broadening may be due to inhomogeneous effects (e.g., slight positional disorder in the anionic site) or may reflect the presence of paramagnetic species in the natural carbonates (e.g., Mn^{2+}).

The new measurements reveal the presence of both BO$_3$ and BO$_4$ groups in both aragonite and calcite. In contrast, Sen et al. (1994) concluded, from their spectra analysis, that BO$_3$ groups are predominantly incorporated into calcite. Inspection of their data confirms the presence of a small amount of BO$_4$ groups in their calcite
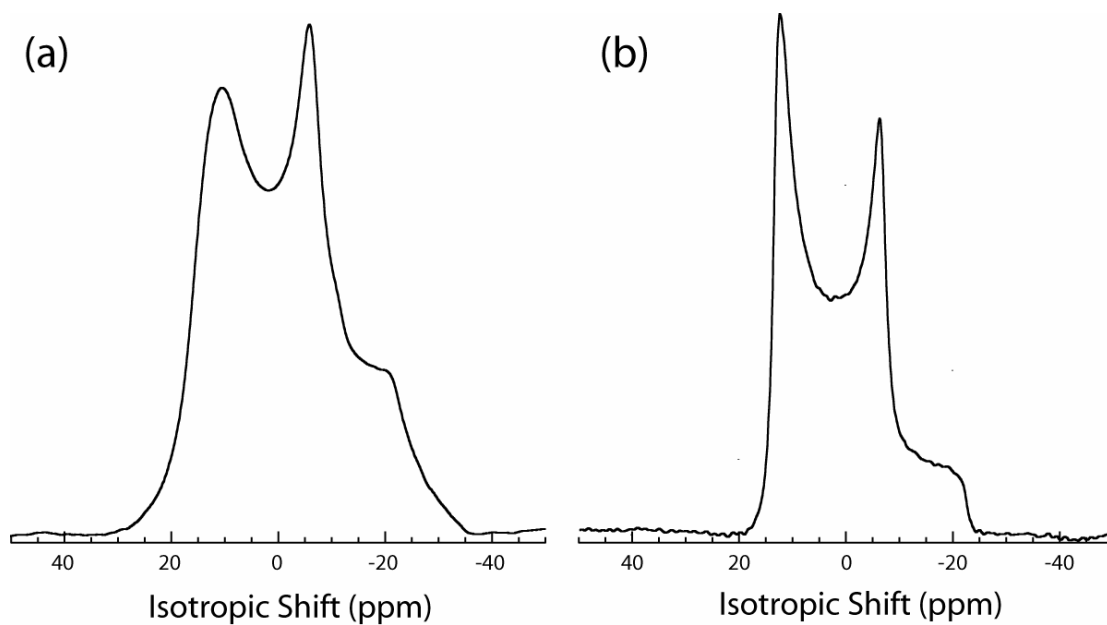
Figure 4.5 – A comparison of ^{11}B MAS NMR spectra of boric acid, $B(OH)_3$: (a) acquired without high power RF ^{1}H decoupling; (b) acquired with high power RF ^{1}H decoupling ($\omega_1/2\pi$ = 75 kHz). Note that, without decoupling, one observes both line broadening and spectral distortion.
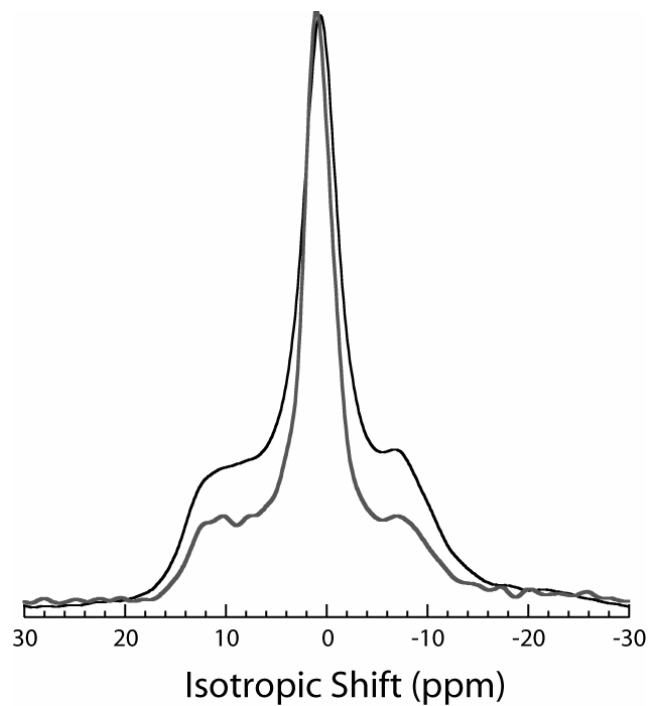
Figure 4.6 – An overlay of ^{11}B MAS NMR spectra of the coral *Porites sp.*, in bold black: acquisition with high power RF ^{1}H decoupling. In black: acquisition without RF decoupling. The apparent increase in BO3 intensity in the absence of high power RF ^{1}H decoupling suggests greater H coordination in the case of the BO4 groups.

sample. It is noteworthy, however, that the calcite ^{11}B NMR spectrum acquired by Sen et al. (1994) differs significantly from the spectral signature of BO_3 groups that we observe in this study. Notably, Sen et al. (1994) report a η of up to 0.67 and a Cq on the order of 3.0 MHz. These values are vastly different from what is expected and observed for the trigonal $B(OH)_3$ and indicate that the symmetry of the EFG surrounding [11]B in their calcite sample is not radially symmetric. Sen et al. (1994) acquired their data at a static magnetic field of 9.4 T, whereas the present experiments were acquired at ~7.05 T. In order to compare the calcite spectrum of Sen et al. (1994) with the one we obtained of the foraminiferal calcite (Fig. 4.3a), we simulated the Sen et al. (1994) spectrum as it would appear at ~7.05 T. This comparison is presented in Figure 4.7 revealing that the boron site detected by Sen et al. (1994) is completely different from the present observations for the foraminiferal calcite.

Clearly, we are observing different borate structures. A clue to what Sen et al. (1994) likely detected may be found in an extensive theoretical analysis of boric acid adsorption on humic acids (Tossell, 2006). One of the species for which Tossell (2006) calculated NMR and NQR properties was the corner-sharing borate carbonate complex, $B(OH)_2CO_3^-$. His calculations yield a theoretical value for η of 0.54 and a Cq of 3.15 MHz. Not surprisingly, covalent bonding of the $B(OH)_3$ group to the CO_3^{2-} anion significantly distorts the trigonal arrangement of oxygen atoms and the EFG far from cylindrical symmetry. In Figure 4.8, we present a simulation of the [11]B MAS spectrum for $B(OH)_2CO_3^-$ along with the boron site observed in calcite by Sen et al. (1994).
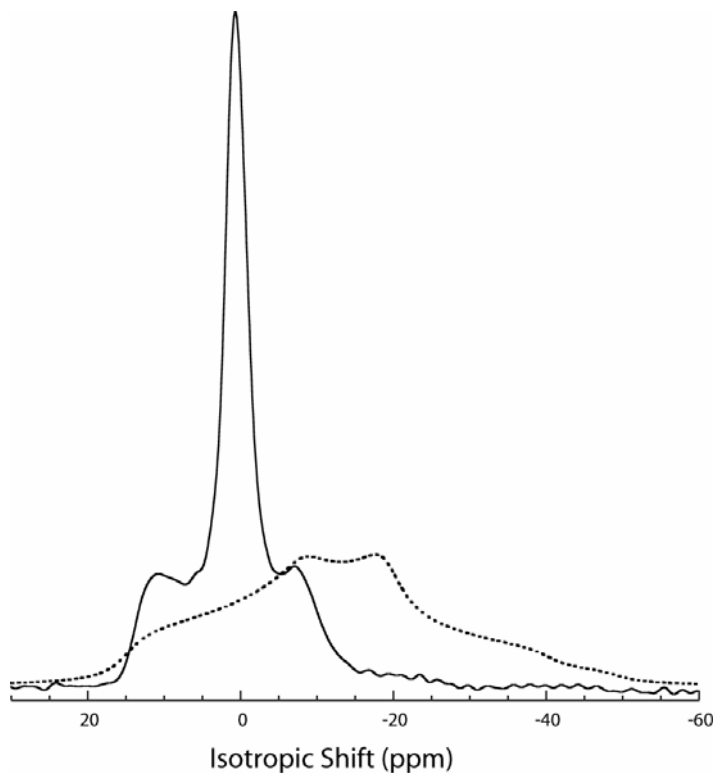
Figure 4.7 – A comparison of the ^{11}B MAS NMR spectrum of foraminifera calcite (this study, where both BO3 and BO4 are observed, solid line) with a simulation (for an external magnetic field of 7 Tesla) of the boron site previously observed and reported in synthetic calcite (at an external magnetic field of 9.4 Tesla) (Sen et al., 1994, dotted line). The enormous differences in peak shape results from large differences in the symmetry of the electric field gradient (η) as well as in the magnitude of the quadrupolar coupling parameter (C_Q).
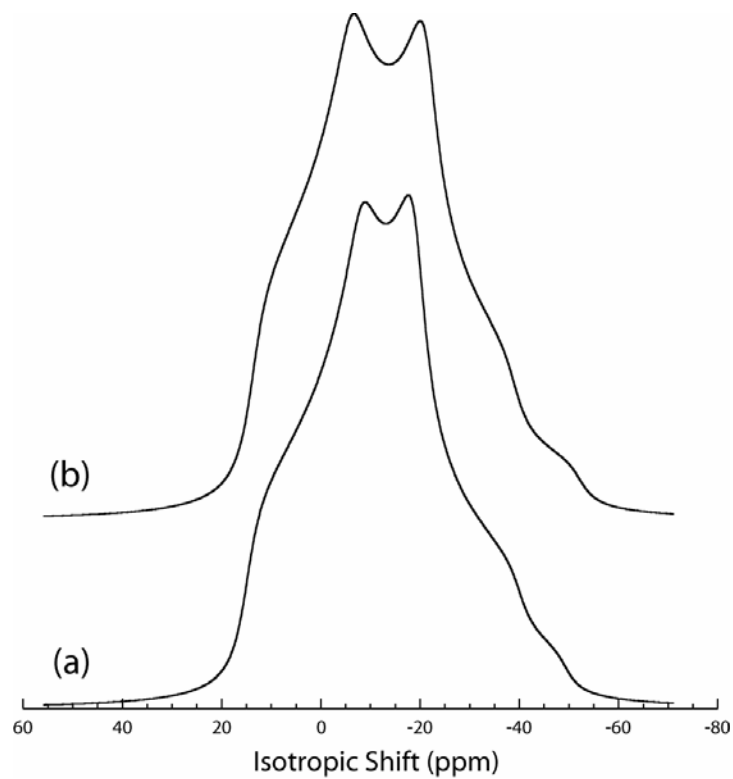
Figure 4.8 – A comparison of simulations of: (a) the boron site previously observed and reported in synthetic calcite (at an external magnetic field of 9.4 Tesla) (adopted from Sen et al., 1994); (b) the MAS quadrupolar powder pattern predicted for corner linked mixed borate-carbonate species $B(OH)_2CO_3^-$ (adopted from Tossell, 2006).

The spectra of these two sites are very similar supporting the previous suggestion by Tossell (2006) that Sen et al. (1994) had actually detected $B(OH)_2CO_3^-$ impurities incorporated in calcite. Intriguingly, Sen et al.'s (1994) study likely identified boron incorporation as $B(OH)_2CO_3^-$ in their synthetic calcite, a species not observed in carbonate samples analyzed in this study.

4.4   Discussion

The principle goal of using boron isotopes in carbonates is to accurately predict the pH of ambient solutions. The equation relating solution pH, boron isotopic composition of boron species incorporated in the carbonate mineral ($\delta^{11}B_{BSp}$) and of seawater ($\delta^{11}B_{sw} = 39.5‰$) is expressed as:

$$pH = pK_B - \log\left(\frac{\delta^{11}B_{sw} - \delta^{11}B_{BSp}}{\delta^{11}B_{sw} - {}^{11-10}K_B \delta^{11}B_{BSp} - 1000 \times ({}^{11-10}K_B - 1)} \right) \qquad (4.3)$$

which depends on three key variables: 1) the boron isotope exchange constant between borate ion and boric acid in solution - $^{11\text{-}10}K_B$, 2) the boron species partitioning into carbonate, which ultimately determines $\delta^{11}B_{BSp}$, and 3) the boric acid stoichiometric dissociation constant – pK^*_B. In our earlier publication (Klochko et al., 2006) we address the first variable; in this study we address the second, in particular the deviations in $\delta^{11}B$ of biogenic and inorganic precipitates from empirical calibration studies (Sanyal et al., 1996; Sanyal et al., 2000; Sanyal et al., 2001; Hönisch et al., 2004).

Three key observations of the culture data require explanation. First, with the exception of a single data point, all carbonates precipitated under controlled pH conditions were enriched in ^{11}B relative to seawater borate, as characterized by the

larger fractionation constant (Klochko et al., 2006) (Fig. 4.1). Second, the ^{11}B

enrichments are more pronounced at lower pH; and third, δ^{11}B values between

calcifying species are variable. Since metabolic and inorganic processes may

differentially affect boron isotope distributions in carbonates, we address biogenic

and inorganic precipitates separately.

4.4.1 *Biologically-driven effects*

Boron isotope redistribution during biosynthesis of carbonate is likely, given

that biomineralizing organisms may actively modify seawater composition (carbonate

ion concentration and saturation state) at the site of calcification (Erez, 2003; Weiner

and Dove, 2003). Saturation is usually maintained by seawater isolation and active

modification, and is usually accompanied by elevation of both pH and alkalinity in

the calcifying fluid (Weiner and Dove, 2003). Current models suggest that Ca^{2+}, CO_2,

and other seawater constituents enter the site of calcification through vacuolization in

foraminifera (Erez, 2003), whereas in corals, endergonic enzymatic reactions that

exchange protons for Ca^{2+} result in higher pH at the site of calcification (Allemand et

al., 1998; Cohen and McConnaughey, 2003). Micro-sensor studies indicate that the

pH of the calcifying fluid in the foraminifera *G.sacculifer* rises to as high as 8.6 in

daylight (Jorgensen et al., 1985). Similarly, pH in the symbiotic coral *Galaxea* rises

from 8.2 to 8.5 at the polyp surface and further to 9.3 in the calcifying fluid (Al-

Horani et al., 2003). Unfortunately, it is not known whether there is a preference for

neutral $B(OH)_3^0$ or charged $B(OH)_4^-$ during boron uptake into the calcifying site or if

there is simply a bulk uptake of seawater boron species. In either case, if the pH of

the calcifying fluid is higher than that of seawater, re-equilibration between

$B(OH)_3^0/B(OH)_4^-$ must occur upon their introduction in these higher pH conditions. Hence, reaction (1) shifts to the right to satisfy chemical equilibrium. As a result, some borate in the calcifying fluid could be formed from the dissociation of boric acid and thus bear its ^{11}B enriched isotopic signature. This effect would be more pronounced at lower ambient seawater pH because the pH adjustment to reach supersaturation would be larger, hence requiring the conversion of more boric acid to borate ion (Fig. 4.1).

This proposed mechanism, however, cannot explain significant differences in $\delta^{11}B$ data between various cultured organisms (the so-called "species effect") (Sanyal et al., 1996; Sanyal et al., 2001; Hönisch et al., 2004). In this analysis, we accept the literature data at face value, although the accuracy of the NTIMS (negative ion thermal ionization mass spectrometry) approach has been recently questioned (Foster, 2008) given the differences in ionization characteristics between foraminiferal carbonate (containing trace organic material) and the normalizing standard solution (boric acid + boron free seawater). Although relative differences in $\delta^{11}B$ may be reconstructed using NTIMS with some degree of confidence, the 4‰ range reported from different laboratories for the same species of planktonic foraminifera highlights the difficulty of generating accurate $\delta^{11}B$ data using this approach (see Foster, 2008).

In addition to inter-species $\delta^{11}B$ variations and enrichments, ^{11}B enrichments are observed in inorganic calcite relative to aqueous borate, where biological effects would not be present (Fig. 4.1). This observation suggests that inorganic processes, likely associated with the complexation of boron species during carbonate precipitation, may also result in boron isotope redistribution.

4.4.2 Inorganic effects

Inorganic effects may manifest themselves during the complex mechanism of boron incorporation from solution to its position in the carbonate structure (Fig. 4.9). For example at the dissociation/isotope exchange stage (Stage I), pH-driven distribution of the $B(OH)_4^-$ and $B(OH)_3$ species as well as the isotope exchange between these species occurs in solution. This stage, which defines the isotopic composition of both species in solution at a set pH, is fairly well characterized. The subsequent steps in the boron incorporation pathway into the carbonate are less well defined. It has been proposed that $B(OH)_4^-$ species preferentially adsorb on to the carbonate surface; subsequent coordination change from BO_4 to BO_3 could then occur during incorporation into the growing carbonate, hence preserving the solution pH derived [11]B isotopic abundance (Sen et al., 1994; Hemming et al., 1998).

Boron incorporated into carbonate minerals precipitated inorganically under pH-controlled conditions (Sanyal et al., 2000) appears to carry an isotopic signature close to the aqueous borate, supporting the idea that borate is preferentially incorporated into the carbonate. Nevertheless, at lower pH there appears to be a progressive enrichment in [11]B relative to aqueous borate. For example, the positive offset between $\delta^{11}B$ of inorganic calcite (Sanyal et al., 2000) and aqueous borate (Klochko et al., 2006) is ~ 4, 2 and 1‰ at pH = 7.6, 8.2 and 8.5, respectively (Fig. 4.1). As boric acid ($B(OH)_3$) becomes the predominant boron species in seawater at pH < 8.587 (Dickson, 1990), and its relative concentration increases with decreasing pH, it is reasonable to assume that its contribution to the incorporation of boron into

the carbonate should also increase leading to larger deviations of the $\delta^{11}B$ in carbonates from the borate curve.

Based on this ^{11}B MAS NMR study of three modern biogenic carbonates, we observe a substantial presence of BO_3 (36-46%) in both aragonite and calcite minerals. If all the boric acid were to come directly from the seawater, then the isotopic composition of studied carbonates should be close to that of seawater (~ 39.5 ‰), which is inconsistent with the $\delta^{11}B$ data available for the natural and synthesized carbonates. This suggests that changes in coordination of the boron species indeed occur during carbonate precipitation (Sen et al., 1994; Hemming et al., 1998).

It is interesting to consider whether such a coordination change might occur through an intermediate phase, such as hypothesized by Tossell (2006). In that study, it was proposed that boron incorporation does not occur by simple adsorption of the borate species to the carbonate surface. Instead, chemical reactions between HCO_3^- and either $B(OH)_3$ or $B(OH)_4^-$ take place on carbonate surfaces during the early growth phase (Stage II) (Tossell, 2006). During this "chemosorption" stage, $B(OH)_2CO_3^-$ isomers of either trigonal (oxygen corner-sharing) or tetrahedral (oxygen four-ring) coordination form on the surface (Fig. 4.9).

As the free energy of formation of these two isomers are very similar, the likelihood of either reaction occurring will essentially be equal. During Stage III, the $B(OH)_2CO_3^-$ isomers, once in the carbonate structure, may break down to the simpler forms and coordination of BO_3 or BO_4, which could explain why we detect only simple BO_3 and BO_4 groups in natural carbonates by NMR.
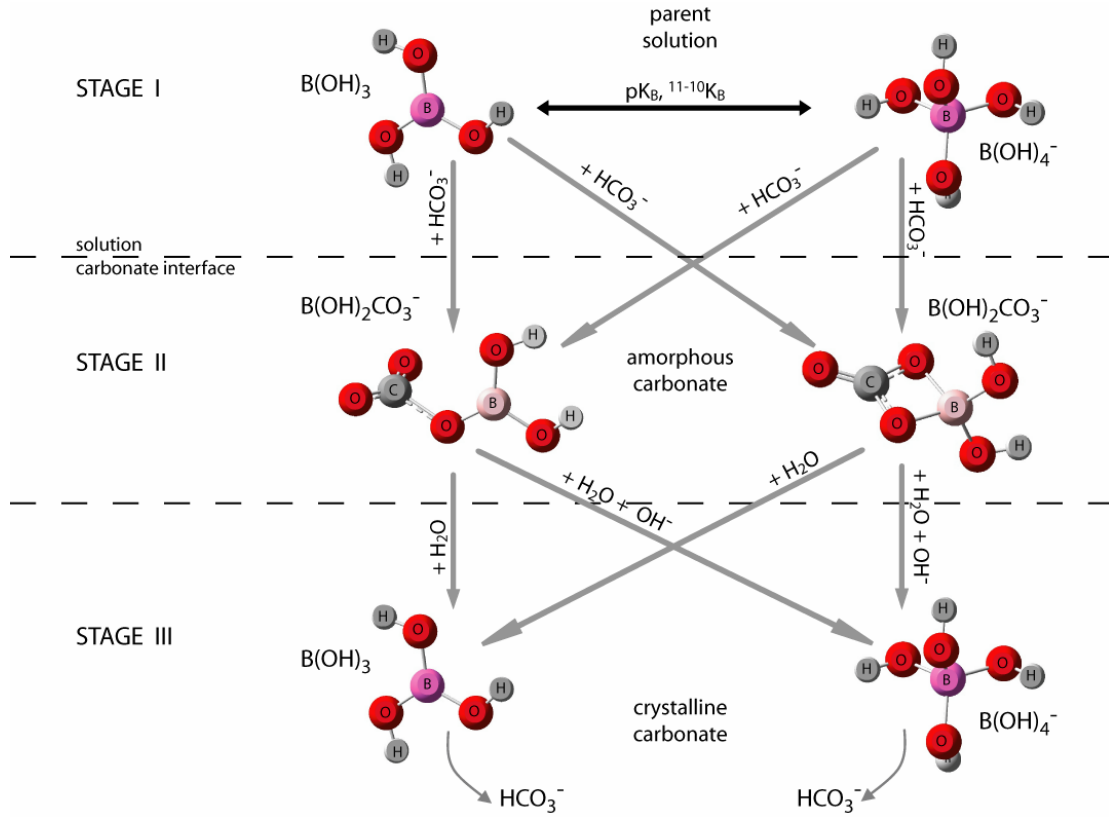
Figure 4.9 – Proposed stage-model of boron incorporation into a carbonate. Schematic representations of molecular structures are adopted from Tossell (2006). Complete reactions for the processes graphically presented in the model are the following:

(1) $B(OH)_3 + H_2O \Leftrightarrow B(OH)_4^- + H^+$

(2) $^{10}B(OH)_3 + {}^{11}B(OH)_4^- \Leftrightarrow {}^{11}B(OH)_3 + {}^{10}B(OH)_4^-$

(3) $B(OH)_3 + HCO_3^- \Leftrightarrow B(OH)_2CO_3^- + H_2O$

(4) $B(OH)_4^- + HCO_3^- \Leftrightarrow B(OH)_2CO_3^- + H_2O + OH^-$

(5) $B(OH)_2CO_3^- + H_2O \Leftrightarrow B(OH)_3 + HCO_3^-$

(6) $B(OH)_2CO_3^- + H_2O + OH^- \Leftrightarrow B(OH)_4^- + HCO_3^-$

Although, $B(OH)_2CO_3^-$ isomer formation was investigated (McElligott and Byrne, 1998; Tossell, 2006), the existence of these isomers has never been demonstrated. Nevertheless, it is interesting to note that the ^{11}B MAS NMR spectra of the synthetic calcite analyzed by Sen et al. (1994) is consistent with the simulated spectra of the oxygen-corner-sharing $B(OH)_2CO_3^-$ species (Tossell, 2006) (Fig. 4.8). The rate at which Sen et al.'s synthetic calcite was precipitated may have been fast enough that the $B(OH)_2CO_3^-$ anion was incorporated directly whereas, in the case of biogenic calcite, this species is hydrolyzed prior to precipitation (Stage III). While speculative, the study of Tossell (2006) suggests that any of the reactions during Stages II and III of boron incorporation in carbonate minerals could result in boron isotope redistribution and are most likely to determine the ultimate bulk boron isotopic composition observed in carbonates.

4.5   Conclusions

Based on our ^{11}B MAS NMR study of three modern biogenic carbonates: two coral aragonites and one foraminiferal calcite, we find no evidence for a strong dependency of boron coordination on crystal structure. Rather, we observe close similarity between these carbonate samples in terms of the relative proportion of boron species, with BO_3 and BO_4 groups representing roughly 36-46% and 54-64%, respectively. Boric acid incorporation may contribute to the ^{11}B enrichment observed in inorganic and biogenic precipitated carbonates, even more so at lower pH, but it is unlikely that all the BO_3 coordinated species detected in calcite and aragonite of our NMR study could come directly from seawater. The observed BO_3/BO_4 inventory in

these minerals is likely the product of some reconstructive surface processes occurring during mineralization, which might involve boron isotope fractionation.

Together, these NMR results and our earlier experimental measurements of $^{11-10}K_B$ in aqueous solutions (Byrne et al., 2006; Klochko et al., 2006) indicate that the controls on the boron isotope composition in biological marine carbonates are more complex that previously suggested. We believe that additional testing of the proxy is warranted prior to its further application in paleoceanographic research. In this regard we are presently conducting pH controlled inorganic precipitation experiments (e.g., Kim et al., 2006) to quantitatively evaluate boron speciation and isotope distribution in carbonates, which should provide more rigorous constraints on the system.

CHAPTER 5 - THE INORGANIC EFFECTS OF PH CONTROLLED PRECIPITATION OF ARAGONITE ON BORON ISOTOPIC COMPOSITION AND SPECIATION IN CARBONATES

5.1   Introduction

The application of boron isotopes in carbonate to estimate pH and pCO_2 of ancient oceans relies on the three main proxy conditions, including

1) The pH dependent speciation of dissolved boron, which is governed by the boric acid dissociation constant (pK_B^*),

2) Isotope exchange between aqueous boric acid $B(OH)_3^o$ and borate ions $B(OH)_4^-$ with distinctly lighter isotopic compositions relative to boric acid, controlled by the boron isotope fractionation constant ($^{11-10}K_B$), and

3) The preferential incorporation of borate ion into both inorganic and biogenic carbonates without further fractionation.

In this regard, both the boric acid dissociation constant (pK_B^*) and boron isotope fractionation constant ($^{11-10}K_B$) have been experimentally constrained (Dickson, 1990; Klochko et al., 2006, respectively). However, the partitioning of boron species in carbonates and the magnitude of isotope fractionation associated with the incorporation of boron as either boric acid or borate remains largely unresolved.

To create working curves for pH estimates from $\delta^{11}B$ measurements of inorganic carbonate, several boron precipitation studies have been conducted across a

range of set pH conditions (Sanyal et al., 1996; Sanyal et al., 2000; Sanyal et al., 2001; Hönisch et al., 2004). Notably, the boron isotopic compositions of both synthetic and natural carbonates obtained in those studies roughly follow a pH-dependent trend, but the absolute values are variably enriched in [11]B relative to those expected for borate ion at various pH levels. This observation suggests that either boric acid is also partially incorporated into the carbonate lattice, or that biologically-driven effects associated with pH adjustment at the site of calcification are taking place during the carbonate growth, or both.

Our recent NMR study of boron speciation has revealed that boron is represented by both boric acid and borate in almost equal amounts in natural carbonates (Klochko et al., 2009). Elevated abundances of boric acid in carbonates may be explained by the conversion of borate to boric acid during precipitation on carbonate surfaces. On the other hand, incorporation of both species remains possible, especially in solutions with pH < 8.6, where boric acid is dominant (Klochko et al., 2009).

In that regard, a focused investigation of boron speciation by NMR and measurement of the boron isotope contrast between solutions and aragonite precipitated across a range of set pH conditions by ICP-MS has great appeal. Since both biological and inorganic processes may potentially affect boron speciation and isotopic composition in carbonates, it is important to constrain each effect separately. To isolate purely inorganic effects on the boron isotope co-precipitation with carbonates, we have designed a series of pH-controlled δ^{11}B calibration experiments of inorganic calcite and inorganic aragonite. Results to date reveal that precipitates

106

from our experiments at pH = 8.7 fall exactly along the borate ion $\delta^{11}B$ curve

predicted by our empirically determined boron isotope fractionation factor (Byrne et

al., 2005; Klochko et al., 2006). Upon completion, we hope to better constrain the

pH/$\delta^{11}B$ relationship across a wide range of pH further testing our measured constant.

Once completed these studies will provide the necessary inorganic baseline for paleo-

studies of inorganic carbonate accumulations (i.e. Neoproterozoic cap carbonates;

reference) and future investigations of the purely biological effects on the boron

isotope distributions in carbonates.

5.2   Experimental design

5.2.1 Scope of the project

This project was specifically designed to investigate boron speciation in

inorganic calcite and aragonite – as well as the magnitude of boron isotope

fractionation between solution and a carbonate precipitated in a given solution –

across a range of controlled pH conditions: low pH ~ 7.3, mid pH ~ 8.7 and high pH

~ 10 (Table 5.1).

The earlier inorganic calcite precipitation study (Sanyal et al., 2000) was

conducted in starting solutions with total boron concentration (B_T) of 74 ppm (6.8

mmol/kg H_2O), which is ~ 15 times that of natural seawater (~ 4.8 ppm, or 0.4

mmol/kg H_2O). It has been shown that an increase in boron concentration by a factor

of 125 (600 ppm or 0.05 mol/kg H_2O) has no observable effect on the boron isotope

equilibrium exchange between boric acid and borate in solution (see Chapter 3;

Table 5.1 – Scope of the project

Phase	Boron concentration	pH		
		7.3	**8.7**	**10**
Aragonite	Low boron concentration (0.42 mmol/kg H_2O)	-	completed	pilot study completed
	High boron concentration (7.9 mmol/kg H_2O)	-	completed	-
Calcite	Low boron concentration (0.42 mmol/kg H_2O)	-	-	-
	High boron concentration (7.9 mmol/kg H_2O)	-	pilot study completed	-

Klochko et al., 2006). However, higher boron concentration in solution may affect

overall boron uptake as well as the resulting boron isotope fractionation between the

calcium carbonate and the parent solution. To investigate potential effects of the

boron concentration on the magnitude of boron isotope exchange between carbonate

and a solution, experiments for each carbonate phase and each experimental pH will

be conducted. These will entail two different solutions with two different total boron

concentrations including a) natural seawater: 0.42 mmol/kg H_2O (or 4.5 ppm), and b)

a solution comparable to that used by a study by Sanyal et al. (2001): 7.9 mmol/kg

H_2O (or 85 ppm). The total boron concentrations in solutions will henceforth be

reported in mmol/kg H_2O.

5.2.2 *Constant addition method of inorganic carbonate precipitation*

Inorganic carbonate precipitation experiments were conducted using the

"constant addition" method (Kim et al., 2006), which is illustrated in Fig.5.1. In this

method, thermally and isotopically equilibrated starting solution was placed in an air-

tight Teflon® reaction vessel. Two titrant solutions containing: 1) $NaHCO_3/Na_2CO_3$

(with relative proportions depending on the pH of the experiment), and 2) $CaCl_2$

solution, were simultaneously injected at a constant and selected rate of 0.05 ml/h by

a dual syringe pump. The addition of the two titrants to the experimental solution led

to supersaturation and the spontaneous nucleation of calcite or aragonite. The

experimental solution was stirred constantly with a floating magnetic stir bar. During

the experiment an aliquot of the solution was sampled with a plastic syringe every
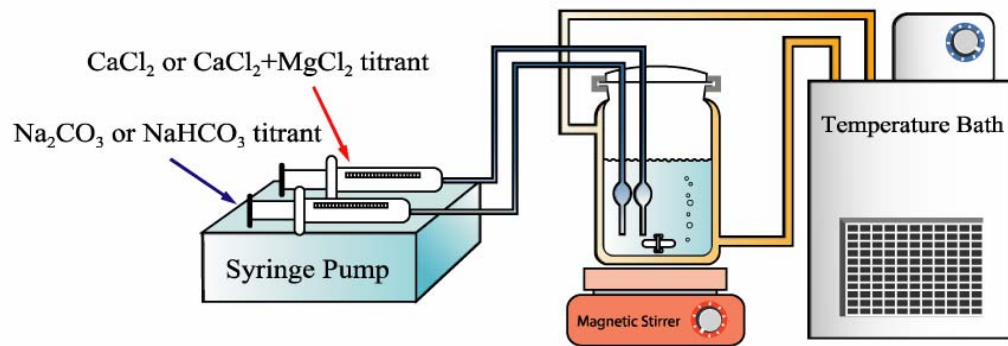
Figure 5.1 – Schematic illustration of the constant addition method for inorganic carbonate precipitation experiments (from Kim et al., 2006).

two days including the first and last. These solutions were filtered through a Millipore

0.45 μm Durapore® syringe filter, and stored in plastic vials for boron concentration

and isotope analyses. The pH of the experimental solutions was monitored daily with

a VWR® Symphony SP70P (#14002-860) pH electrode with a precision of better than

± 0.01 pH units. Before each application, the pH electrode was calibrated using three

of four NIST-traceable buffers at 25°C (i.e., 4.00, 7.00, 10.00, and 11.00). The

reaction vessel was connected to a NESLAB® circulating temperature bath set for

25°C; the temperature of the experimental solutions were monitored daily with a

digital thermometer.

5.2.3 *Solution preparation*

The experimental starting solutions and the titrants were prepared

gravimetrically by dissolving Sigma-Aldrich® analytical grade reagents in18 MΩ

Milli-Q® water. These solutions were stored in a closed container and placed in a

temperature controlled incubator at the constant temperature of 25 ± 0.01^{o}C) until

thermal and isotopic equilibria were established (~ 10 days). The chemical

composition of the two titrants and the starting experimental solutions were adjusted

so that the pH of the experimental solution remained nearly invariant during the

course of the carbonate precipitation (Table 5.2). This chemical adjustment required a

substantial amount of method development, which included running precipitation

experiments with variety of chemical compositions, and monitoring changes, in

particular focusing on pH variability.

Table 5.2 – Chemical composition of the titrants and starting solutions.

Experiment		1	2 (A)	2 (B)	3 (A)	3 (B)	4 (B)	5 (A)	5 (B)	6 (A)	6 (B)
		UMD Arag Oct3107	UMD Arag Apr2208A	UMD Arag Apr2208B	Aug.28, 2008 Arag(A)	Aug.28, 2008 Arag(B)	Oct.2, 2008 Arag(B)	Oct.20, 2008 Arag(A)	Oct.20, 2008 Arag(B)	Dec.19, 2008_Blank Arag(A)	Dec.19, 2008_Blank Arag(B)
Starting solution, mmol/kg H_2O	$NaHCO_3$	0	5	5	8.75	5	5	8.75	5	8.75	8.75
	Na_2CO_3	10	5	5	1.25	5	5	1.25	5	1.25	1.25
	H_3BO_3	5	10	10	0.42	7.9	7.9	0.42	7.9	0	0
	$CaCl_2*2H_2O$	0.25	2	2	0.5	0.5	1	0.5	0.5	0.5	0.5
	$MgCl_2*6H_2O$	1	0.5	0.5	2	2	4	2	2	2	2
	NaCl	0	700	700	685	685	685	685	685	685	685
Titrant (-), mmol/kg H_2O	$NaHCO_3$	0	0	0	40	40	60	60	60	60	60
	Na_2CO_3	80	80	80	40	40	20	20	20	20	20
	NaCl	0	700	700	580	580	620	620	620	620	620
Titrant (+), mmol/kg H_2O	$CaCl_2*2H_2O$	3	3	3	3	3	3	3	3	3	3
	H_3BO_3	0	0	10	5	20	20	10	20	0	0
	NaCl	0	700	700	695	695	695	695	695	695	695
Ionic strength		0.06	0.79	0.79	0.71	0.76	0.77	0.71	0.76	0.71	0.71
pH of starting solution		10.12	8.63	8.63	8.62	8.73	8.71	8.61	8.72	8.67	8.67

The first experiment in the series (Exp.1; UMD_Arag_Oct3107) was conducted at pH = 10.12 as a pilot precipitation to investigate the magnitude of pH fluctuations, boron concentration changes, carbonate yield and mineralogy at a set pH setting. Therefore, for simplicity, the experimental and the titrant solutions for this particular precipitation were prepared in low ionic strength media (I = 0.06) with no boron in the titrants. All the experiments that followed were conducted in NaCl media (I = 0.71-0.79).

The next two experiments (Exp. 2(A) and 2(B); UMD_Arag_Apr2208) were designed to test for boron concentration changes during the inorganic calcite precipitation. The starting solutions for both experiments (Exp. 2(A) and Exp. 2(B)) were identical (B_T = 10 mmol/kg H_2O); however, boric acid was also added to one of the titrants (B_T = 10 mmol/kg H_2O) for the Exp. 2(B) to maintain constant supply of boron into the reaction vessel.

Experiments 3-5 were part of the method development for the inorganic aragonite precipitation at "mid" pH ~ 8.7 with "low" (B_T = 0.42 mmol/kg H_2O) and "high" (B_T = 7.9 mmol/kg H_2O) boron concentration in the starting solutions. The relative proportions of $NaHCO_3/Na_2CO_3$ in the titrant solutions were adjusted for each experiment to reduce pH variability (Table 5.2).

Two blank aragonite precipitation experiments (Exp. 6(A) and 6(B)) were conducted to test for boron contamination.

Upon the termination of each experiment, one last aliquot of a sample solution was collected. The remaining sample solution was run through a vacuum filtration system using 0.45 μm Durapore® membrane filters until all the suspended calcium

113

carbonate was collected. Salts were thoroughly rinsed with 5-6 liters of 18 MΩ Milli-Q$^®$ water, followed by ultra-pure methanol. The calcium carbonate on the filter was placed to dry in the oven at ~ 50°C overnight. The carbonate was then collected from the filter and weighed. An average carbonate yield from a 4-week precipitation experiment was ~ 50 mg.

Plastic vials for solution and carbonate samples were pre-cleaned in 3 M HCl solution for 24 hours at ~ 80°C, and then thoroughly rinsed with 18 MΩ Milli-Q$^®$ water. After cleaning, vials were stored in a sealed plastic container. When sampling solutions the vials were rinsed with an aliquot of a sample solution, which was discarded, and then a second aliquot taken and stored.

5.3   Instrumental analyses

5.3.1 *X-ray diffraction*

X-ray diffraction analyses (XRD) of the carbonate samples were performed by Peter Y. Zavalij of the X-ray Crystallographic Center at the Department of Chemistry & Biochemistry, University of Maryland. A Bruker D8 Advance diffractometer used in the analyses was equipped with Cu-sealed tube and LynxEye PSD detector Twenty minute exposures were taken using monochromatic, Cu Kα radiation. Samples were spinned to average grain orientations. Crystal structure of the carbonate phases were established via their characteristic diffraction patterns. In either case, the calcite and aragonite samples have been determined to be 99% mineralogically pure.

5.3.2 Scanning Electron Microscopy

Images of the two carbonate phases (Fig. 5.2) were obtained by AMRAY 1620D Scanning Electron Microscopy (SEM) at 20 kV by Tim Mougel (director of the Laboratory for Biological Ultrastructure) at the University of Maryland. Samples were coated with < 20nm layer of Au:Pd alloy with 60%:40% relative abundances.

5.3.3 ^{11}B MAS NMR

^{11}B MAS NMR analyses were performed by George Cody at the W. M. Keck solid-state NMR facility at the Geophysical Laboratory, Carnegie Institution for Science. The instrument used in this study is a three channel Varian-Chemagnetics Infinity solid-state NMR spectrometer. The static field strength of the magnet is ~ 7.05 T. The Larmor frequency of ^{11}B in this static magnetic field is 96.27 MHz. For the current experiments, ~ 50 mg of powdered samples were placed in 5mm diameter zirconia rotar cells. The sample was spun at a magic angle of 54.7^o at a frequency ($\omega_r/2\pi$) of 12 kHz.

5.3.4 Boron concentration and isotope analyses

The isotopic composition of the inorganic carbonates were determined with a new method developed at the University of Bristol using multi-collector inductively coupled plasma mass spectrometry (MC-ICPMS) (Foster, 2008). Unlike the more standard negative ion thermal ionization mass spectrometry (NTIMS) approach
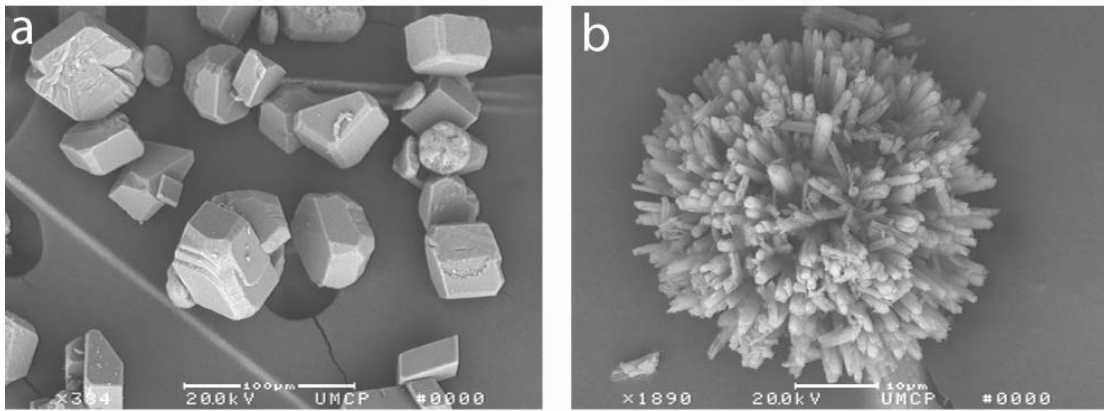
Figure 5.2 – Scanning electron micrograph (SEM) images of (a) inorganic calcite+vaterite (Exp. 2(A)) and (b) inorganic aragonite (Exp. 1).

previously used to analyze boron in carbonates (e.g. Pelejero et al., 2005; Hönisch et al., 2008), for MC-ICPMS it is necessary to first separate boron from the predominantly Ca matrix of the dissolved marine carbonate. This is achieved using the boron specific resin Amberlite IRA 743 (Foster, 2008). Samples were dissolved in 0.5 M HNO_3 and buffered to a pH of 5 using a 2 M Na acetate 0.05 M acetic acid buffer. Column yields using this procedure were determined using isotope dilution and are consistently ~95%. All boron isotope analyses were carried out using a ThermoFinnigan Neptune MC-ICPMS. Instrumental mass bias was corrected by using the average value of bracketing, intensity-matched (to within 10 %) NIST SRM 951 boric acid standards. As a consequence, boron isotope ratios are essentially determined as delta values. Each analysis consisted of a 2 minute simultaneous collection of masses 11 and 10 on Faraday cups. Solution concentrations were typically 30-50 ppb boron.

Boron concentration analyses were conducted as part of the trace element analyses (Ca, Mg, Sr, Na, Mn, Li, B, Ba, Cd, U, Al, Cu, Fe, Nd and Zn) on a Thermo Finnigan Element 2 ICP-MS. The B/Ca ratio determined in these analyses is precise and accurate to 5% (at 95% confidence).

5.4   Results and Discussion

5.4.1 Overview

At the time of writing this dissertation the time-consuming carbonate precipitation experiments were still underway. The results presented here include 1)

quantification of pH drift in the experimental system, 2) the mineralogy of precipitates determined by XRD, and 3) variations in solution and carbonate B abundance and isotope composition by MC-ICPMS. Specific results of the pilot experiment for inorganic aragonite precipitation at pH ~ 10 (Exp.1) and the experiment for inorganic calcite precipitation (Exp. 2(A) and 2(B)) will be presented, but the discussion concentrates on the method development for the inorganic aragonite precipitation at pH ~ 8.7. This part of the project has been successfully completed and the results are presented here (Table 5.3).

5.4.2 pH drift

pH variability during carbonate synthesis has been a primary concern in the method development, insofar as the sole purpose of this project is to constrain boron isotopic composition and speciation in carbonates precipitated at a set pH. The pH drift observed at the early stages of the method development (Exp. 1-3) was a characteristic increase in pH values (Fig. 5.3a). As described above, pH in the reaction vessel was regulated via constant addition of the titrant solutions with various proportions of $NaHCO_3/Na_2CO_3$. In that regard, it is interesting to compare the pH variations during Exp. 3, 4 and 5.

During Exp. 3(A), pH of the parent solution increased from 8.62 to 9.28 pH units ($\Delta pH = 0.66$); and during Exp. 3(B), pH of the parent solution increased from 8.73 to 9.08 pH units ($\Delta pH = 0.35$). Titrants for these experiments contained 40 mmol/kg H_2O $NaHCO_3$ and 40 mmol/kg H_2O Na_2CO_3.
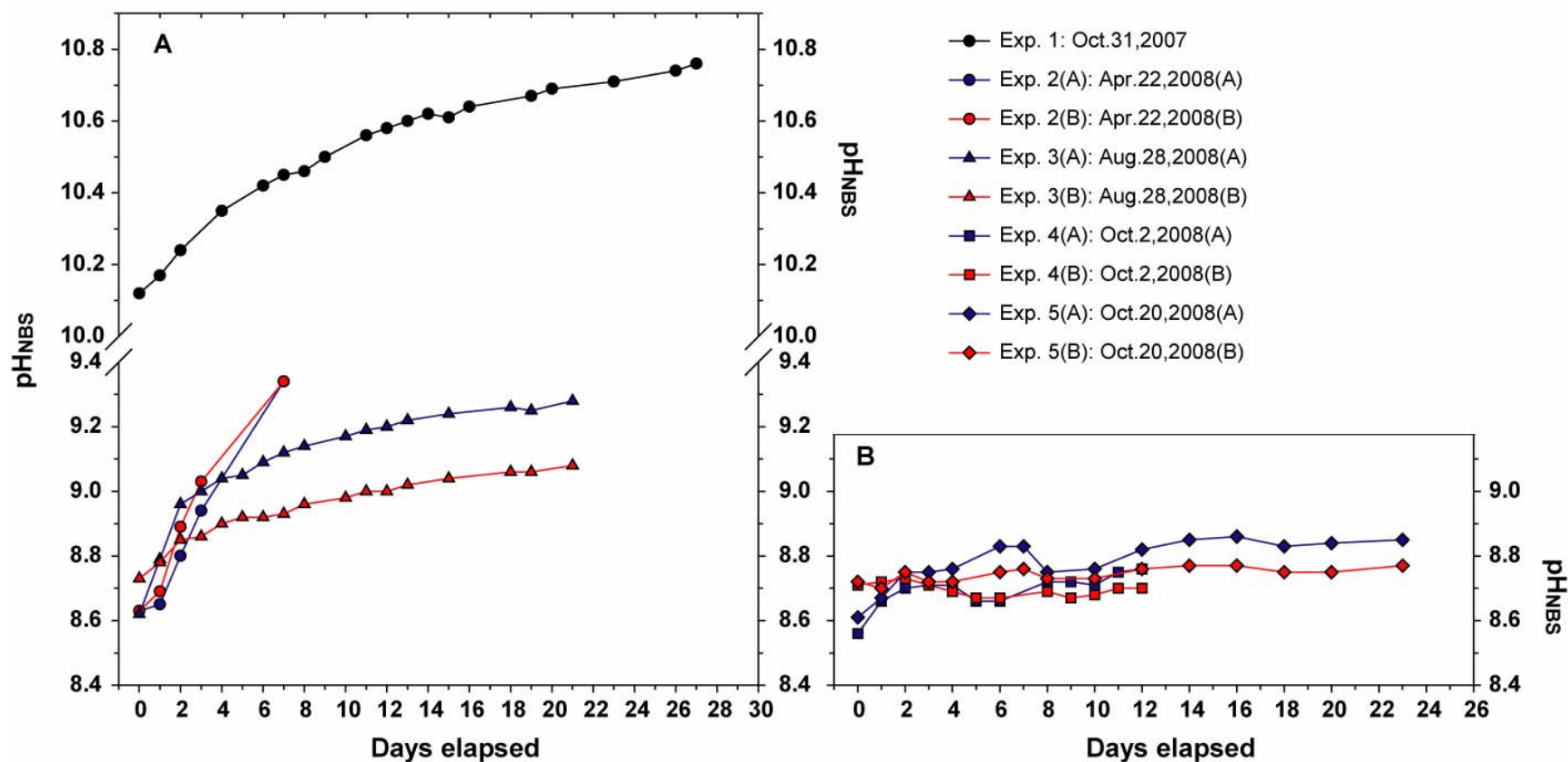
Figure 5.3 – pH variations during carbonate precipitation experiments monitored with VWR® Symphony SP70P (#14002-860) pH electrode with precision better than ± 0.01 pH units.

The pH drift was significantly reduced during Exp. 4 (A: ΔpH = 0.2, B: ΔpH = 0.06) and 5 (A: ΔpH = 0.25, B: ΔpH = 0.07) by adjusting $NaHCO_3$ and Na_2CO_3 concentrations to 60 and 20 mmol/kg H_2O, respectively (Fig. 5.3b). Notably, the pH drift in solutions (A) with lower boron concentration (B_T = 0.42 mmol/kg H_2O) was always larger than in solutions (B) with higher boron concentration (B_T = 7.9 mmol/kg H_2O). This should be expected, insofar as the boric acid is part of total seawater alkalinity. The degree of deviation from equilibrium conditions depends on the presence of a buffer in solution. At ~ 20 fold increase in B_T the buffer provided by the conversion of boric acid $B(OH)_3{}^o$ to borate $B(OH)_4{}^-$ is significant, suppressing any large perturbations in the carbonate system.

5.4.3 Boron concentration and isotopic composition

Aliquots of solutions collected during each of the completed precipitation experiments have been analyzed for boron concentration. A significant decrease in dissolved boron was observed during the experiments with no constant boron addition via titrants. For example, during aragonite precipitation in Exp. 1, boron concentration dropped ~ 6 fold from 6.4 to 1.58 mmol/kg H_2O; and during calcite precipitation in Exp. 2(A), boron concentration decreased from 10.47 to 7.56 mmol/kg H_2O. Ideally, it is desirable to maintain constant boron concentration throughout the duration of the precipitation experiment. To address this issue, boron was constantly supplied to the reaction vessel via a titrant at a 0.5 ml/h rate throughout the experiments. This adjustment resulted in a small overall increase in

Table 5.3 – Experimental details, boron isotope and concentration data. Boron concentration data has 5% uncertainty (at 95% confidence).

Experiment	Sample ID	Type	Duration hrs	carbonate recovered, mg	Ionic str.	pH drift min-max	pH, ave.	B, ppm	[B], mmol/kg H_2O	$\delta^{11}B$	2σ
1	**UMD Arag Oct3107**	**aragonite**	**648**	**~ 50**		**10.12 - 10.61**	**10.52**	**98**		**-9.73**	**0.19**
	UMD_Arag_Oct3107#1	starting solution			0.06				6.40		
	UMD_Arag_Oct3107#2	solution							5.28		
	UMD_Arag_Oct3107#3	solution							4.66		
	UMD_Arag_Oct3107#4	solution							4.66		
	UMD Arag Oct31-07#5	solution							3.27	-12.85	0.14
	UMD Arag Oct31-07#9	solution							2.62		
	UMD Arag Oct31-07#14	final solution							1.58	-12.78	0.15
2 (A)	**UMD Arag Apr2208A**	**calcite**	**168**	**60**		**8.63 - 9.34**	**8.87**	**124**		**-26.06**	**0.17**
	UMD Arag Apr2208 #1A	starting solution			0.79				10.47	-13.02	0.16
	UMD Arag Apr2208 #3A	solution							9.22		
	UMD Arag Apr2208 #4A	final solution							7.56	-12.94	0.19
2 (B)	**UMD Arag Apr2208B**	**calcite**	**168**	**80**		**8.63 - 9.34**	**8.92**	**140**			
	UMD Arag Arp2208 #1B	starting solution			0.79				9.91	-12.96	0.17
	UMD Arag Arp2208 #3B	solution							10.40		
	UMD Arag Arp2208 #4B	final solution							8.93	-12.88	0.16

Table 5.3 – *Continued…*

Experiment	Sample ID	Type	Duration hrs	carbonate recovered, mg	Ionic str.	pH drift min-max	pH, ave.	B, ppm	[B], mmol/ kg H₂O	δ¹¹B	2σ
3 (A)	Aug.28, 2008_ Arag(A)	aragonite	503	44.1		8.62 - 9.28	9.10	19		-20.88	0.20
	Aug.28, 2008_ Arag(A)#1	starting solution			0.71				0.42	-12.34	0.19
	Aug.28, 2008_ Arag(A)#5	solution							1.07		
	Aug.28, 2008_ Arag(A)#9	solution							1.36		
	Aug.28, 2008_ Arag(A)#13	final solution							1.67	-12.77	0.19
3 (B)	Aug.28, 2008_ Arag(B)	aragonite	503	44.7		8.73 - 9.08	8.95	107		-22.87	0.19
	Aug.28, 2008_ Arag(B)#1	starting solution			0.76				8.84	-12.83	0.19
	Aug.28, 2008_ Arag(B)#5	solution							8.82		
	Aug.28, 2008_ Arag(B)#9	solution							9.00		
	Aug.28, 2008_ Arag(B)#13	final solution							9.32	-12.83	0.17
4 (B)	Oct.2, 2008_Arag(B)	aragonite	276	26.7		8.67 - 8.73	8.70	163		-26.67	0.15
	Oct2 2008_Arag(B)#1	starting solution			0.77				8.25	-12.96	0.20
	Oct2 2008_Arag(B)#3	solution							8.63		
	Oct2 2008_Arag(B)#4	final solution							8.93	-12.92	0.20

Table 5.3 – *Continued…*

Experiment	Sample ID	Type	Duration hrs	carbonate recovered, mg	Ionic str.	pH drift min-max	pH, ave.	B, ppm	[B], mmol/ kg H$_2$O	δ^{11}B	2σ
5 (A)	**Oct.20, 2008_Arag(A)**	**aragonite**	**576**	**48.3**		**8.61 - 8.86**	**8.73**	**30**		**-25.23**	**0.20**
	Oct20 2008_Arag(A)#1	starting solution			0.71				0.45	-12.32	0.18
	Oct20 2008_Arag(A)#5	solution							1.79		
	Oct20 2008_Arag(A)#9	solution							2.97		
	Oct20 2008_Arag(A)#11	final solution							3.70	-12.86	0.19
5 (B)	**Oct.20, 2008_Arag(B)**	**aragonite**	**576**	**48.9**		**8.70 - 8.77**	**8.74**	**90**		**-25.99**	**0.15**
	Oct20 2008_Arag(B)#1	starting solution			0.76				7.98	-12.83	0.22
	Oct20 2008_Arag(B)#7	solution							8.64		
	Oct20 2008_Arag(B)#11	solution							9.24	-12.84	0.17
6 (A)	**Dec.19, 2008_BlankArag(A)**	**aragonite**	**715**	**59.3**		**8.67 - 9.05**		**0.63**			
	Dec.19, 2008_BlankArag(A)#1	starting solution			0.71				0.005		
	Dec.19, 2008_BlankArag(A)#5	final solution							0.008		
6 (B)	**Dec.19, 2008_BlankArag(B)**	**aragonite**	**715**	**69.0**		**8.67 - 9.03**		**0.21**			
	Dec.19, 2008_BlankArag(B)#1	starting solution			0.71				0.006		
	Dec.19, 2008_BlankArag(B)#5	final solution							0.008		

123

dissolved boron during experiments with higher starting boron abundances (Experiments (B): B_T = 7.9 mmol/kg H_2O). This increase was more pronounced during experiments with lower starting boron abundances (Experiments (A): B_T = 0.42 mmol/kg H_2O). As expected, boron concentrations were higher in carbonates precipitated from solutions with higher boron abundances relative to those with lower boron abundances.

The boron concentration in blank solutions (Exp. 6 (A, B)) was found to be as low as 0.005-0.008 mmol/kg H_2O, which is two to three orders of magnitude lower than those in the experiments. Similarly, boron concentrations in blank carbonates were found to be 3-4 orders of magnitude lower than those of other precipitates with boron in starting solutions.

Boron isotope analyses of both starting and final solutions for each experiment have shown that the boron isotopic composition of the parent solutions remained unchanged (-12.92 ± 0.25‰ (2σ), except for the Exp. 3(A) where δ^{11}B of solutions increased from -12.34 ± 0.19‰ to -12.77 ± 0.19‰). Small solution δ^{11}B variations during the precipitation cannot be absolutely ruled out at this point in the experiments; future analyses of the remaining solution aliquots will address this question.

Boron concentrations and isotopic compositions in the inorganic calcite and aragonite materials were in the range of abundances and compositions of natural biogenic carbonates. Boron concentrations ranged from 19 to 163 ppm. Boron isotopic compositions have demonstrated distinctly light boron isotope signatures

124

ranging from -20.88 ± 0.20‰ (2σ) to -26.06 ± 0.17‰ (2σ) compared to parent

solution -12.92 ± 0.25‰ (2σ). The magnitude of the offset towards lighter values in

carbonates compared to the parent solution is typical for marine carbonates.

5.4.4 Boron speciation

To determine boron speciation in carbonates across the range of experimental

pH conditions from 8.6 to 10, inorganic carbonates precipitated during this study have

been analyzed by ^{11}B MAS NMR (Klochko et al., 2009). Unfortunately, the results

of this effort are as yet inconclusive. The few analyses attempted thus far produced

anomalously low spectra, which are undistinguishable from the background spectra.

Such problems typically occur when the abundance of boron in the precipitates is too

low and below detection limits. However, total boron abundances in the experimental

carbonates determined by MC-ICPMS are high and are comparable with those of the

natural carbonates analyzed in Klochko et al. (2009). Therefore, there is likely to be a

different explanation for the lack of signal in the present sample set, which is likely

the result of insufficient material for the NMR analysis. Typically ~ 200 mg of

carbonate material is used; however, due to the slow growth of aragonite and calcite

in our equilibrium experiments, the largest sample produced for the NMR analyses

was ~80 mg. It seems most likely that this sample size is too small and increasing

yields (hence longer reactions) from the precipitation experiments will help in the

future NMR analyses of boron speciation.

5.4.5 $\delta^{11}B$ – pH calibration

Insofar as the pH stability was achieved during three of the inorganic

carbonate precipitation experiments in this study, the results of these – Exp. 4(B),

Exp. 5(A) and Exp.(B) – are of special interest for our δ^{11}B-pH calibration study.

The pH variability during these experiments has been especially low during

experiments (B) with higher boron concentration $B_T = 7.9$ mmol/kg H_2O (Fig. 5.3b),

which allows us to put a solid constraint on the boron isotopic composition of the

inorganic aragonite at pH ranges 8.67-8.73 and 8.70-8.77 (Exp. 4(B) and 5(B),

respectively).

The boron isotopic composition of inorganic aragonites precipitated in this

study (Exp. 4(B), Exp. 5(A) and Exp.(B)) at pH ~ 8.7, as well as results of previous

culture and precipitation studies across the pH range of interest are plotted in Fig.5.4.

In order to plot the results of the three experiments of this study, pH values

determined in this study on the "NBS" pH scale were converted to the "total" pH

scale using -0.14 correction factor. The values not corrected for "NBS" are also

plotted for comparison. Within analytical uncertainty, there is no observed difference

in isotopic composition between the aragonite samples precipitated in high-boron and

low-boron solutions at pH ~8.7.

Most importantly, the boron isotopic composition of all three aragonite

samples reflect the boron isotopic composition of aqueous borate predicted using the

the $^{11-10}K_B = 1.0272$ (boron fractionation factor) empirically determined by Klochko

et al., 2006. We thus conclude that boron incorporation into inorganic aragonite
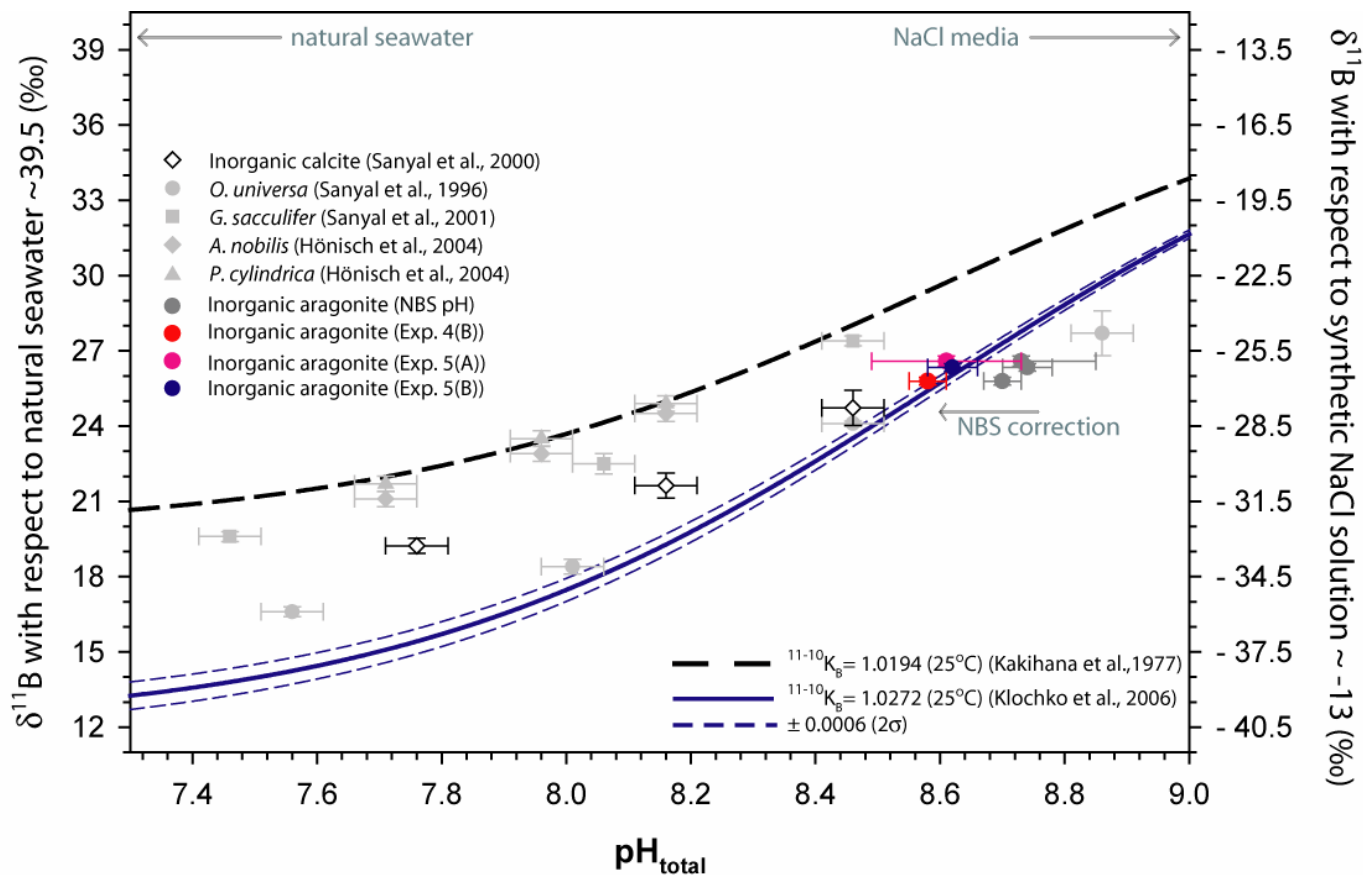
Figure 5.4 – The results of the biogenic carbonates culture experiments (Sanyal et al., 1996; 2001; Hönisch et al., 2004), inorganic calcite precipitation experiments (Sanyal et al., 2000) and inorganic aragonite precipitation experiments (this study: Exp.4(B), 5(A), 5(B)). The pH_{NBS} values from this study and (Sanyal et al., 1996; 2000; 2001) were recalculated to fit the total pH scale ($pH_T = pH_{NBS} - 0.14$). Data from this study, not corrected for "NBS" is plotted in dark grey for comparison.

occurs via preferential uptake of borate ions from solution without isotope fractionation at pH range of parent solutions 8.67-8.73 and 8.70-8.77. The NMR study (Chapter 3; Klochko et al. 2009), however, shows almost equal abundances of borate ion and boric acid in the biogenic samples. Coupled together these observations suggest that structural rearrangement of borate ion must occur during mineral incorporation without further fractionation (Klochko et al., 2009).

Furthermore, the fact that these inorganic precipitates formed at pH ~8.7 fall exactly on the predicted isotopic composition for solution borate ion supports the view that observed ^{11}B enrichments observed in cultured biogenic aragonite relative to aqueous borate ion (Hönisch et al., 2004) may be a purely biological effect driven by pH increase at the site of calcification in corals.

5.4.6 *Future work*

It is too soon to predict whether samples precipitated at higher and lower pH will also confirm our previous study of the boron isotope fractionation constant (Klochko et al., 2006). However, the success in the experiments at pH ~8.7 justify the feasibility of our analytical design and measurements. Once completed, with both aragonite and calcite precipitates grown across the pH interval of interest and measured by both NMR and MC-ICPMS techniques, this study should provide the most rigorously constrained working curve relating δ^{11}B compositions in ancient inorganic carbonates with paleo-pH estimates.

CHAPTER 6 - CONCLUSIONS

The boron isotopic composition measured in marine carbonates is considered to be a tracer of seawater pH. However, an accurate application of this proxy has been hampered by our lack of intimate understanding of chemical kinetics and thermodynamic isotope exchange between the two dominant boron-bearing species in seawater: boric acid $B(OH)_3^o$ and borate ions $B(OH)_4^-$, as well as their subsequent partitioning into a carbonate lattice. In this dissertation I have taken on a task of a systematic empirical re-evaluation of the fundamental parameters and assumptions, on which boron isotope paleo-pH proxy is based. As a result of this research we have come to strikingly different values of the boron isotope exchange constant in solution, boron speciation and partitioning in carbonates, suggesting that the most parameters and assumptions that were believed to be previously constrained and have been widely applied to the $\delta^{11}B$-pH reconstructions were incorrect.

Our empirical analysis of the boron isotope fractionation constant between dissolved boron species ($B(OH)_3^o$ and $B(OH)_4^-$) have shown a significantly larger value $^{11-10}K_B = 1.0272 \pm 0.0006$ (2σ) than a widely used theoretical estimate of 1.0194 (Kakihana et al., 1977). Determination of this constant in various media, temperature and total boron concentrations presented here in Chapters 2-3 and in Klochko et al. (2006) is an important milestone on our way to better understanding of the boron isotopic signatures observed in marine carbonates, especially because it has highlighted more discrepancies in our current view of the proxy.

More specifically, a thorough evaluation of empirical $\delta^{11}B$-pH calibrations of cultured foraminifera, corals and inorganic precipitates (Sanyal et al., 1996; Sanyal et

al., 2000; Sanyal et al., 2001; Hönisch et al., 2004), which have been used to validate

the applicability of the proxy, has shown that none of the data sets have reflected

boron isotopic composition of the aqueous borate (believed to be preferentially

uptaken by the marine carbonates); and there are significant offsets in isotopic

composition between the datasets. These discrepancies between the experimentally

predicted boron isotopic composition of aqueous borate and the isotopic composition

of the calibrated carbonates have led us to propose that (a) species vital effects, and

particularly the pH modification in the micro-environments of biogenic calcifiers;

combined with (b) pH-dependent incorporation of both boron species into a

carbonates, could result in unique slightly heavier isotopic signatures (Klochko et al.,

2006; Klochko et al., 2009).

Our own investigation of boron structural composition in modern marine

carbonates of different mineralogy (calcite and aragonite) calcified in modern

seawater (pH ~ 8.2) has indeed shown dual presence of trigonally-coordinated boric

acid and tetrahedrally-coordinated borate in almost equal abundances (Chapter 4;

Klochko et al., 2009). The results were contrary to the findings of the previous and

the only study of boron speciation in carbonates, which reported 100% trigonal

presence in aragonite and 90% tetrahedral presence in calcite (Sen et al., 1994).

Although such large presence of trigonal boric acid reported in both studies cannot be

entirely attributed to the boric acid incorporation directly from seawater, some

fractional boric acid incorporation into carbonates cannot be ruled out, especially at

pH < 8.6.

To date, the community has recognized the importance of our new empirical constant and several publications have considered it in their reconstructions of paleo-pH (Foster, 2008; Hönisch et al., 2008; Kasemann et al., 2009; Liu et al., 2009; Wei et al., 2009). However, it is important to realize that the boron isotope fractionation constant determined in Klochko et al. (2006) is only applicable to the isotope exchange between boric acid and borate in solution. Further investigation of potential boron isotopic fractionation associated with inorganic and biological effects during carbonate precipitation is needed to constrain the proxy. In the absence of a detailed knowledge of said effects, different groups have chosen various approaches for their paleo-pH reconstructions. For example, in their reconstruction of the deep water Pleistocene pH variations using benthic foraminifera, Hönisch et al. (2008) have chosen to use Kakihana's relationship ($^{11-10}K_B = 1.0194$) combined with constant species-specific downward offset inferred from the earlier calibration study (Sanyal et al., 2001). Paleo reconstructions of surface pH of mid-late Holocene in South China Sea (Liu et al., 2009) and ocean acidification during the last 200 years in the Great Barrier Reef (Wei et al., 2009) using *Porites* fossilized corals, have also applied Kakihana's value ($^{11-10}K_B = 1.0194$) with no additional correction factors. Alternatively, a reconstruction of pH variations in the Caribbean Sea during the last 130 Kyr using planktonic foraminifera (Foster, 2008) has applied the new empirical constant of $^{11-10}K_B = 1.0272$ (Klochko et al., 2006) combined with a $+ 0.8$‰ "vital effect" correction factor, which was obtained in their own core-top $\delta^{11}B$-pH calibration.

Regardless of the choice of the constant applied in these studies, all publications agree that there is a lack of understanding of biological effects on the boron isotopic composition of the marine carbonates, and until those are constrained the reconstruction of the absolute paleo-pH changes will remain a challenge. Moreover, the situation is complicated by our inability to predict purely inorganic effects associated with the potential pH-dependent boric acid partitioning into the carbonates at pH < 8.6. To this end we have initiated a δ^{11}B-B speciation-pH calibration project designed to investigate boron isotope fractionation and speciation in inorganic carbonates precipitated across a range of pH conditions. Although this project is still underway, our results obtained from the aragonite precipitates grown at pH range of parent solutions 8.67-8.73 and 8.70-8.77 are in excellent agreement with the boron isotopic composition of the aqueous borate predicted by the empirical $^{11-10}K_B$ = 1.0272 determined in Klochko et al. (2006), suggesting the boron incorporation into inorganic aragonite occurs via preferential uptake of borate ions from solution without isotope fractionation at this pH range.

Our future efforts will be directed to extending these precipitation experiments to pH ranges lower and higher then ~ 8.7, and inorganic calcite, which would provide the community with an important inorganic baseline for the future calibration studies.

BIBLIOGRAPHY

Al-Horani F. A., Al-Moghrabi S. M., and de Beer D. (2003) The mechanism of calcification and its relation to photosynthesis and respiration in the scleractinian coral *Galaxea fascicularis*. *Marine Biology* **142**, 419–426.

Allemand D., Tambutte E., Girard J.-P., and Jaubert J. (1998) Organic matrix synthesis in the scleractinian coral stylophora pistillata: role in biomineralization and potential target of the organotin tributyltin. *Journal of Experimental Biology* **201**, 2001-2009.

Baes C. F. and Mesmer R. E. (1976) *The Hydrolysis of Cations*. Wiley-Interscience, John Wiley and sons. New York. pp. 512.

Berner R. A. (1975) The role of magnesium in the crystal growth of calcite and aragonite from seawater. *Geochimica et Cosmochimica Acta* **39**, 489-504.

Berner R. A. (1978) Equilibrium kinetics, and the precipitation of magnesium calcite from seawater. *American Journal of Science* **278**, 1435-1477.

Berner R. A. (2004) A model for calcium, magnesium and sulfate in seawater over Phanerozoic time. *American Journal of Science* **304**, 438-453.

Bevington P. R. and Robinson D. K. (2003) *Data reduction and error analysis for the physical sciences*. McGraw-Hill.

Blanchon P. and Shaw J. (1995) Reef drowning during the last deglaciation: Evidence for catastrophic sea-level rise and ice-sheet collapse. *Geology* **23**, 4-8.

Broeker W. S. and Denton G. H. (1990) What drives glacial cycles? *Scientific American* **January**, 48-56.

Byrne R. H. and Kester D. R. (1974) Inorganic speciation of boron in seawater. *Journal of Marine Research* **32**, 119-127.

Byrne R. H. (1987) Standardization of standard buffers by visible spectrometry. *Analytical Chemistry* **59**, 1479-1481.

Byrne R. H., McElligott S., Feely R. A., and Millero F. J. (1999) The role of pH_T measurements in marine CO_2-system characterizations. *Deep-Sea Research* **46**, 1985-1997.

Byrne R. H., Yao W., Klochko K., Tossell J. A., and Kaufman A. J. (2006) Experimental evaluation of the isotopic exchange equilibrium $^{10}B(OH)_3 + ^{11}B(OH)_4^- = ^{11}B(OH)_3 + ^{10}B(OH)_4^-$ in aqueous solution. *Deep-Sea Research Part I* **53**, 684-688.

Caldeira K. and Berner R. A. (1999) Seawater pH and the atmospheric carbon dioxide. *Science* **286**, 2043a.

Catanzaro E. J., Champion C. E., Garner E. L., Marinenko G., Sappenfield K. M., and Shields W. R. (1970) Boric acid; isotopic and assay standard reference materials, Vol. 260-17 (ed. U. N. B. o. Standards).

Clayton T. D. and Byrne R. H. (1993) Spectrophotometric pH measurements: total hydrogen ion concentration scale measurements and at-sea results. *Deep-Sea Research* **40**, 2115-2129

Clayton T. D., Byrne R. H., Breland J. A., Feely R. A., Millero F. J., Campbell D. M., Murphy P. P., and Lamb M. F. (1995) The role of pH measurements in modern oceanic CO_2-system characterizations: Precision and thermodynamic consistency. *Deep-Sea Research* **42**, 411-429.

Cobb K. M., Hunter D. E., and Charles C. D. (2001) A central tropical Pacific coral demonstrates Pacific, Indian, and Atlantic decadal climate connections. *Geophysical Research Letters* **28**, 2209-2212.

Cobb K. M., Charles C. D., Edwards R. L., Cheng H., and Kastner M. (2003) El Niño Southern Oscillation and tropical Pacific climate during the last millennium. *Nature* **424**, 271-276.

Cohen A. and McConnaughey T. A. (2003) Geochemical perspectives on coral mineralization. *Reviews in Mineralogy and Geochemistry* **54**, 151-187.

Cohen M. H. and Reif F. (1957) Quadrupole effects in nuclear magnetic resonance studies of solids. *Solid State Physics* **5**, 322-348.

Cotton F. A. and Wilkinson G. (1972) *Advanced inorganic chemistry*. John Wiley and Sons Interscience. New York. pp. 1145.

Culberson C. and Pytkowicz R. M. (1968) Effect of pressure on carbonic acid, boric acid and the pH in seawater. *Limnology and Oceanography* **13**, 403-417.

Dickson A. G. (1990) Thermodynamics of the dissociation of boric acid in synthetic seawater from 273.15 to 318.15 K. *Deep-Sea Research* **37**, 755–766.

Dickson A. G. and Goyet C. (1994) Handbook of methods for the analysis of the various parameters of the carbon dioxide system in sea water (ed. O. R. N. L. Carbon Dioxide Information Analysis Center). U.S. Department of Energy.

Dyrssen D. and Hansson I. (1973) Ionic medium effects in sea water - a comparison of acidity constants of carbonic acid in sodium chloride and synthetic seawater. *Marine Chemistry* **1**, 137-149.

Erez J. (2003) The source of ions for biomineralization in foraminifera and their implications for paleoceanographic proxies. *Reviews in Mineralogy and Geochemistry* **54**, 115-149.

Fallon S. J., McCulloch M. T., Van Woesik R., and Sinclair D. J. (1999) Corals at their latitudinal limits: Laser ablation trace element systematics in Porites from Shirigai Bay, Japan. *Earth and Planetary Science Letters* **172**, 221-238.

Feely R. A., Sabine C. L., Lee K., Berelson W., Kleypas J., Fabry V. J., and Millero F. J. (2004) Impact of anthropogenic CO_2 on the $CaCO_3$ system in the oceans. *Science* **305**, 362-366.

Feng J., Lee Y. J., Reeder R. J., and Phillips B. L. (2006) Observation of bicarbonate in calcite by NMR spectroscopy. *American Mineralogist* **91**, 957-960.

Foster G. L. (2008) Seawater pH, pCO_2 and $[CO_3^{2-}]$ variations in the Caribbean Sea over the last 130 kyr: A boron isotope and B/Ca study of planktic foraminifera. *Earth and Planetary Science Letters* **271**, 254-266.

Gallup C. D., Edwards R. L., and Johnson R. G. (1994) The timing of high sea levels over the past 200,000 years. *Science* **263**, 796-800.

Gallup C. D., Cheng H., Taylor F. W., and Edwards R. L. (2002) Direct determination of the timing of sea level change during termination II. *Science* **295**, 310-313.

Ganapathy S., Schramm S., and Oldfield E. (1982) Variable-angle sample-spinning high resolution NMR of solids. *Journal of Chemical Physics* **77**, 4360-4365.

Gillardet J. and Allègre C. J. (1995) Boron isotopic compositions of corals: seawater or diagenesis record? *Earth and Planetary Science Letters* **136**, 665-676.

Hansson I. (1973) A new set of acidity constants for carbonic acid nd boric acid in sea water. *Deep-Sea Research* **20**, 461-478.

Hardie L. A. (1996) Secular variation in seawater chemistry: An explanation for the coupled secular variation in the mineralogies of marine limestones and potash evaporites over the past 600 my. *Geology* **24**, 279-283.

Hemming N. G. and Hanson G. N. (1992) Boron isotopic composition and concentration in modern marine carbonates. *Geochimica et Cosmochimica Acta* **56**, 537-543.

Hemming N. G., Reeder R. J., and Hanson G. N. (1995) Mineral-fluid partitioning and isotopic fractionation of boron in synthetic calcium carbonate. *Geochimica et Cosmochimica Acta* **59**, 371-379.

Hemming N. G., Reeder R. J., and Hart S. R. (1998) Growth-step-selective incorporation of boron on calcite surface. *Geochimica et Cosmochimica Acta* **62**, 2915-2922.

Hershey J. P., Fernandez M., Milne P. J., and Millero F. J. (1986) The ionization of boric acid in NaCl, Na-Ca-Cl and Na-Mg-Cl solutions at 25ºC. *Geochimica et Cosmichimica Acta* **50**, 143-148.

Hirao T., Kotaka M., and Kakihana H. (1979) Raman spectra of polyborate ions in aqueous solution. *Journal of inorganic Nuclear Chemistry* **41**, 1217-1220.

Hoffman P. F., Kaufman A. J., Halverston G. P., and Schrag D. P. (1998) A Neoproterozoic snowball Earth. *Science* **281**, 1342-1346.

Hönisch B. and Hemming N. G. (2004) Ground-truthing the boron isotope-paleo-pH proxy in planktonic foraminifera shells: Partial dissolution and shell size effects. *Paleoceanography* **19, doi: 10.1029/2004PA001026**.

Hönisch B., Hemming N. G., Grottoli A. G., Amat A., Hanson G. N., and Bijma J. (2004) Assessing scleractinian corals as recorders for paleo-pH: Empirical calibration and vital effects. *Geochimica et Cosmochimica Acta* **68**, 3675-3685.

Hönisch B. and Hemming N. G. (2005) Surface ocean pH responce to variations in pCO$_2$ through two full glacial cycles. *Earth and Planetary Science Letters* **236**, 305-314.

Hönisch B., Bickert T., and Hemming N. G. (2008) Modern and Pleistocene boron isotope composition of the benthic foraminifer *Cibicidoides wuellerstorfi*. *Earth and Planetary Science Letters* **272**, 309-318.

Imbrie J., Berger A., Boyle E. A., Clemens S. C., Duffy A., Howard W. R., Kukla G., Kutzbach J. E., Martinson D. G., McIntyre A., Mix A. C., Molfino B., Morley J. J., Peterson L. C., Pisias N. G., Prell W. L., Raymo M. E., Shackleton N. J., and J.R. T. (1993) On the structure and origin of major glaciation cycles, 2. The 100,00-year cycle. *Paleoceanography* **8**, 699-735.

Ingri N. (1963) Equilibrium studies of polyanions containing B^{III}, Si^{IV}, Ge^{IV} and V^{V}. *Svensk Kemisk Tidskrift* **75**(4), 199-230.

IPCC. (2001) *Climate Change 2001: The scientific basis. Contribution of the working group I to the third assessment report of the Intergovernmental Panel on Climate Change (IPCC)*. Cambridge University Press, UK.

Jabo A. (2001) The Fractionation of carbon and nitrogen isotopes in scleractinian corals. M.Sc. thesis, University of Maryland.

Jorgensen B. B., Erez J., Revsbech N. P., and Cohen Y. (1985) Symbiotic photosynthesis in a planktonic foraminifera *Globigerinoides sacculifer* (Brady), studied with microelectrodes. *Limnological Oceanography* **30**(6), 1253-1267.

Kakihana H. and Kotaka M. (1977) Equilibrium constants for boron isotope-exchange reactions. *Bulletin of the Research Laboratory for Nuclear Reactors* **2**, 1-12.

Kakihana H., Kotaka M., Satoh S., Nomura M., and Okamoto M. (1977) Fundamental studies on the ion-exchange separation of boron isotopes. *Bulletin of Chemical Society of Japan* **50**, 158–163.

Kasemann S. A., Hawkesworth C. J., Prave A. R., Fallick A. E., and Pearson P. N. (2005) Boron and calcium isotope composition in Neoproterozoic carbonate rocks from Namibia: evidence for extreme environmental change. *Earth and Planetary Science Letters* **231**, 73-86.

Kasemann S. A., Schmidt D. N., Bijma J., and Foster G. L. (2009) In situ boron isotope analysis in marine carbonates and its application for foraminifera and palaeo-pH. *Chemical Geology* **260**, 138-147.

Kelley D. S., Karson J. A., Blackman D. K., Früh-Green G. L., Butterfield D. A., Lilley M. D., Olson E. J., Schrenk M. O., Roe K. K., Lebon G. T., and Rivizzigno P. (2001) An off-axis hydrothermal vent field near the Mid-Atlantic Ridge at 30°N. *Nature* **412**, 145-149.

Kelley D. S., Karson J. A., Früh-Green G. L., Yoerger D., Shank T. M., Butterfield D. A., Hayes J. M., Schrenk M. O., Olson E. G., Proskurowski G., Jakuba M., Bradley A., Larson B., Ludwig K., Glickson D., Buckman K., Bradley A. S., Brazelton W. J., Roe K., Elend M. J., Delacour A., Bernasconi S. M., Lilley M. D., Baross J. A., Summons R. E., and Sylva S. P. (2005) A serpentinite-hosted submarine ecosystem: The Lost City Hydrothermal Field. *Science* **307**, 1428-1434.

Kilbourne K., Quinn T. M., Taylor F., Delcroix T., and Gouriou Y. (2004a) ENSO-related Salinity Variations Recorded in the Skeletal Geochemistry of a Porites Coral from Espiritu Santo, Vanuatu. *Paleoceanography* **19(4)** PA4002 10.1029/2004PA001033.

Kilbourne K., Quinn T. M., and Taylor F. (2004b) A fossil coral perspective on western tropical Pacific climate ~350 ka. *Paleoceanography* **19(1)**, PA1019, 10.1029/2003PA000944.

Kim S.-T., Hillaire-Marcel C., and Mucci A. (2006) Mechanisms of equilibrium and kinetic oxygen isotope effects in synthetic aragonite at 25°C. *Geochimica et Cosmochimica Acta* **70**, 5790–5801.

137

Klochko K., Kaufman A. J., Yao W., Byrne R. H., and Tossell J. A. (2006) Experimental measurement of boron isotope fractionation in seawater. *Earth and Planetary Science Letters* **248**, 261–270.

Klochko K., Cody G. D., Tossell J. A., Przemyslaw D., and Kaufman A. J. (2009) Re-evaluating boron speciation in biogenic calcite and aragonite using ^{11}B MAS NMR. *Geochimica et Cosmochimica Acta* **73**, 1890-1900.

Lemarchand D., Gaillardet J., Lewin É., and Allègre C. J. (2002) Boron isotope systematics in large rivers: implications for the marine boron budget and paleo-pH reconstruction over the Cenozoic. *Chemical Geology* **190**, 123-140.

Liu Y. and Tossell J. A. (2005) *Ab initio* molecular orbital calculations for boron isotope fractionations on boric acids and borates. *Geochimica et Cosmochimica Acta* **69**, 3995-4006.

Liu Y., Liu W., Peng Z., Xiao Y., Wei G., Sun W., He J., Liu G., and Chou C.-L. (2009) Instability of seawater pH in the South China Sea during the mid-late Holocene: Evidence from boron isotopic composition of corals. *Geochimica et Cosmochimica Acta* **73**, 1264-1272.

Ludwig K. A., Kelley D. S., Butterfield D. A., Nelson B. K., and Früh-Green G. (2006) Formation and evolution of carbonate chimneys at the Lost City Hydrothermal Field. *Geochimica et Cosmochimica Acta* **70**, 3625-3645.

Lyman J. (1956) Buffer mechanisms of seawater, University of California.

Massiot D., Fayon F., Capron C., King I., Le Calvé S., Alonso B., Durand J.-O., Bujoli B., Gan Z., and Hoatson G. (2002) Modelling one- and two-dimensional solid-state NMR spectra. *Magnetic Resonance in Chemistry* **40**, 70-76.

McElligott S. and Byrne R. H. (1998) Interaction of $B(OH)_3^0$ and HCO_3^- in seawater: formation of $B(OH)_2CO_3^-$. *Aquatic Geochemistry* **3**, 345-356.

McIntyre A., Ruddiman W. F., Karlin K., and Mix A. C. (1989) Surface water response of the equatorial Atlantic Ocean to orbital forcing. *Paleoceanography* **4**, 19-55.

Millero F. J., Lee K., and Roche M. P. (1998) Distribution of alkalinity in the surface waters of the major oceans. *Marine Chemistry* **60**, 111 – 130.

Morse J. W. and Mackenzie F. T. (1990) *Geochemistry of Sedimentary Carbonates*. Elsevier.

Mucci A. (1986) Growth kinetics and composition of magnesian calcite overgrowths precipitated from seawater: Quantitative influence of orthophosphate ions. *Geochimica et Cosmochimica Acta* **50**, 2255-2265.

Oi T., Kato J., Ossaka T., and Kakihana H. (1991) Boron isotope fractionation accompanying boron mineral formation from aqueous boric acid-sodium hydroxide solutions at 25°C. *Geochemical Journal* **25**, 377-385.

Oi T. (2000a) Calculations of reduced partition function ratios of monomeric and dimeric boric acids and borates by the ab initio molecular orbital theory. *Journal of Nuclear Science and Technology* **37**, 166-172.

Oi T. (2000b) *Ab initio* molecular orbital calculations of reduced partition function ratios of polyboric acids and polyborate anions. *Zeitschrift für Naturforschung* **55a**, 623-628.

Oi T. and Yanase S. (2001) Calculations of reduced partition function ratios of hydrated monoborate anion by the *ab initio* molecular orbital theory. *Journal of Nuclear Science and Technology* **38**, 429-432.

Pagani M., Lemarchand D., Spivack A., and Gaillardet J. (2005) A critical evaluation of the boron isotope-pH proxy: The accuracy of ancient ocean pH estimates. *Geochimica et Cosmochimica Acta* **69**, 953-961.

Palmer M. R., Spivack A. J., and Edmond J. M. (1987) Temperature and pH controls over isotopic fractionation during adsorption of boron on marine clay. *Geochimica et Cosmochimica Acta* **51**, 2319–2323.

Palmer M. R., Pearson P. N., and Cobb S. J. (1998) Reconstructing past ocean pH-depth profiles. *Science* **282**, 1468-1471.

Palmer M. R. and Pearson P. N. (2003) A 23,000-year record of surface water pH and pCO2 in the western equatorial Pacific Ocean. *Science* **300**, 480-482.

Pearson P. N. and Palmer M. R. (1999) Middle Eocene seawater pH and atmospheric carbon dioxide concentrations. *Science* **284**, 1824-1826.

Pearson P. N. and Palmer M. R. (2000) Atmospheric carbon dioxide over the past 60 million years. *Nature* **406**, 695-699.

Pelejero C., Calvo E., McCulloch M. T., Marshall J. F., Cagan M. K., Lough J. M., and Opdyke B. N. (2005) Preindustrial to modern interdecadal variability in coral reef pH. *Science* **309**, 2204-2207.

Petit J. R., Jouzel J., Raynaud D., Barkov N. I., Barnola J.-M., Basile I., Benders M., Chappellaz J., Davis M., Delayque G., Delmotte M., Kotlyakov V. M.,

Legrand M., Lipenkov V. Y., Lorius C., Pépin L., Ritz C., Saltzman E., and Stievenard M. (1999) Climate and atmospheric history of the past 420,000 years from the Vostok ice core, Antarctica. *Nature* **399**, 429-436.

Plummer L. N. and Busenberg E. (1982) The solubilities of calcite, aragonite and vaterite in CO_2-H_2O solutions between 0-90°C and an evaluation of the aqueous model for the system $CaCO_3$-CO_2-H_2O. *Geochimica et Cosmochimica Acta* **46**, 1011-1040.

Prothero D. R. and Schwab F. L. (2003) *Sedimentary geology: an introduction to sedimentary rocks and stratigraphy*. Macmillan.

Quinn T. M., Taylor F. W., Crowley T. J., and Link S. M. (1996) Evaluation of sampling resolution in coral stable isotope records: A case study using records from New Caledonia and Tarawa. *Paleoceanography* **11**, 529-542.

Quinn T. M., Taylor F. W., Crowley T. J., Henin C., Joannot P., and Join Y. (1998) A multi-century coral stable isotope record from a New Caledonia coral: Interannual and decadal sea surface temperature variability in the southwest Pacific since 1957 A.D. *Paleoceanography* **13**, 412-426.

Quinn T. M. and Sampson D. E. (2002) A multiproxy approach to reconstructing sea surface conditions using coral skeleton geochemistry. *Paleoceanography* **17**, 1062.

Roy R. N., Roy L. N., Vogel K. M., Moore C. P., Pearson T., Good C. E., and Millero F. J. (1993) Thermodynamics of the dissociation of boric acid in seawater. *Marine Chemistry* **44**, 243-248.

Sanchez-Valle C., Reynard B., Daniel I., Lecuyer C., Martinez I., and Chervin J.-C. (2005) Boron isotopic fractionation between minerals and fluids: New insights from in situ high pressure-high temperature vibrational spectroscopic data. *Geochimica et Cosmochimica Acta* **69**, 4301-4313.

Sandberg P. A. (1983) An oscillating trend in Phanerozoic nonskeletal carbonate mineralogy. *Nature* **305**, 19-22.

Sanyal A., Hemming N. G., Hanson G. N., and Broecker W. S. (1995) The pH of the glacial ocean as reconstructed from boron isotope measurements on foraminifera. *Nature* **373**, 234-236.

Sanyal A., Hemming N. G., Broecker W. S., Lea D. W., Spero H. J., and Hanson G. N. (1996) Oceanic pH control on the boron isotopic composition of foraminifera: Evidence from culture experiments. *Paleoceanography* **11**, 513-517.

Sanyal A., Hemming N. G., and Broecker W. S. (1997) Changes in pH in the eastern equatorial Pacific across stage 5-6 boundary based on boron isotopes in foraminifera. *Global Biogeochemical Cycles* **11**, 125-133.

Sanyal A., Nugent M., Reeder R. J., and Bijma J. (2000) Seawater pH control on the boron isotopic composition of calcite: Evidence from inorganic calcite precipitation experiments. *Geochimica et Cosmochimica Acta* **64**, 1551-1555.

Sanyal A., Bijma J., Spero H. J., and Lea D. W. (2001) Empirical relationship between pH and the boron isotopic composition of *G. sacculifer*: Implications for the boron isotope paleo-pH proxy. *Paleoceanography* **16**, 515-519.

Sen S., Stebbins J. F., Hemming N. G., and Ghosh B. (1994) Coordination environments of boron impurities in calcite and aragonite polymorphs: An ^{11}B MAS NMR study. *American Mineralogist* **79**, 818-825.

Sigman D. and Boyle E. (2000) Glacial/Interglacial variations in atmospheric carbon dioxide. *Nature* **407**, 859-869.

Sonoda A., Makita Y., Ooi K., Takagi N., and Hirotsu T. (2000) pH-dependence of the fractionation of boron isotopes with N-Methyl-D-Glucamine resin in aqueous solution systems. *Bulletin of Chemical Society of Japan* **73**, 1131-1133.

Spivack A. J. and Edmond J. M. (1987) Boron isotope exchange between seawater and the oceanic crust. *Geochimica et Cosmochimica Acta* **51**, 1033-1043.

Spivack A. J., You C. F., and Smith H. J. (1993) Foraminiferal boron isotope ratios as a proxy for surface ocean pH over the past 21 Myr. *Nature* **363**, 149-151.

Spivack A. J. and You C.-F. (1997) Boron isotopic geochemistry of carbonates and pore waters, Ocean Drilling Program Site 851. *Earth and Planetary Science Letters* **152**, 113-122.

Stanley S. M. and Hardie L. A. (1998) Secular oscillations in the carbonate mineralogy of reef-building and sediment-producing organisms driven by tectonically forced shifts in seawater chemistry. *Palaeogeography, Palaeoclimatology, Palaeoecology* **144**, 3-19.

Sundquist E. T. (1999) Seawater pH and atmospheric carbon dioxide. *Science* **286**, 2043a.

Tossell J. A. (2006) Boric acid adsorption on humic acids: Ab initio calculation of structures, stabilities, ^{11}B NMR and [11]B,[10]B isotopic fractionations of surface complexes *Geochimica et Cosmochimica Acta* **70**, 5089-5103.

Tossell J. A. (unpublished).

Urey H. C. (1947) The thermodynamic properties of isotopic substances. *Journal of Chemical Society* **57**, 562-581.

Vengosh A., Kolodny Y., Starinsky A., Chivas A. R., and McCulloch M. T. (1991) Coprecipitation and isotopic fractionation of boron in modern biogenic carbonates. *Geochimica et Cosmochimica Acta* **55**, 2901-2910.

Wei G., McCulloch M. T., Mortimer G., Deng W., and Xie L. (2009) Evidence for ocean acidification in the Great Barrier Reef of Australia. *Geochimica et Cosmochimica Acta* **73**, 2332-2346.

Weiner S. and Dove P. M. (2003) An overview of biomineralization processes and the problem vital effect. *Reviews in Mineralogy and Geochemistry* **54**, 1-29.

Wilkinson B. H. and Algeo T. J. (1989) Sedimentary carbonate record of calcium-magnesium cycling. *American Journal of Science* **289**, 1158-1194.

Zeebe R. (2005) Stable boron isotope fractionation between dissolved $B(OH)_3$ and $B(OH)_4^-$. *Geochimica et Cosmochimica Acta* **69**, 2753-2766.

Zeebe R. E. and Wolf-Gladrow D. A. (2001) *CO$_2$ in seawater: equilibrium, kinetics and isotopes*. Elsevier.

Zeebe R. E. and Sanyal A. (2002) Comparison of two potential strategies of planktonic foraminifera for house building: Mg^{2+} or H^+ removal? . *Geochimica et Cosmichimica Acta* **66**, 1159-1169.

Zeebe R. E., Wolf-Gladrow D. A., Bijma J., and Hönisch B. (2003) Vital effects in foraminifera do not compromise the use of $\delta^{11}B$ as a paleo-pH indicator: Evidence from modeling. *Paleoceanography* **18**(2), 1043.

Zhang H. and Byrne R. H. (1996) Spectophotometric pH measurements of surface seawater at in-situ conditions: absorbance and protonation behavior of thymol blue. *Marine Chemistry* **52**, 17-25.